Transport of microplastic debris in estuaries

Isabel Jalón-Rojas, Sophie Defontaine, María Bermúdez, Manuel Díez-Minguito

Transport of microplastic debris in estuaries

Isabel Jalón-Rojas [1,*], Sophie Defontaine [1], María Bermúdez [2], Manuel Díez-Minguito [2]

[1] *CNRS, Univ. Bordeaux, UMR 5805 EPOC, Allée Geoffrey Saint-Hilaire, 33615 Pessac, France*
[2] *IISTA, Dept. Structural Mechanics and Hydraulics Engineering, University of Granada, Avenida del Mediterráneo, Edificio CEAMA, Granada E-18006, Spain*

[*] *Corresponding author: Isabel Jalón-Rojas (isabel.jalon-rojas@u-bordeaux.fr)*

Abstract

This Chapter provides insight into the physical, hydrodynamic and biochemical processes governing the transport of microplastics in estuarine environments. The focus is mainly on the physical and hydrodynamical processes that control microplastic transport, although the role of biochemical processes on their dynamical behaviour is discussed. The chapter begins by describing the microplastic physical properties and their variability with the time spent in the environment due to weathering, biofouling, and flocculation. This variability makes them different from other suspended particulate matter and critically affects their buoyancy, deposition and erosion rates. The more prominent hydrodynamic processes driving the transport of microplastics are then discussed. Next, four case studies are presented to illustrate microplastic dynamics in different types of estuaries, from well-mixed to strongly stratified. Finally, sampling and numerical approaches for analysing the dispersion of microplastics in estuaries are reviewed.

Citation

Jalón-Rojas, I., Defontaine, S., Bermúdez, M., Díez-Minguito, M. (2024). Transport of microplastic debris in estuaries. Reference Module in Earth Systems and Environmental Sciences: Treatise on Estuarine and Coastal Science, 2nd Edition, Elsevier, https://doi.org/10.1016/B978-0-323-90798-9.00022-6

Highlights

- The chapter introduces the physical, hydrodynamics and biochemical processes driving the transport of microplastics in estuaries, providing a concise foundation for the interdisciplinary community studying plastic pollution and deepening in forefront results.
- A thorough foundation on sinking, erosion and beaching processes is presented, highlighting the intrinsic behaviour of microplastics in relation to their wide range of physical properties and the effects of biochemical processes such as biofouling and flocculation.
- A wide range of hydrodynamic processes for which there are first signs of evidence that they may play a key role in the transport and trapping of microplastics are described, including tidal-scale processes, residual circulation and internal asymmetries.
- Four study cases illustrate estuarine microplastic dynamics under contrasting environmental conditions in different estuaries, from well-mixed to strongly stratified, with a particular focus on flushing and trapping physical mechanisms. Microplastic dispersion and transport trends are site-specific and highly dependent on the particle physical properties. Nevertheless, Estuarine MicroPlastic Maxima (EMPM) seem to be a common feature in estuaries.
- The main observation techniques and modelling methods to advance knowledge of MP transport are presented, focusing on the limitations of sampling strategies and the recommendation to capture the representative time scales of estuarine variability.

---

1. Introduction

Plastics[1] are indispensable materials used in nearly all aspects of our daily lives, such as packaging, textile, health, agriculture, building and electronics. Humanity is now producing more than 380 tons of plastic every year, a figure that is expected to increase over the next years (Geyer et al., 2017). The combination of this huge production, low-reusing and recycling rates, and poor policies promoting a circular plastic economy imply a great input of plastic waste into the aquatic environment. For instance, Borrelle et al. (2020) estimated that from 19 to 23 Mt of plastic litter - or 11% of the global plastic waste - entered aquatic ecosystems in 2016.

Plastic pollution of aquatic ecosystems brings about a variety of environmental and socio-economical issues, including physical and behavioural effects on aquatic organisms (e.g. Cole et al., 2011; Andrady, 2011), habitat modifications (Gall and Thompson, 2015), loss of ecosystem services (Smith, 2012), damage of urban infrastructures (Njeru, 2006), and economic losses such as tourism revenues (McIlgorm et al., 2011). Microplastics[1] (MPs) - particles[1] of plastic[1] litter with a size ranging from 1 μm to 5 mm (Frias and Nash, 2019) - are particularly problematic due to their abundance, their susceptibility to travel over long distances, and their capacity to enter the food chain (Cózar et al., 2017; Wright et al., 2013). Microplastics present in the aquatic environment are classified into primary or secondary depending on their source. Primary MPs are intentionally manufactured to be that size (e.g. microbeads[1] from personal care products). Secondary MPs, the predominant category, originate from the breakdown of larger plastic items, mainly through exposure to UV radiation and mechanical abrasion. A third intermediate category includes MPs derived from the wear and tear of plastic products, such as car tires and synthetic fibres from laundry.

At the land-ocean interface, estuaries are privileged pathways of MPs. According to Morales-Caselles et al. (2021), around three-quarters of plastic waste reported in the ocean comes from land-based sources, mostly via rivers and estuaries (Lebreton et al., 2017). Other than rivers, sources of MPs in estuaries include atmospheric transport (Allen et al., 2021), direct run-off (Treilles et al., 2021), and ocean- or estuarine-based sources such as ports, sewage or vessels (Napper et al., 2022). However, not all plastic entering estuaries are flushed into the ocean (van Emmerik et al., 2022). In the same way that sediments and particulate organic matter are trapped in estuaries (Burchard et al., 2018), MPs might also accumulate in convergence zones. Estuarine benthic sediments, riverbanks and riparian vegetation could constitute important sinks for MPs (Simon-Sánchez et al., 2019; Martin et al., 2019; Tramoy et al., 2020a). This potential accumulation can prevent a significant portion of MPs generated in river catchments from reaching the sea, but also may significantly affect the growth of plant species in saltmarsh edges and benthic communities such as microphytobenthos (e.g. Díez-Minguito and de Swart, 2020; Miró et al., 2020).

Even although MPs could get trapped, they can be remobilised from these hot-spots at different time scales from tidal to pluriannual (e.g. Tramoy et al., 2020a) and accumulate in a different location. A major challenge for scientists is to assess the relationships between sources and sinks of MPs at the continuum river-estuary-ocean. This is a complex task, and general rules do not exist because sources and sinks are very site-specific. Systematic studies aiming to identify MP concentration trends in conjunction with the physical drivers of their transport and trapping in

[1] Term defined in Section 2

different types of estuaries are crucial to gain insight into this research issue, as well as to evaluate environmental and socio-economical risks, and prevent waste from reaching the ocean.

In recent years, the number of studies in estuaries has rapidly increased (e.g. Yonkos et al., 2014; Cohen et al., 2019), although the distribution, fluxes and fate of MPs remain largely unknown. This is partially due to the novelty of the area of study and the complexity of this research issue. Studies on MP transport are relatively less abundant than studies on ecotoxicity, adsorption or ageing (Rozman and Kalčíková, 2022) and mainly focused on ocean and regional scales (e.g. Lobelle et al., 2021; Baudena et al., 2022). The wide range of sizes, shapes, and densities make the dynamical behaviour and the water-bed exchange of MP complex. On top of that, the absorption of chemical contaminants and the formation of biofilms and aggregates further enhance this complexity (Kooi and Koelmans, 2019). The complex sedimentary behaviour plays a particularly relevant role in the transport of MP in estuaries. Compared to the open ocean, estuaries are generally very shallow, and the three-dimensional structure in the water column greatly contributes to material transport, including light neutrally buoyant particles (Jalón-Rojas et al., 2019b). Deep knowledge of the dynamical properties of MPs under the effect of biogeochemical processes is therefore essential to progress in understanding estuarine MP transport.

This chapter provides a comprehensive and coherent overview of the physical mechanisms and hydrodynamical processes involved in the transport and trapping of MPs in estuarine environments. It includes the introduction to fundamental concepts and processes, most of them common to sediment transport research, recent findings on the specific dynamical behaviour of MPs, and site-specific examples to elucidate and gain insight into estuarine MP transport and the spatio-temporal distribution of this pollutant. The chapter mainly focuses on physical mechanisms, although the effects of biochemical processes such as biofouling[2] or flocculation[2] on transport processes are discussed. While many of the mechanisms described here also drive the transport of macroplastic[2] debris, the chapter mainly focused on the transport of MPs. Two of the major differences are the significant influence of windage (i.e., direct drift by wind) for macro-debris and the distinct sinking behaviour of micro and macro debris as it relies on the size and shape of the items (Section 4.3). These differences imply that the resulting distribution of micro and macro debris at different time scales may follow different patterns under the effect of the same environmental conditions.

Given the interdisciplinary nature of plastic pollution research, this chapter begins with a list of definitions (Section 2) aiming to facilitate the reading and understanding of the different terms and concepts by readers with different backgrounds.

Section 3 describes the physical properties of MPs and the processes that modify such properties in the aquatic environment, such as weathering, biofouling, mechanical degradation and subsequent fragmentation, and flocculation.

Section 4 provides a comprehensive picture of the mechanisms of MP transport, explaining fundamental concepts, and introducing recent knowledge on the dynamical behaviour of MPs and new parameterisations. The section includes processes such as advection, turbulent diffusion, beaching, washing-off, deposition, salting, rolling, sliding, and elaborates on vertical processes such as sinking, buoyancy and resuspension.

Understanding MP transport patterns requires thorough knowledge of the driving hydrodynamics

[2]Term defined in Section 2

in estuaries. Section 5 provides a comprehensive description of what is known about the different hydrodynamic processes that affect the transport of microplastic in estuaries.

The relative influence of the various physical processes on the trapping and exporting dynamics of MPs in different types of estuaries is evaluated in detail in Section 6 through four case studies. The presented examples include observations, idealised simulations and realistic simulations. Even if there is a bias toward our own work in European Atlantic estuaries, the selected case studies represent a wide range of types of estuaries according to the circulation-stratification diagrams by Geyer and MacCready (2014); Valle-Levinson (2008), from well-mixed to salt-wedge estuaries.

Section 7 illustrates different observation strategies and techniques and different types of modelling tools to advance the knowledge of MP transport processes and spatial-temporal patterns in estuaries. Finally, Section 8 summarises several key ideas presented in this Chapter, including research perspectives.

2. Definitions

- **Biofouling:** Growth and accumulation of micro and macro living organisms (bacteria, algae, invertebrates) on living or non-living surfaces. This coating is named biofilm.

- **Bottom shear stress:** Force per unit area exerted by the fluid in motion on the bed, in a direction parallel to the bed surface. Shear stress (τ, in $N \cdot m^{-2}$ or Pa) is calculated as a function of the shear velocity (u^*, in $m \cdot s^{-1}$) and water density (ρ, in $\mathrm{kg} \cdot \mathrm{m}^{-3}$):

$$\tau = \rho(u^*)^2 \tag{1}$$

- **Buoyancy:** Upward force defined by the Archimedes Principle "A body immersed in a fluid will experience an upward force due to hydrostatic pressure equal and opposite to the weight of the fluid displaced by the body". Buoyancy forces also arise from the variations of density in a fluid subject to gravity leading to a wide range of phenomena in fluid mechanics (Turner and Turner, 1979), including stratification[3] in estuaries.

- **Dimensionless particle diameter:** Dimensionless number introduced by Shield (1936) typically used in sediment studies to describe the particle size by considering the particle Reynolds number, i.e. the nature of the surrounding flow and its settling velocity. It is calculated as follows:

$$D^\star = \left(\frac{\frac{\rho_s - \rho_w}{\rho_w} g}{\nu^2}\right)^{1/3} D \tag{2}$$

  where ρ_s is the particle density, ρ_w is the water density, g is the gravity acceleration, ν is the kinematic velocity of the fluid, and D is the particle size.

- **Estuarine circulation:** Tidally-averaged[3] along-channel velocity through an estuarine cross-section.

[3]Term defined in Section 2

- **Estuarine Microplastic Maxima (EMPM):** Similarly to Estuarine Turbidity Maxima (ETM)[4] definition, EMPM are defined as zones of elevated suspended microplastic concentration (hot-spots) in estuaries (Díez-Minguito and de Swart, 2020).

- **Estuarine Turbidity Maxima (ETM):** Region of elevated tidally-averaged[4] suspended sediment concentration that often occurs in coastal-plain, salt-wedge, and river-dominated estuaries, where they influence the morphodynamic development, biogeochemical cycling, and contaminant redistribution of these systems (Jay et al., 2015; Burchard et al., 2018).

- **Exchange flow:** term used to emphasises that the estuarine circulation[4] is commonly structured in space (e.g., incoming flows of denser water and outflows of lighter waters near the surface). This flow may be primarily responsible for exchanging water and substances between the estuary and the ocean (Geyer and MacCready, 2014).

- **Flocculation:** Aggregation of fine organic or inorganic particles into flocs due to cohesive forces and organic polymers and coatings (Andersen et al., 2021).

- **Microbead:** Manufactured microplastic of less than 1 mm used in a mixture as an abrasive, i.e. to exfoliate, polish or clean (modified from ECHA (2020)).

- **Macroplastic:** Plastic object or fragment characterised by an external dimension higher than 5 mm.

- **Microplastic (MP):** "Any synthetic solid particle or polymeric matrix, with regular or irregular shape and with size ranging from 1 μm to 5 mm, of either primary or secondary manufacturing origin, which are insoluble in water" (Frias and Nash, 2019). Natural polymers that have not been chemically modified are excluded (ECHA, 2020).

- **Nanoplastic:** Idem than microplastics[4] but with size (all dimensions) between 1 nm and 1 μm (Gigault et al., 2018).

- **Particle:** Minute piece of matter with defined physical boundaries (ECHA, 2020). Also referred to as item.

- **Plastic:** Synthetic or semi-organic polymers[4] made from raw material such as oil, petroleum, and plants through the use of chemicals and condensation to induce molecular bonding. Their capacity to deform irreversibly without breaking (or plasticity) makes it possible for plastics to be moulded into solid objects of various shapes.

- **Polymer:** Materials made of long, repeating chains of joined individual molecules. They have unique properties (e.g. density, hardness, tensile strength, machinability, formability, etc.) depending on the type of molecules and how they are joined. Polymers range from natural biopolymers, such as wool or cotton, to synthetic plastics, such as polystyrene.

- **Stokes drift:** Net drift velocity in the direction of wave propagation caused by a phase lag between wave elevation and wave currents. Stokes drift is present under progressive wave

[4]Term defined in Section 2

conditions such as surface gravity waves and tides. It induced a landward accumulation of water and momentum, resulting in a water level gradient that generates a seaward return flow called Stokes return flow.

- **Richardson number (Ri):** Dimensionless number that evaluates the relative importance of the vertical shear (changes in current velocities with depth) and the stratification[5] induced by gravitational effects. Turbulent mixing induced by vertical shear is expected to overcome buoyancy[5] forces and breakdown stratification when the Richardson number is below the threshold value of 0.25. Otherwise, a stable stratified configuration prevails over turbulent mixing.

$$Ri = -\frac{g}{\rho_0}\frac{\partial\rho/\partial z}{(\partial\overline{u}/\partial z)^2}, \tag{3}$$

where g is the gravity acceleration, ρ_0 the reference density and $\overline{u}$ the mean horizontal velocity.

- **Rouse number (Ro):** Dimensionless number that indicates the mode of particles transport through several threshold values: bed load ($Ro > 2.5$), 50% suspended ($1.2 < Ro < 2.5$), 100% suspended ($0.8 < Ro \leq 1.2$) and wash load ($Ro \leq 0.8$).

$$Ro = \frac{w_s}{\kappa u^\star}, \tag{4}$$

where w_s is the settling velocity, κ is the von Karman's constant and u^* is the shear velocity. Transport modes are explained in detail in Section 4.

- **Stratification:** Division of the water column into layers with different densities caused by differences in salinity, temperature or both. It is one of the most important characteristics of estuaries as it affects vertical mixing and, therefore, the vertical distribution of chemicals, biota and particles. Stratification arises due to the input of freshwater into saline embayments, wherein the influence of gravity causes the freshwater to override the saltwater (Chapter 2.03 of this treatise).

- **Tidal pumping:** Covariance between suspended particulate matter concentration and current velocity. For example, in a flood-dominant estuary, more particles are resuspended during the flood tidal phase (characterized by stronger currents), which results in up-estuary pumping of particles despite a net down-estuary advective flux (Scully and Friedrichs, 2007).

- **Tidal range:** Height difference in water level elevation between successive high and low tide.

- **Tidally-averaged or subtidal or residual:** Averaged value of a parameter over a tidal cycle. According to Geyer and MacCready (2014), this term indicates that a low-pass filter has been applied to the time series of a property to reveal its low frequency features.

[5]Term defined in Section 2

3. Physical Properties of Microplastics and their Variability

3.1. Size

Microplastics[6] are commonly defined as plastic particles having the largest dimension smaller than 5 mm. In contrast, nanoplastics[6] have the largest dimension smaller than 1 μm. In this chapter, the nanoscale is left aside as the physico-chemical behaviour and biological interactions of nanoplastics are dissimilar from those of microplastics (Ter Halle and Ghiglione, 2021), and most of the sampling techniques used in estuaries do not cover the nanoscale (minimum sampling size of 5 μm). In practice, the size limitation of MPs is fully dependent on the used sampling technique, which generally varies from 5 μm (manta nets) to 300 μm (filtration) (Section 7). The size range of MPs is similar to that of natural sediments such as clay, silt and sand, hence similarities can be found between MP and fine sediment dynamics (Browne et al., 2010; Rodrigues et al., 2019).

Small MPs seem to be predominant in the aquatic environment. Figure 1 shows the size distributions of MPs from 9 observation studies compiled by Kooi and Koelmans (2019). The sampling location, mainly the sea surface, or the plastic type were highlighted for some studies. Data shows two different patterns. Either there is a decrease in particle concentration with increasing sizes, or an initial increase in concentration with particle size, followed by a decrease similar to the first-mentioned pattern. There are two possible explanations for this second pattern. Either the smallest particles are easily overlooked in the sample analyses, leading to a bias; either wind mixing, biofouling[6] or aggregation decrease the abundance of small MPs in surface waters (Kooi and Koelmans, 2019).

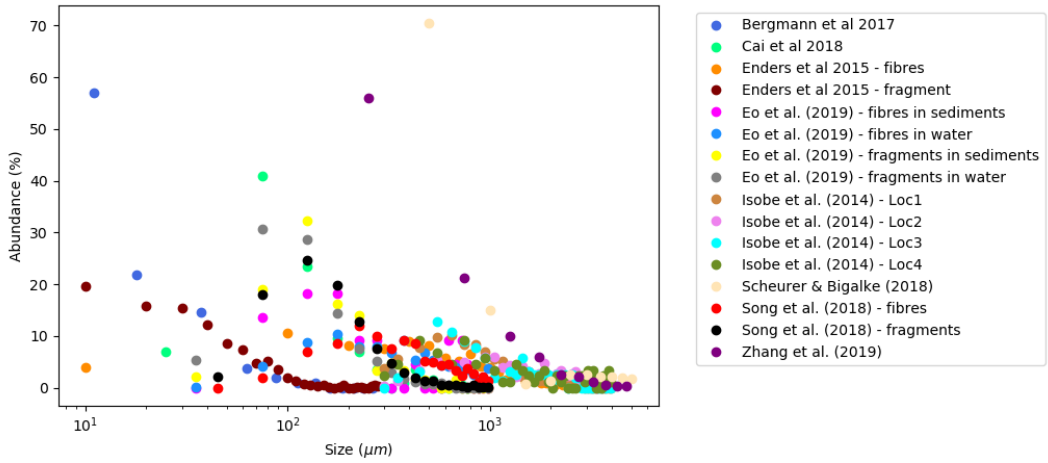

Figure 1: Microplastic abundance in function of particle sizes (after Kooi and Koelmans, 2019).

3.2. Density

There is a wide diversity of plastics present in the marine environment and their density depends to a large extent on the chemical composition. Some of the most commonly found polymers[6] are polyethylene (PE), polyethylene terephthalate (PET), polypropylene (PP), polystyrene (PS),

[6]Term defined in Section 2

Polyvinyl chloride (PVC) and polyamide (PA) (Geyer et al., 2017). The density of such polymers[7] ranges from 0.89 to 0.98 $\mathrm{g \cdot cm^{-3}}$ for PE, from 0.96 to 1.45 $\mathrm{g \cdot cm^{-3}}$ for PET, from 0.83 to 0.92 $\mathrm{g \cdot cm^{-3}}$ for PP, from 0.95 to 1.10 $\mathrm{g \cdot cm^{-3}}$ for PS, from 1.10 to 1.58 $\mathrm{g \cdot cm^{-3}}$ for PVC and from 1.02 to 1.15 for PA (Waldschlager and Schuttrumpf, 2019a; Zhang, 2017). The density of plastic material may deviate from the original polymer density due to the addition of stabilisers, fillers and additives during the manufacturing. This property plays an important role in its dynamics. MPs with a lower density than the ambient water density will tend to float, while MPs with a greater density than the ambient water density will tend to sink. More details on the sinking behaviour of MPs are given in Section 4.3. Microplastics of the same size and shape but different density may therefore not be subjected to the same forcing. For instance, MPs floating at surface waters will suffer wind forcing, while high-density sinking MPs will be subjected to bed shear instabilities.

3.3. Shape and colour

MPs exist in different colours and shapes (see examples in Figure 2). During inspection procedures, MPs are generally classified under shape categories, such as beads, fibres, pellets, fragments, foam and films. The most abundant MP shape category in the aquatic environment is fibres (48.5%), followed by fragments, beads, films, and foam (Burns and Boxall, 2018). Shape hugely impacts the dynamical behaviour of MPs as detailed in Section 4.3. For instance, a fibre, a film and a sphere of same major dimension and density, will not settle or rise at the same velocity. Consequently, MPs of different shapes can be subject to different forcing and show different spatial and temporal distributions. MP shape is usually quantified through parameters such as the Corey shape factor (Kooi and Koelmans, 2019). This widely-used parameter is calculated from the three mean lengths of the particle as

$$CSF = \frac{c}{\sqrt{a \cdot b}} \tag{5}$$

where a, b, and c are the longest, intermediate, and shortest sides. Other parameters are based on the equivalent spherical diameter, roundness, surface area and perimeter (Kowalski et al., 2016; Kooi and Koelmans, 2019; Van Melkebeke et al., 2020).

During inspection procedures, MPs are also classified by colours, as it may help to deduce the original source of MPs. However, even the colour of microplastics may play a role in their fate as it makes them look like prey for marine organisms. In particular, transparent, white, yellowish and blue particles are preferentially ingested (Oben Mbeng et al., 2021; Parvin et al., 2021).

[7] Term defined in Section 2

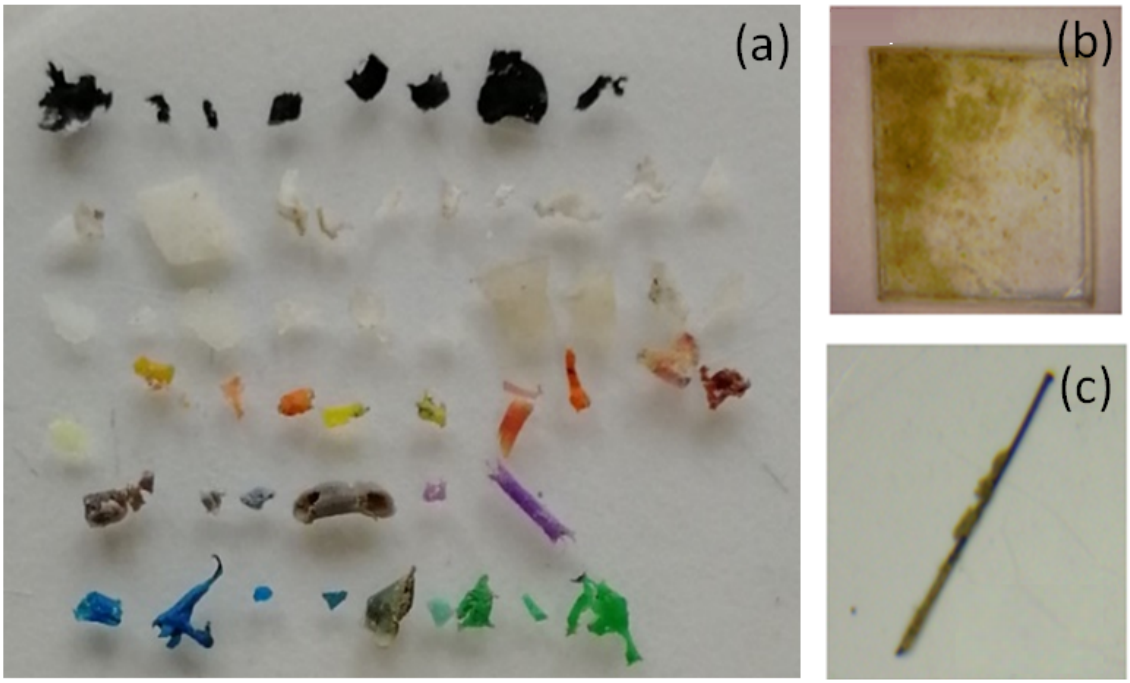

Figure 2: (a) Example of MPs of different sizes, shapes and colours from the surface waters of Arcachon Bay (Photo: F. Le-Bihanic, ARCPLASTIQUE project); (b) biofouled MP sheet; (c) biofouled MP fibre (Jalón-Rojas et al., 2022)

3.4. Alteration of physical properties: weathering and aggregation

The physical and dynamical properties of MPs vary in time and space in aquatic environments due to various physical, chemical and biological processes, thereby resulting in significant modification of their dynamics. In coastal waters, MPs are exposed to weathering by wave action, solar exposure, mechanical shear, thermal oxidation, and biological degradation. Wind, waves, and tides generally cause their mechanical abrasion on beaches or on the bed (Cooper and Corcoran, 2010; Sipe et al., 2022). Solar exposure induces a photodegradation of the polymer[8] matrix leading to embrittlement (Andrady et al., 1998). Despite the durability of plastic polymers, weathering causes the generation of cracks up to the MP fragmentation into smaller pieces. However, fragmentation is a long iterative process. It takes decades to centuries to degrade an entire plastic bottle into microplastics.

Weathered MPs exhibit altered physical and dynamical properties, such as size, colour, mechanical properties, specific surface area and sorption capacity, compared to pristine ones (Liu et al., 2020). The impact of weathering on MPs relies on their composition. For instance, a laboratory experiment that exposed MPs to UV light for 12 months and mechanical abrasion for 2 months demonstrated that PS and PP were more significantly fragmented than PE (Song et al., 2017). Smaller sized MPs produced by fragmentation may also be more easily ingested by marine organisms. Readers can refer to Jahnke et al. (2017) and Liu et al. (2020) for more details on weathering processes.

After spending some time in aquatic environments, a biofilm can develop on the MP surface. This process called biofouling[8] consists of the generation of a coating made of living micro- and macro-organisms (e.g. bacteria, plankton, algae, mussels). Figure 2.b-c illustrates examples of

[8]Term defined in Section 2

biofouled MP. The time necessary for generating a biofilm fluctuates depending on the MP size and surface area, the type of polymer[9], the biological activity, and ambient water characteristics (Karkanorachaki et al., 2021; Rummel et al., 2017). Weathering enhances the formation of biofilm by increasing the specific surface area of MPs. Biofouling affects size, shape and, to a greater extent, MPs density. The consequences of these changes on the MP dynamical behaviour, particularly on buoyancy and sinking, are discussed in Section 4.3. Biofouling is supposed to be the main reason that makes initially negatively-buoyant particles sink below the upper water (Amaral-Zettler et al., 2021).

This accumulation of biomass on the MP surface also promotes aggregation with sediment or other MPs due to the binding properties of biofilm. Small MPs in the size range of cohesive sediments (i.e., clay, silt, and fine sand; $0.1\tilde{}250\,\mu$m) can aggregate with fine sediments into flocs as a result of cohesive forces and organic polymers and coating (Andersen et al., 2021). This process of flocculation[9] implies an increase of size and modifies the density of the virgin particle by forming pores between the aggregated particles filled with ambient waters. These changes also influence the sinking behaviour of MPs (Section 4.3). The first studies of MPs flocculation suggest that the timescale of flocculation is relatively short. For example, it takes only two hours for PVC MPs incubated in a solution of $100\,\mathrm{mg}\cdot\mathrm{L}^{-1}$ suspended sediment concentration to flocculate (Andersen et al., 2021). Moreover, particles such as films, fibres or foam which are characterised by a high surface area to volume ratio are prone to biofouling and aggregation (Ryan, 2015).

4. Transport Mechanisms: Fundamentals and Influence of Biological and Chemical Processes

This section describes the different modes of MP motion in estuarine and coastal environments and the underlying processes. Even though this is a relatively young research topic, decades of research in sedimentology and hydrodynamics aiming to understand the transport of natural sediments, flocs, and aggregates (see, e.g., compilation in Winterwerp and Van Kesteren, 2004) provide the theoretical background and foundations to describe the transport behaviour of MPs. Nonetheless, the heterogeneous nature of MPs implies that some concepts and parameterisations must be revised or adapted. In particular, as described in Section 3.4, weathering, biofouling, and aggregation processes can modify the physical properties of particles significantly, affecting their transport behaviour. Some of these processes, such as biofouling[9] and flocculation[9], can be particularly important in highly productive (Kvale et al., 2020) and hyperturbid (e.g. Andersen et al., 2021) systems, respectively, and must be considered when studying MP transport. Here, the fundamental processes of transport are described, as illustrated in classical literature on sediment research (e.g. Chapter 2.15 of this book), and introduce recent advances from experimental, observational, and numerical works aiming to understand, quantify or parametrise the transport behaviour of MPs.

Depending on their physical properties, MPs are transported in estuaries as wash load, in suspension, or as bed load. A MP is considered as suspended when it is floating within the water column. MPs are kept in suspension by turbulent mixing (Section 4.1), against gravity (settling, Section 4.3). Wash load also refers to suspended particles but, unlike suspended load, the effect of

[9]Term defined in Section 2

particle (positive) buoyancy[10] dominates over turbulent mixing (Section 4.3). Positive buoyant MPs are typically transported as wash load, close to the water surface (Iwasaki et al., 2017). Neutral buoyant MPs and very small particles such as fibres are typically transported as wash load, uniformly distributed across the flow field (Lefebvre et al., in prep). Bed load refers to transport in a thin layer near the bed surface. Negative buoyant MPs can be transported as bed load, especially large high-density MPs, or in suspension (Ballent et al., 2012; Waldschlager and Schuttrumpf, 2019b). In this chapter, the focus is on the wash and suspended transport modes. Transport modes can be affected by biofouling and aggregation processes. For example, pristine low-density particles initially transported as wash load at surface waters can switch to the sediment-load mode after colonisation by organisms or flocculation with fine sediments (Figure 2.b-c). Below, the different processes of MP transport are addressed (outlined in Figure 3), particularly the settling and the effects of biofouling and flocculation on it.

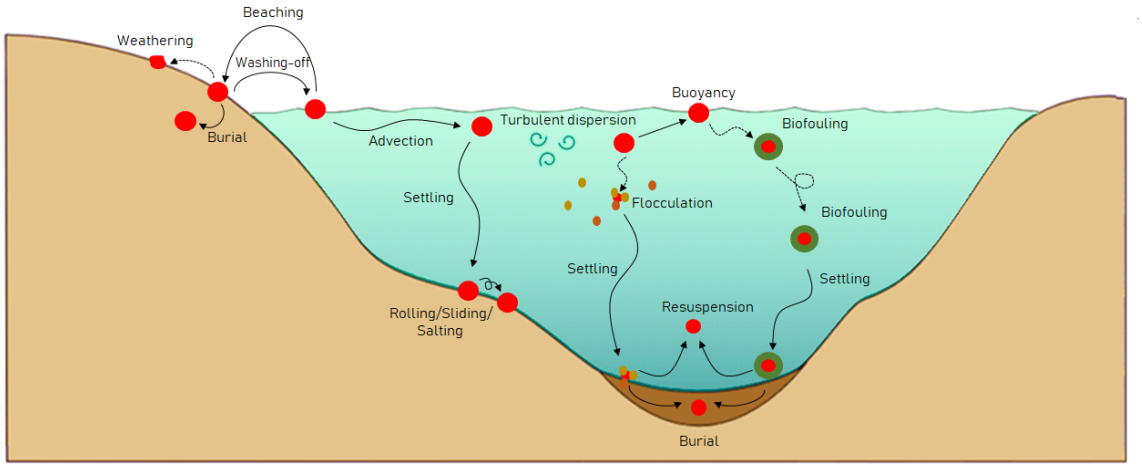

Figure 3: Key processes affecting the transport of microplastics.

4.1. Advection and turbulent diffusion

Advection is the transport of MPs caused by the movement of a fluid. It requires currents in the fluid to transport MPs by advection at an average rate equal to the average water velocity in the environment. The currents in estuaries are induced by tides, river inflow, wind and density gradient, as explained in Section 5. For example, for a cluster of MPs arriving at the upper estuary by seaward river currents, advection will move all the particles downstream. Mathematically, fluid motion is described as a vector field $v(x, y, z, t)$ that represents the velocity of the fluid at the point (x, y, z) at the instant t.

Turbulent diffusion or dispersion is the spread of a cloud of substance or particles such as MPs by random and chaotic (turbulent) motion. In the example of a cloud of MPs arriving at the upper estuary, while advection carries the centre of mass of the cluster downstream, diffusion spreads out the cloud to a larger, less concentrated region (see Figure 4). Turbulent diffusion occurs in non-uniform turbulent flows by the fluctuations in the velocity fields at scales smaller than the cloud, or by horizontal or vertical velocity gradients at scales larger than the cloud, which cause horizontal

[10]Term defined in Section 2

or vertical shear dispersion (Fischer et al., 1979). It is considered analogous to molecular diffusion, but it occurs much more rapidly, becoming a fundamental transport process. The turbulent diffusion in the horizontal and vertical dimensions is usually called horizontal dispersion and vertical mixing, respectively. Vertical mixing is particularly important in estuarine dynamics, as it impacts the stratification[11] and thus exchange flow[11] (Geyer et al., 2008). Different estuarine physical processes such as tidal straining or turbulence damping by stratification may affect vertical mixing and, therefore, MP transport as detailed in Sections 5 and 6.

Our inability to predict an instantaneous fluid velocity field, and therefore turbulence, translates into uncertainty in estimating the transport of MPs by turbulent dispersion and vertical mixing. As for molecular diffusion, the quantitative assessment of turbulent dispersion is based on Fick's law (Fick, 1855) and a diffusion coefficient K [m^2s^{-1}], also called dispersion coefficient or eddy diffusivity at the horizontal dimension (K_h), or eddy viscosity at the vertical dimension (K_v). The dispersion coefficient is the rate at which particles (or a substance) can spread. It depends on the mixing length (eddies can vary from small Kolmogorov microscales to subtropical gyres) and the turbulent intensity (Okubo and Ebbesmeyer, 1976), being several orders of magnitudes larger than molecular diffusivity. Consequently, it varies with the environment and the fluid conditions, rather than on the properties of the particles or substance; at a turbulent scale, the dispersion coefficient for salt, heat or MPs has the same size.

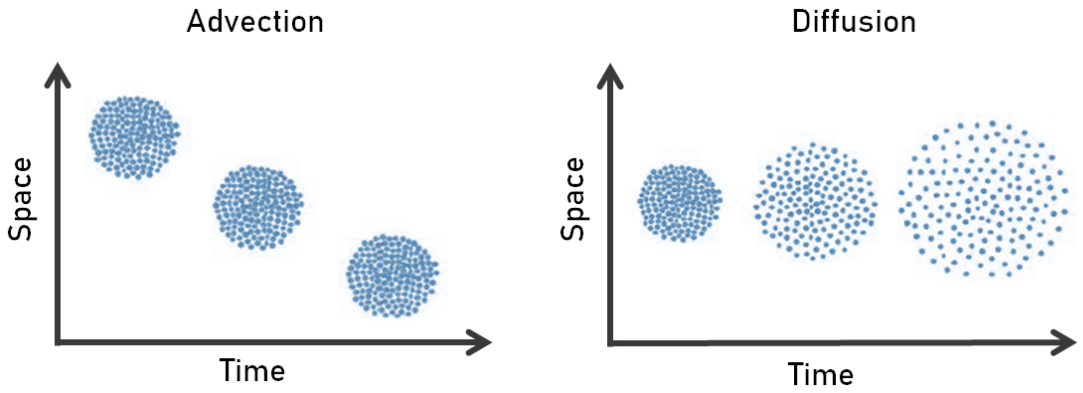

Figure 4: Schematic representation of the spatial and temporal variability of a cloud of particles transported by advection and diffusion.

4.2. Beaching, washing-off and burial

MPs can reach land and beach on river banks, intertidal flats, salt marshes, tidal inlets and beaches. Beached MPs can be washed-off or be trapped or buried on the coast. Although these phenomena of stranding and remobilisation to the water still lack hindsight, recent research provided insight into the role of nearshore physical processes (e.g. Stokes drift[11] and wind-driven currents) and the effect of different factors, particularly at sandy beaches: environmental conditions, the physical properties of MPs, and beach-specific factors such as the morphology, orientation, and type of sediment (Bowman et al., 1998; Chubarenko et al., 2018b; Ryan et al., 2018; Pinheiro et al., 2019; Lo et al., 2020; Forsberg et al., 2020).

[11]Term defined in Section 2

MPs transported in surface layers (either positively buoyant MPs or negatively buoyant MPs kept in suspension by turbulence) can be dragged by shoreward currents to the beach (Chubarenko et al., 2018a). The nature of these shoreward currents (induced by tides, river flow, wind, and/or waves) depends on the specific system and the estuarine region and can vary significantly over time depending on the environmental conditions. The direct action of wind (windage) can also lead to the beaching of macro-debris. Figure 5 presents the monthly variability of the beached MPs concentration at three regions - the inner bay, the mouth and the outer bay- of a mesotidal lagoon (Arcachon Bay, French Atlantic coast), together with the time series of several environmental forcing (significant wave height, wind velocity, and river flow) over the same period, (Lefebvre et al., 2021). The tidal range[12] was similar for the different sampling dates. The highest concentrations of beached MPs were found during energetic hydrodynamic conditions (strong wind, wave and river-flow conditions). The fact that the different environmental factors followed a similar seasonal variability (as they respond to the same large-scale atmospheric forcing; Castelle et al., 2017; Jalón-Rojas and Castelle, 2021), makes the assessment of the individual role of each factor on beaching a difficult task. Nevertheless, some interesting results are highlighted:

1. Wind is a key factor for beaching: onshore (westerly) strong wind favoured the MP beaching, particularly at the mouth and inner bay sites, which are protected from swell and exposed to onshore wind. Laboratory experiments have also demonstrated that low-density MPs beached under onshore winds, while offshore winds pushed them back (Forsberg et al., 2020).
2. Strong waves can enhance the transport of MPs toward the coast through the Stokes drift[12] and the beaching of MPs at the outer bay. Curiously, this site presented the lowest MP concentration and the poorest correlation with waves and wind characteristics. This may be explained by the fact that strong onshore wind events dispersed MPs toward the upper beach before the sampling, as also suggested in previous studies (Browne et al., 2010), making the study of beaching even harder. Readers can refer to Alsina et al. (2020) for more details on the effects of Stokes drift on MP transport.
3. The highest beaching concentrations also matched with flood events, particularly at the mouth and inner bay sites. This factor is not directly linked to beaching in this bay, but it can favour the entrance of MPs into the lagoon. Karthik et al. (2018) also highlighted a relationship between river flow and MPs concentration at beaches of the southeast coast of India.

[12]Term defined in Section 2

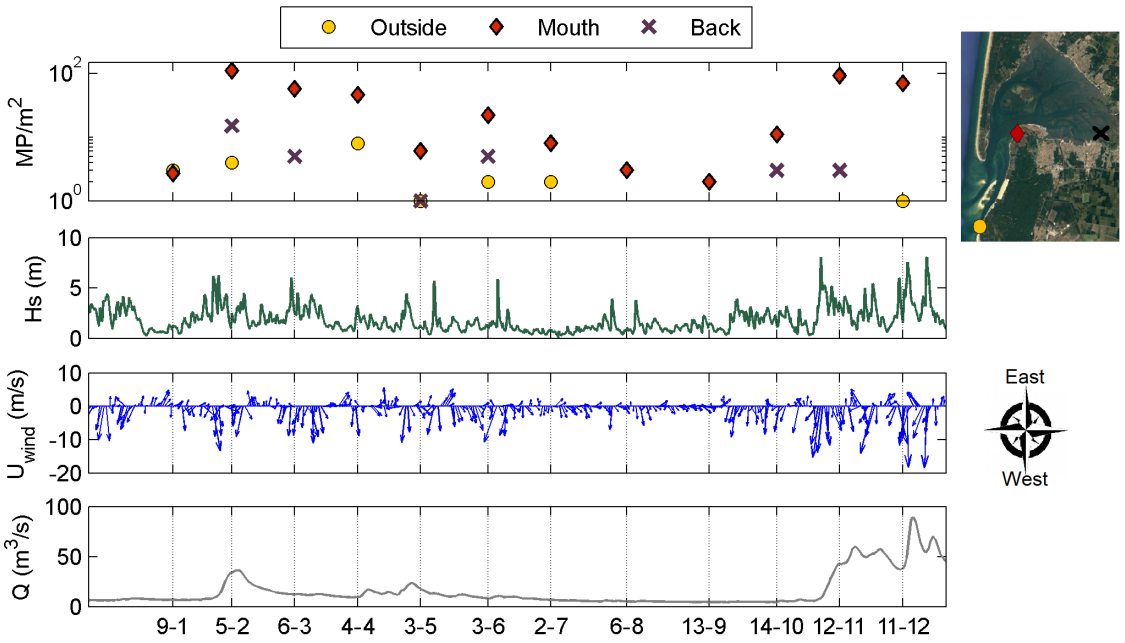

Figure 5: Monthly variability of a) MPs concentration (in $\mathrm{MP} \cdot \mathrm{m}^{-2}$) at three beaches of Arcachon Bay (no data means that concentration was $0\,\mathrm{MP} \cdot \mathrm{m}^{-2}$), b) significant wave height (H_s, in m), c) wind speed ($m \cdot s^{-1}$) and direction (see wind rose) and d) mean daily discharge of the Leyre river (Q, in $m^3 \cdot s^{-1}$). Data from December 1st 2018 to December 31st 2019 (after Lefebvre et al., 2021)

.

Negatively-buoyant heavy MPs that sink at local waters and are hardly transported by surface on-shore currents cannot beach. Nevertheless, similarly to sands, this kind of particles can be transported up-slope to the shore through repetitive upward jumps from the bottom (see erosion and saltation processes in Section 4.4) and subsequent onshore transport by the Stokes drift at beaches influenced by waves, at the lower or outer estuary (Chubarenko et al., 2018a; Forsberg et al., 2020; Jalón-Rojas et al., 2022). Figure 6 presents the result of the laboratory experiments carried out by (Forsberg et al., 2020), aiming to understand the cross-shore transport and beaching of different types of MPs (low- and high-density spheres, sheets and fibres) in a wind-wave flume under controlled conditions. The presented case study corresponds to the reference case consisting of regular waves and no-wind. Nearly all heavy plastic sank to the bottom after release and progressively moved onshore as explained above, due to the enhanced Stokes drift by wave asymmetry (see also Section 5.2) in the shoaling zone. The local balance between return flow and wave forcing trapped these particles in the breaking zone. Low-density particles were transported onshore by Stokes drift and, near the breaking point, most of the particles were advected to the beach by the roller across the surf zone. Interestingly, most of the sheets, characterised by a more neutral buoyancy[13], were transported offshore by return flow and trapped in the surf zone.

MPs and litter stranded in beaches can be washed off by the incoming tides (Johnson, 1989; Johnson and Eiler, 1999; Hinata et al., 2017), swash waves and wave-induced nearshore currents

[13]Term defined in Section 2

(Isobe et al., 2014; Kataoka and Hinata, 2015), or be buried by sediments. A study on Israeli Mediterranean beaches (Bowman et al., 1998) suggests that, unlike the previous example in French Atlantic beaches, stormy events favour the remobilisation of debris, rather than beaching. The balance between input and export of debris may be beach-specific and depend on the environmental conditions and other beach characteristics. For example, Bowman et al. (1998) suggested that morphological elements such as ridge and runnel can trap litter, and beach wide plays a vital role in the deposition/remobilisation rates. According to this study, narrow beaches characterised by a higher range of dynamics presented lower depositional rates. Sediments can also play a key role in stranding MPs. For example, beach rocks provide sheltered habitats where MPs can deposit in great amounts (Pinheiro et al., 2019).

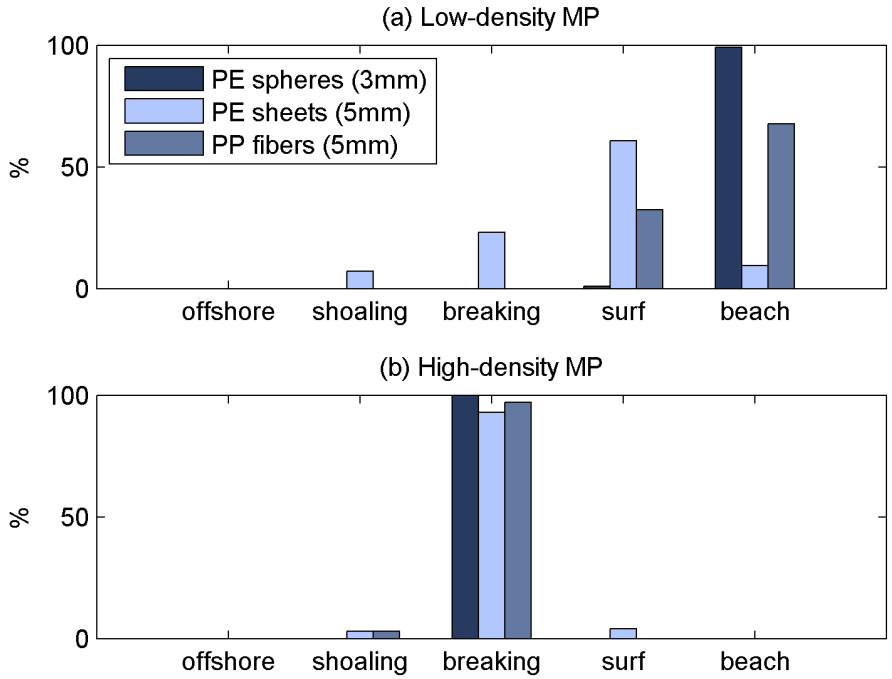

Figure 6: Cross-shore distribution of (a) low-density and (b) high-density MPs at the end of the experiment carried out by Forsberg et al. (2020) in a wind-wave flume (after Forsberg et al., 2020).

In the upper and middle estuarine regions, there are evidences that MP beaching and washing-off processes are controlled by tides and flooding events. Tramoy et al. (2020b) released 50 plastic bottles equipped with GPS-trackers in the Seine River and Seine Estuary (France) that were subject to several beaching/remobilisation events. All the bottles were beached at least one time at different sites. Except one, bottles were stranded for periods longer than 12h (one complete tidal cycle). The stranding/transport time ratio was nearly three times lower in the estuary than in the river. Water level changes by river flow also played an essential role in beaching and straining, particularly on the riverbanks upstream. In this region, debris can be stranded in floodable areas near the main channel (Tramoy et al., 2020a) and be remobilised due to water level changes induced by river discharge, wind, and waves induced by navigation.

Vegetation can be an important element to trap stranded plastic debris in estuarine intertidal zones. For example, Gonçalves et al. (2020) quantified litter retention in the Amazonian estuary

and found a higher number of items in the vegetated habitats (around 73% of the recovered litter). do Sul et al. (2014) showed that mangrove forests tend to retain plastic debris for long periods, from months to years.

Further research based on laboratory experiments, field observations and numerical modelling is needed to further understand processes of beaching, remobilisation and burial at the different estuarine regions. Among the great unknowns, it should be highlighted the flux of MPs between the intertidal areas and the main channel, and the processes governing these exchanges.

4.3. Buoyancy and settling: effect of biofouling and flocculation

A particle submerged in a still fluid is subject to the gravity force, a drag force caused by the motion of the particle through the fluid and the buoyancy[14] force defined by Archimedes' principle (Figure 7) (Dietrich, 1982; Hallermeier, 1981). When these forces are in equilibrium, negatively buoyant particles settle at a constant speed called settling, terminal or sinking velocity; positively buoyant particles rise at a constant speed called rising or upward terminal velocity. The (settling or raising) terminal velocity of any particle depends on the particle physical properties (density, size, shape, roundness, surface texture; Dietrich, 1982; Ballent et al., 2012), and this is the case of MPs (Kowalski et al., 2016; Khatmullina and Isachenko, 2017).

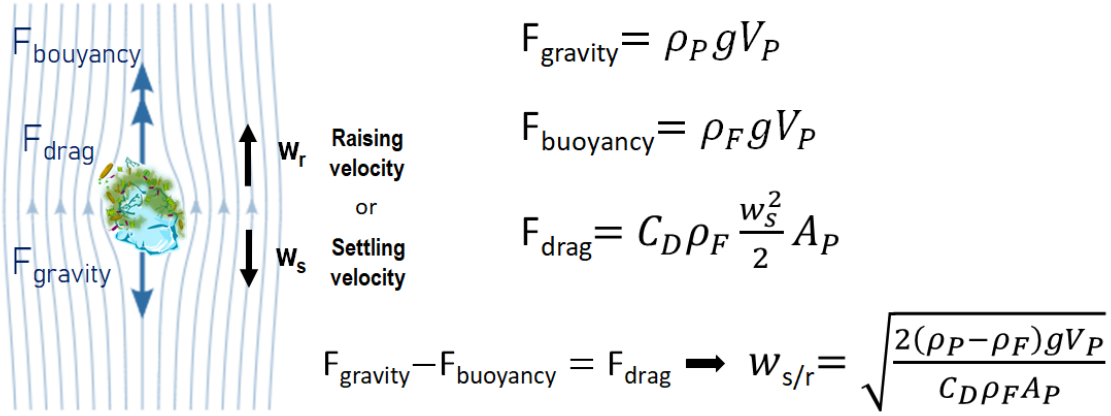

Figure 7: Settling or raising velocity [$\mathrm{m} \cdot \mathrm{s}^{-1}$] from the force balance of falling or raising (biofouled) microplastic. ρ_P [$\mathrm{kg} \cdot \mathrm{m}^{-3}$] is the particle density, ρ_F [$\mathrm{kg} \cdot \mathrm{m}^{-3}$] is the fluid density, g is the gravitational acceleration [$m \cdot s^{-2}$], V_P is the particle volume, A_P is the cross-sectional area of the particle, and C_D [$-$] is the dimensionless drag coefficient. See detailed formulation at Dietrich (1982). The illustration of the biofouled microplastics was extracted from Rummel et al. (2017).

Figure 7 summarises the terminal velocity equation of a particle in still water. Other than particle physical properties, the estimation of terminal velocities [m/s] requires the estimation of the drag coefficient C_D, which quantifies the drag force. This coefficient usually depends on the particle Reynolds number, which relies in turn on the terminal velocity:

$$R = \frac{w_{s/r} \rho_w D_p}{\nu} \tag{6}$$

[14]Term defined in Section 2

where ν is the fluid kinematic viscosity $[m^2 s^{-1}]$ and D_p is the particle size. Terminal velocities of particles are therefore calculated iteratively from empirical formulations of the drag coefficient and the Reynolds number equation.

Several experimental studies have measured the settling and rising velocities of different types of MPs, evaluated the pertinence of existing drag models, and even proposed new drag model formulations. Kowalski et al. (2016) was the first study entirely dedicated to conducting sinking experiments with MP fragments of different sizes and densities. It revealed a significant deviation between their measurements and predictions using the drag model by Dietrich (1982), classically used for sediments. Khatmullina and Isachenko (2017) evaluated the settling behaviour of spherical and cylindrical particles. Waldschlager and Schuttrumpf (2019a) conducted not only settling but also rising experiments on a wide range of MPs and determined the influence of particle shape on the terminal velocity. They showed (e.g.) that fibres and films will generally have a lower settling velocity than spheres. Van Melkebeke et al. (2020) also evaluated the settling behaviour of different types of MPs, including films, whereas Jalón-Rojas et al. (2022) explored the settling and rising behaviour of thick sheets and small fibres. Except for Melkebeke, which proposed a single drag model to predict the settling behaviour of all the types of particles, all the other studies proposed shape-specific formulations. Table 1 compares values of settling and rising velocities estimated by these studies, together with the type of particles considered at each experiment.

Figures 8 and 9 illustrate the terminal velocities of MPs observed by Van Melkebeke et al. (2020) and Jalón-Rojas et al. (2021), respectively, as a function of the dimensionless diameter[15], which considers both particle density and size. In general, terminal velocity increases with the particle density and size (Figure 7). However, there are some exceptions depending on shape as it affects the mass to surface ratio and, consequently, the drag forces do not apply similarly for each shape category. For the same density, velocities of fibres are much smaller than for other shapes and independent of their length (Figure 9.a). Settling and rising velocities of sheets increase with size up to a threshold and then decrease (Figure 9.b-c). This is related to the fact that larger sheets oscillate about a horizontal axis in their own plane, which increases the drag coefficient and slows down the vertical motion.

[15]Term defined in Section 2

Study	Vertical velocity ($\mathrm{mm} \cdot \mathrm{s}^{-1}$)	Density ($kg \cdot cm^{-3}$)	Shapes	Biofouling/Weathering state
		SETTLING		
Kowalski et al. (2016)	6-91	1050-1560	Fragments	Pristine
Khatmullina and Isachenko (2017)	5-127	1130-1168	Spheres, cylinders	Pristine
Waldschlager and Schuttrumpf (2019a)	6.5-314	1020-1580	Pellet, fragment, fibre	Pristine
Waldschlager et al. (2020)	1.6-35.2	1001-1500	Pellet, fragment, foam, film	Weathered/biofouled
Van Melkebeke et al. (2020)	4.5-105	1013-1432	Fragment/fibre	Pristine
Jalón-Rojas et al. (2022)	1.8-70	1170-1600	Sheet/Fibre	Pristine/Biofouled (3 months)
Karkanorachaki et al. (2021)	0-400	No available	Pellet/Film	Biofouled (up to 242 days)
		RAISING		
Waldschlager and Schuttrumpf (2019a)	3.9-184	839-980	Pellet, fragment, fibre	Pristine
Waldschlager et al. (2020))	1.8-198.5	20-983	Pellet, fragment, foam, film	Weathered/biofouled
Jalón-Rojas et al. (2022)	35-74	892- 918	Sheet	Pristine/biofouled

Table 1: Comparison of estimated settling and raising velocity under laboratory conditions.

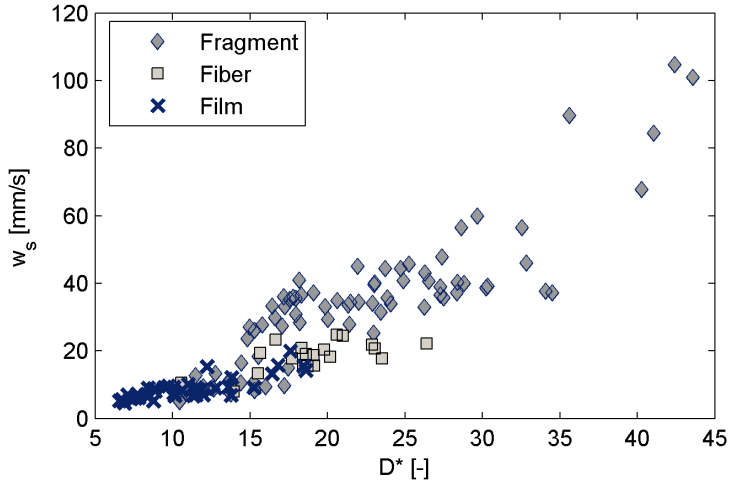

Figure 8: Results of the laboratory experiments carried out by Van Melkebeke et al. (2020): Settling velocity of non-buoyant MP fragments, fibres and films as a function of their dimensionless diameter[17]. (After Van Melkebeke et al., 2020)

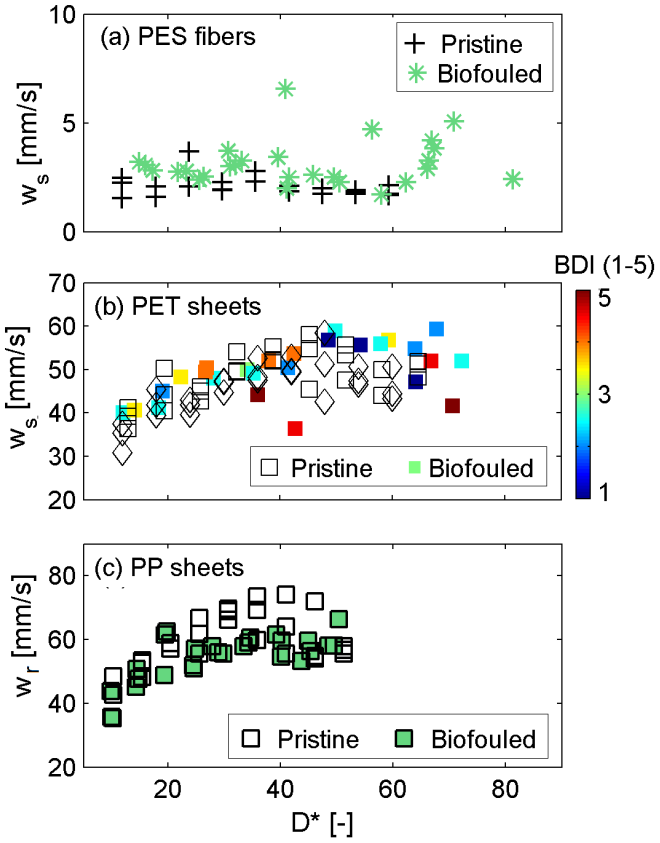

Figure 9: Results of laboratory experiments carried out by Jalón-Rojas et al. (2022): settling (w_s, a-b) and raising (w_r, c) velocities of pristine and biofouled MP fibres (a) and sheets (b-c) as a function of the dimensionless diameter $D^{\star}$[17]. The colorbar in (b) represents the biofilm distribution index (BDI). A high BDI indicates a highly irregular distribution of biofilm.

As introduced in Section 3.4, particle density and therefore settling or rising capacities can significantly change over time under the effect of biofouling[18] (Rummel et al., 2017). Several experimental (e.g. Amaral-Zettler et al., 2021; Fazey and Ryan, 2016) and modelling (e.g. Kooi et al., 2017; Lobelle et al., 2021) studies have demonstrated that floating particles may become negatively buoyant after several weeks in marine waters due to density increase by biofilm attachment. To gain further insight into the dynamical behaviour of biofouled MPs, Jalón-Rojas et al. (2022) measured the vertical velocities of polyester PS fibres (settling), polyethylene terephthalate PET sheets (settling) and polypropylene PP sheets (rising) with two degrees of biological colonisation (pristine and aged 3 months in marine water). Figure 9 illustrates the results of these experiments. Biofouled PES fibres (photo in Fig. 2.c) had slightly higher settling velocities than pristine ones (Fig. 9.a). However, the authors demonstrated that this increase is likely related to changes in fibre orientations during their fall triggered by biofilm rather than to density increase.

In the case of PET sheets, there were no significant differences in settling velocities between pristine and biofouled particles despite the increase in density due to biofouling (Fig. 9.b). For the same size, biofouled sheets (photo in Fig. 2.b) could have either higher or lower settling velocities than pristine sheets. This was explained by a double effect of biofilm. On the one hand, biofilm increased the particle density and therefore its sinking capacity. On the other hand, irregularly-distributed biofilms triggered horizontal oscillations of sheets over their vertical trajectories, increasing drag coefficients and decreasing settling velocities. The balance between these two effects determines the increase or decrease of settling velocity. The distribution of biofilm was quantified through a Biofilm Distribution Index (BDI) in Figure 9.b so that BDI = 1 represents a well-distributed biofilm while BDI = 5 represents a distribution of biofilm highly irregular. This index can be added to drag-model formulations to improve the prediction of settling velocities (see Jalón-Rojas et al., 2022, for details). Biofouled PP sheets were characterised by a thin regular cover of biofilm that did not induce instabilities in motion. In that case, biofilm only increased particle densities and decreased rising velocities (Figure 9.c).

The settling or rising behaviour of particles is thus very sensitive to the nature and degree of biofouling, which can vary in turn for different polymers[18], shapes and environmental conditions. Predicting the evolution of biofilm and terminal velocities over time is therefore a big challenge. With this regard, Karkanorachaki et al. (2021) proposed empirical relationships for different types of MPs and Kooi et al. (2017) developed the first theoretical model based on environmental parameters. This type of model is still based on numerous assumptions but is a promising tool to improve the description of settling behaviour and improve the prediction of MP transport (e.g. Lobelle et al., 2021; Fischer et al., 2021).

Flocculation[18] can also significantly affect the settling behaviour of very small MPs (see description in Section 3.4). A laboratory experiment conducted by Andersen et al. (2021) revealed that polyvinylchloride MPs characterised by sizes ranging $63 - 125\,\mu$m readily floculate with fine cohesive sediments when they are exposed to suspended sediment concentrations observed in hyper-turbid estuaries. Consequently, the resulting aggregates sank faster than individual MPs, at rates characteristic of sediment microflocs or macroflocs. This result implies that small MPs entering estuaries from riverine sources are likely to be trapped in the estuarine turbidity maximum zone, be deposited

[18]Term defined in Section 2

on the bed and become part of fluid mud deposits.

Moreover, the variations of water composition (e.g. salinity, temperature, pH) in estuaries due to the mixing of riverine and marine waters, air-water exchanges and radiation can also impact the sinking behaviour of MPs. Therefore, the MP terminal velocity can vary spatially along the estuarine axis. For example, virgin PS particles have a higher settling velocity in estuarine water than at the coastal sea (Kaiser et al., 2017).

4.4. Deposition, resuspension, bottom transport and burial

Sinking MPs can reach the bottom of the estuary and be deposited. Once deposited, particles can remain there or be remobilised again by currents. This remobilisation process is known as erosion (Van Rijn et al., 1993). Depending on the particle properties and the flow regime, eroded MPs can be resuspended into the water column as suspended load or be transported as bed load. Assuming that MPs behave similar to sediments, they can be transported as bed load by rolling, sliding and saltation. These processes are mainly triggered by gravitational and tractive forces that move particles at velocities slower than the flow (Bagnold, 1973). Sliding and rolling particles remain in continuous contact with the bed while salting particles jump for a short time above the bed. Saltation happens at relatively higher current velocities than rolling and sliding. Resuspension requires higher velocities and more turbulent conditions than bed load transport. This process can be an important source of particles into the estuarine water column, particularly in well-mixed estuaries. For example, Figure 10 shows the concentration of MP fragments observed at three tidal phases and three water depths in the middle Seine estuary (La Roque station, France), Gasperi and Cachot (2021). Given that tide in this estuary is flood-dominant, the peak of MP concentration at middle and bottom depths after the highest flood current velocities evidences the strong resuspension of MPs from the bottom. A considerable amount of suspended particles also occurred during the highest ebb current velocities.

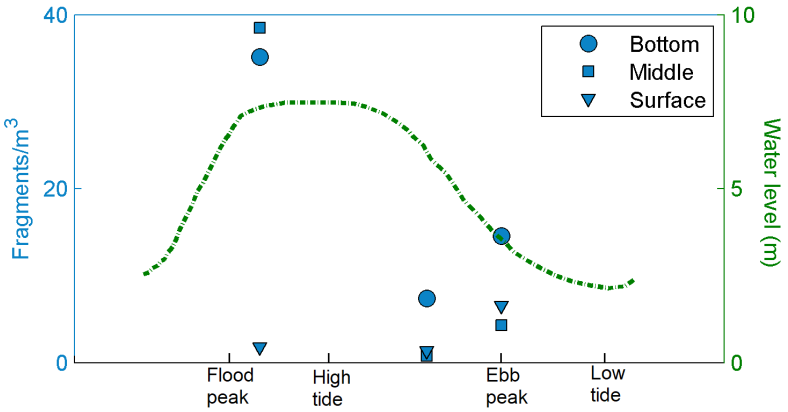

Figure 10: Water level (m) and concentration of MP fragments (MP/m3) observed at three tidal phases and three water depths at La Roque station, in the Seine estuary (after Gasperi and Cachot, 2021).

Understanding and quantifying the erosion behaviour of MPs is essential for a detailed estimation of the transport capacities of MPs in estuaries. Numerical modelling of MP transport requires an accurate parameterisation of erosion behaviour in order to deposit or remobilise particles over time under the influence of the flow velocity field. The beginning of particle erosion occurs when the

bottom shear stress τ[19] reaches the value required to mobilise those particles, known as critical shear stress τ_c, which depends on the particle properties and the sediment bed (Van Rijn et al., 1993; van Rijn, 1998). The critical shear stress of particles can be determined experimentally. The "Shields curve" (Shields, 1936) is often used to relate critical shear stress τ_c $[N \cdot m^{-2}]$ to the particle size D [m] or the particle Reynolds number Re_p $[-]$ (Chubarenko et al., 2018b). This curve is based on experimental tests on natural sediments and establishes the limit between "no motion" and "motion" (see the black line at Figure 11). The dimensionless shear stress parameter or Shield parameter θ $[-]$ relates to the shear stress τ_0 $[N \cdot m^{-2}]$ as

$$\theta = \frac{\tau_0}{(\rho_p - \rho_f)gD} \tag{7}$$

where ρ_p $[kg \cdot m^{-3}]$ is the particle density, ρ_f $[kg \cdot m^{-3}]$ is the fluid density and g is the gravitational acceleration $[m \cdot s^{-2}]$. The particle Reynolds number is defined as

$$R_p = \frac{u^* D}{\nu} \tag{8}$$

where u^* is the shear velocity [m/s] defined as $u^* = \sqrt{\frac{\tau_0}{\rho_p}}$ and ν is the fluid kinematic viscosity [m2/s]. Van Rijn et al. (1993) modified the Shield curve to a more specific curve that considers particle density, water density and water viscosity. Readers can refer to chapter 2.15 of this book for a detailed explanation of the theory and parameterisation of (sediment) erosion.

In a more recent experimental study, Waldschlager and Schuttrumpf (2019b) estimated the critical shear stress of 14 MPs with different shapes, density and sizes on different sediment beds (from fine sand to fine gravel, including mixing sediments), and tested the applicability of Shield diagram. Critical shear stresses ranged from 0.002 N/m2 (polystyrene spheres on a smooth bed, Di = 4.83 mm) and 0.233 N/m2 (pellets of polyethylene terephthalate on fine gravel, Di = 2.7 mm), depending on particle and sediment properties. Figure 11 compares the results of these experiments with the Shield diagram and shows that half of the MPs moves earlier than natural sediment would. Waldschlager and Schuttrumpf (2019b) also evidence the impact of sediment bed through the "hiding-exposure effect": larger particles on a bed of smaller grains are exposed and therefore are more likely to be eroded. Smaller particles on a bed of larger grains are less exposed and therefore more protected from erosion but, on the other hand, also have lower critical shear stress than the bed sediments and can be remobilised more easily than sediments. They proposed the following formulation that takes into account this effect and can be used to determine the critical shear stress of MPs on natural sediment:

$$\Theta_{c,i}^* = 0.5588\Theta_c^*(\frac{D_{50}}{D_i})^{-0.503} \tag{9}$$

where $\Theta_{c,i}^*$ is the critical Shields parameter of the MP [-], Θ_c^* is the critical Shields parameter of the sediment bed [-], D_i [m] is the MP diameter and D_{50} [m] is the median grain size of the sediment bed.

[19] Term defined in Section 2

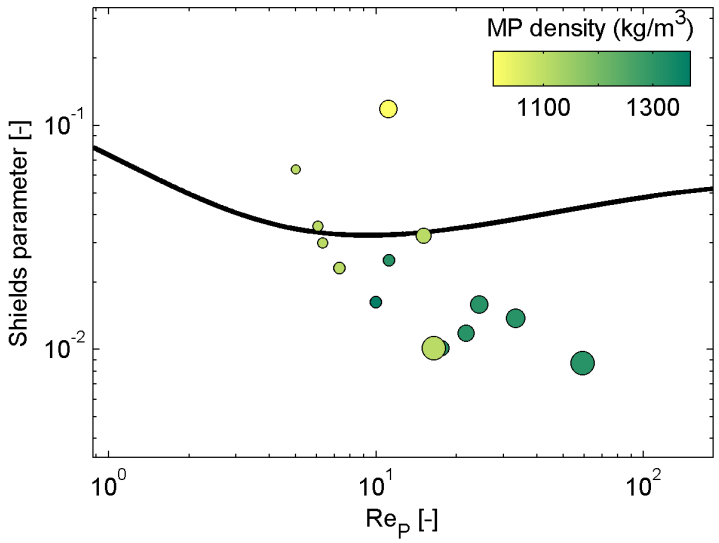

Figure 11: Results of the laboratory experiments carried out by Waldschlager and Schuttrumpf (2019b): dimensionless Shield parameter of different types of MPs as a function of their Reynolds number and comparison with the Shield curve (van Rijn formulation, black line). Circles size indicate the relative size of particles, which ranges from 0.75 mm to 5.04 mm (after Waldschlager and Schuttrumpf, 2019b).

MPs that remain on the bed can be buried by sediments and become part of the sediment bottom. The large presence of MPs observed at bottom sediment samples in estuaries, such as the Loire (Phuong et al., 2018), Seine (Gasperi and Cachot, 2021), Kwazulu-Natal (Naidoo et al., 2015), Ebro (Simon-Sánchez et al., 2019) and Pearl River (Fan et al., 2019)), is evidence of that. Key questions related to burial rates, the role of sedimentary processes on burying or the effect of the type of sediments needs future research. A relevant hypothesis is that the estuarine turbidity maximum[20] may have a key role in trapping MPs, as it favours flocculation of small particles (Section 4.3, Andersen et al., 2021) and is associated with fluid mud layers that can bury MPs. For example, a MPs monitoring campaign performed in the Seine estuary (Gasperi and Cachot, 2021) revealed that the most polluted bottom sediments were found at the location of the Estuarine turbidity maxima (ETM)[20].

5. Physical processes controlling the transport of microplastics

The physical processes that govern the fate of MP debris in estuaries are as varied as those for suspended sediments can be (e.g. Burchard et al., 2018; Dyer, 1995). Their accumulation in hot spots, flushing or trapping can depend on a plethora of hydrodynamic processes, and also on the physicochemical and mechanical properties of the MP discussed in the preceding sections. This section reviews some of the more prominent hydrodynamic processes for which there are signs that they may play a role in the transport of MPs in estuaries. They are schematised in Figure 12.

[20]Term defined in Section 2

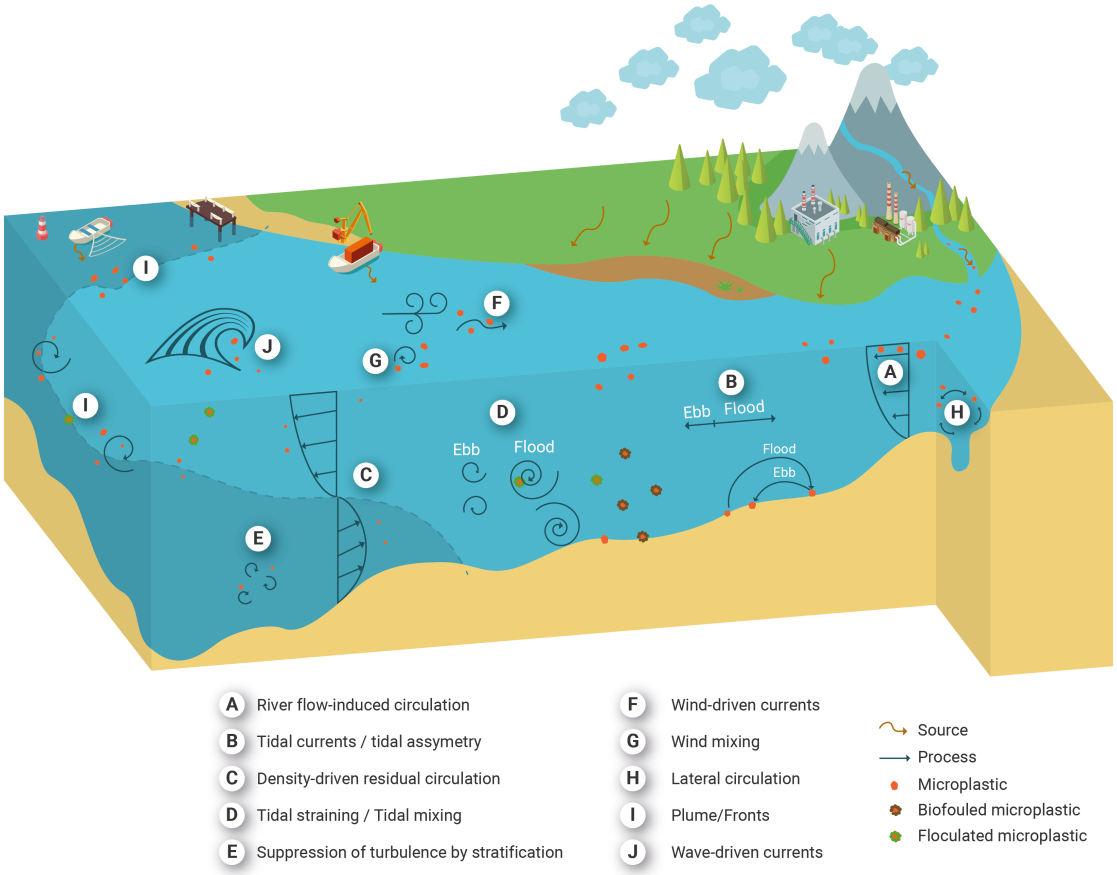

Figure 12: Sketch of different physical processes thought to be relevant in controlling the transport of MP in estuaries.

The relative importance of hydrodynamic processes in the transport of MPs depends on the particular biomorphological setting of the estuary and the spatio-temporal variability of marine, atmospheric and fluvial forcing. Although it is important to be aware that different processes operating at different scales may impact MP concentrations at other scales due to non-linear interactions, it is sometimes convenient to conceptually separate them into two temporal scales of variability: intratidal and subtidal (or tidally-averaged/residual[21]). On one hand, tidal variability mostly occurs at well-defined frequencies from approximately 1/25 to $1/6\,\mathrm{hr}^{-1}$ that can be precisely determined from the equilibrium theory of tides (Dronkers, 1964). Sometimes the term intratidal is used to refer to variations within a particular semidiurnal or diurnal cycle. Tidal variability in currents, elevations and other dependent variables can be modulated at spring-neap or equatorial-tropical cycles. On the other hand, subtidal variability occurs at frequencies lower than $1/25\,\mathrm{hr}^{-1}$. The terms tidal-averaged[21] or residual are often preferred to emphasise that this variability is of lower frequency than tides and emerges when averaging is applied to (e.g.) the current field. Tidal averaging is often necessary to understand the low-frequency variability in time series. Residual

[21]Term defined in Section 2

circulation can be induced by non-linearities in tidal propagation, tidal rectification processes, tidal and internal asymmetries, tidal pumping[22], Stokes drift[22], and changes in estuarine circulation[22]. The latter includes the influence of river flow, gravitational circulation, and wind-driven circulation, among others (Jay, 2010).

5.1. Tidal variability

Since tides are generated by the gravitational pull of the Moon and the Sun, tidal currents and elevations are usually expressed as a sum of harmonics with well-known frequencies (or periods T). The dominant circulation modes in mid-latitude estuaries are usually driven by tidal variability induced by diurnal (mainly $T_{\mathrm{K1}} = 23.93\,\mathrm{hr}$, $T_{\mathrm{O1}} = 25.81\,\mathrm{hr}$, $T_{\mathrm{P1}} = 24.06\,\mathrm{hr}$) and semidiurnal (mainly $T_{\mathrm{M2}} = 12.42\,\mathrm{hr}$, $T_{\mathrm{S2}} = 12.00\,\mathrm{hr}$, $T_{\mathrm{N2}} = 12.65\,\mathrm{hr}$) constituents. Diurnal constituents induce diurnal inequalities in tidal records and their superposition induces the 27.32 days equatorial-tropical variability. The superposition of the M2, S2, and N2 constituents yields spring-neap cycles, including the modulation of characteristic period 28.46 days due to the perigean and apogean tides caused by ellipticity of the lunar orbit (Dronkers, 1964). The superposition of diurnal and semidiurnal constituents alone defines to a larger extent the tidal range[22]. According to their tidal range, an estuary is termed microtidal when its tidal range is less than 2 m, mesotidal when it is between 2 m and 4 m, macrotidal when it is greater than 4 m, and hypertidal when it is greater than 6 m.

Tidal elevations, and particularly currents, also vary along the estuary. Tides transform in their propagation throughout the estuary depending on the balance between channel convergence/divergence and friction (e.g. Savenije, 2005). Channel convergence/divergence affects elevations due to mass conservation and hypsometry. It also affects tidal current due to channel narrowing or widening and dissipation. Friction increases with increasing velocity, shallower water columns and higher river discharge, thereby dissipating energy from the tide. If convergence effects exceed those of friction, the tidal range experiences an increase as the tidal wave propagates landward (hypersynchronous estuary). Where convergence and friction are balanced, the tidal range is expected to remain constant along the estuary. If friction overcomes convergence, the tidal range decreases as the tidal wave propagates landward (hyposynchronous). Notice that the dominant processes may change from stretch to stretch in an estuary, which allows a process-based zonation of estuaries. Moreover, the dominant processes may also change from spring to neap tides or from equatorial to tropical tides. The competing roles of channel convergence and friction may utterly drive subtidal movements, which in turn influence the long-term variability of estuarine suspended particulate matter such as MPs.

Although separately primary semidiurnal and diurnal harmonics are periodic in time, when combining a number of them, such as the M2, K1, and O1 constituents, asymmetrical low-frequency flow patterns can arise, driving a net residual transport (Hoitink et al., 2003). However, the most common form of tidal asymmetry is induced in shallow waters by nonlinear interactions between constituents. These interactions emerge from quadratic non-linearities in the tidal mass and momentum topographtion equations (Parker, 1991) and depend on several factors such as the bathymetry, the topography, the tidal regime and river discharge (e.g. Guo et al., 2015; Jalón-Rojas et al., 2018; Losada et al., 2017). Significant ebb-flood asymmetries can be observed in both elevation

[22]Term defined in Section 2

and current records when the tidal range is not vanishing relative to water column depth. Two primary waves propagating through a nonlinear system (and shallow estuaries indeed are) generate new harmonics with frequencies that are sums or differences of the primary frequencies, viz. overtides and compound tides, respectively. For instance, the mutual nonlinear interaction between M2 and the principal solar constituent, S2, produces, besides the overtide MS4 ($T_{\mathrm{MS4}} = 6.10\,\mathrm{hr}$), the fortnightly compound tide MSf ($T_{\mathrm{MSf}} = 14.76\,\mathrm{days}$). The interaction of the M2 with itself produces the overtide $T_{\mathrm{M4}} = 6.21\,\mathrm{hr}$. Other examples are the nonlinear interactions between diurnal or/and semidiurnal constituents that produce overtides that occur at periods $T_{\mathrm{SO3}} = 8.19\,\mathrm{hr}$, and $T_{\mathrm{MK3}} = 8.17\,\mathrm{hr}$. All of them produce asymmetries in the flow. Nevertheless, compound tides, due to their long periods, rather affect subtidal water levels (Buschman et al., 2009; Losada et al., 2017). Since the M2 is the most energetic constituent in many estuaries, ebb-flood asymmetry in levels and currents is usually described by the superposition of M2 and its first overtide M4 (Blanton et al., 2002; Friedrichs and Aubrey, 1988; Lanzoni and Seminara, 1998; Speer and Aubrey, 1985). If ebb-flood tidal asymmetry results in shorter but more intense floods and longer, weaker ebbs, there is a flood dominance. This typically occurs in estuaries in which tidal variations in channel depth are more important than variations in its width (i.e. channelised estuaries). In an estuary dominated by tidal variations in its width (i.e. estuaries that show large extensions of intertidal flats or marshes), low tide propagates faster, resulting in shorter falling tides and ebb dominance. Additionally, river discharge yields ebb-flood tidal asymmetry by dissipating tidal energy (e.g. Godin, 1991; Horrevoets et al., 2004), changing wave celerity (e.g. Godin, 1985; Losada et al., 2017), and enhancing overtides through the energy transfer from the principal bands to the lower and higher frequencies (e.g. Elahi et al., 2020).

5.2. Tidally-averaged variability

Overall, suspended particulate matter is not constituted by passive tracers, i.e., it does not respond instantaneously to flow oscillations, and it usually shows lags with respect to the flow. Lags can be produced by a variety of causes (Dyer, 1995), such as settling and deposition lags due to flocculation[23] (Section 4.3) and erosion lags due to critical shear stress (Section 4.4), with different processes being important for different particle types. Tidal asymmetry, for instance, may produce a residual transport of particulate matter even when there is no residual movement of water. In a flood-dominated estuary with no net residual movement of water, there would be neither residual movement of floating MPs (considering they are unaffected by wind). On the contrary, sinking MPs would be only transported landward during floods if the bed shear stress during ebbs does not exceed the critical shear stress.

Overall, lags yield non-zero temporal covariances between suspended particulate matter concentrations, water elevations, and currents, thereby producing a net residual transport (Burchard et al., 2018). Several authors have proposed different decompositions of the tidally-averaged[23](and depth-averaged or sectionally-averaged) transport to relate covariances between those variables with their lags, and thus identify the relevant underlying mechanisms that utterly control the transport (e.g. Dyer, 1988, 1995; Becherer et al., 2016; Díez-Minguito et al., 2014; Uncles et al., 1985). Although these studies focused on suspended sediments, transport mechanisms may be extrapolated to a certain extent to MPs. Transport induced by a non-zero temporal covariance between current and

[23]Term defined in Section 2

concentration is often referred to as tidal pumping[24] (Figure 13.a). This transport arises (e.g.) in a flood-dominated estuary in which higher suspended particle concentrations occur during floods than during ebbs. Transport associated with the covariance between current velocity and water depth (Figure 13.b) is commonly referred to as the Stokes[24] transport (e.g. Jay, 1991; Van Sebille et al., 2020). These mechanisms are known to be relevant in the MP transport in several estuaries, such as the Guadalquivir Estuary and the Garonne Tidal River, whose cases are discussed below. Also, tidal pumping seems to be relevant in the MP transport in the middle part of the Seine estuary (see Figure 10). The highest current velocity at mid-flood induces higher resuspension rates, higher vertical mixing, and thus higher concentrations of MP fragments at the lower layers of the water column. Microplastics are then transported further landward during floods and deposited at high-water slacks. Conversely, the weaker peak of MP fragments during ebb currents evidences lower rates of resuspension and subsequent lower seaward transport rates. Consequently, there is a net residual landward transport over each tidal cycle.

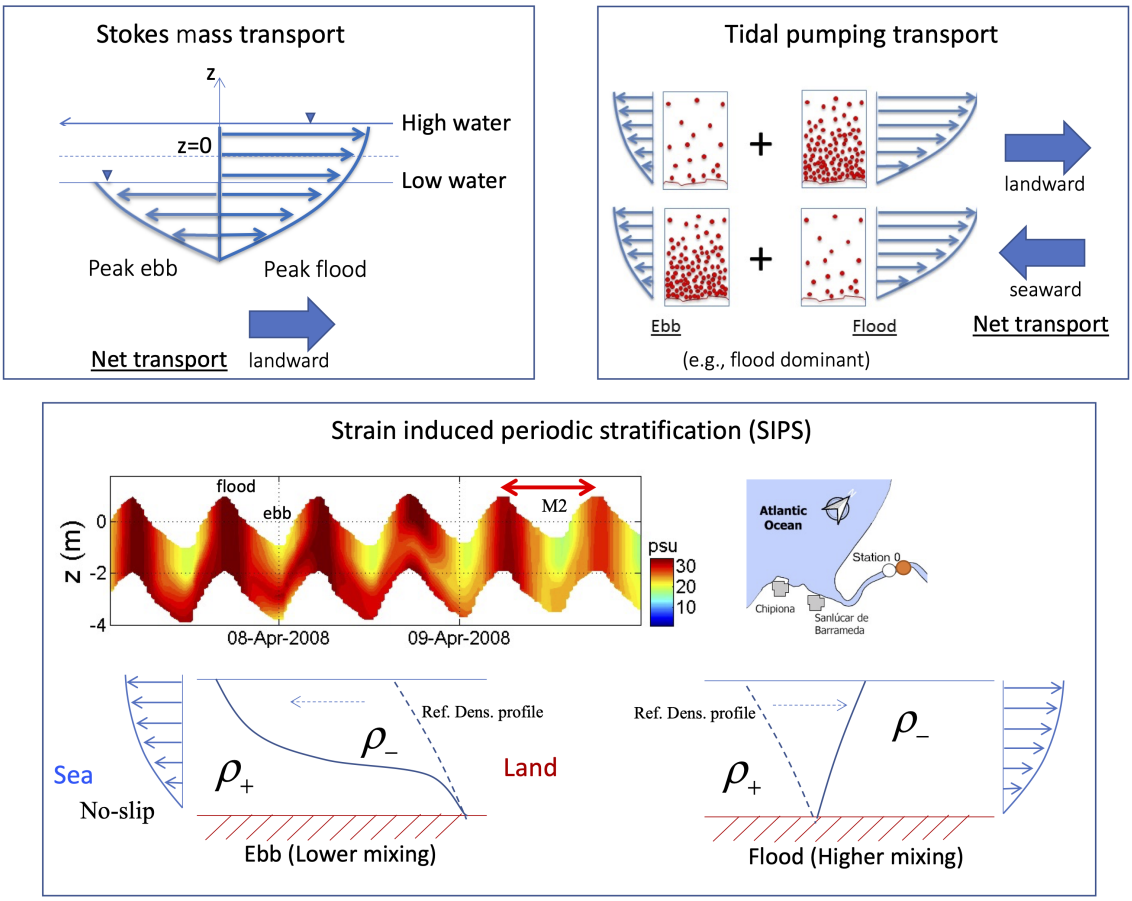

Figure 13: Panel a: Sketch of tidal pumping transport due to the covariance between current (blue arrows) and suspended particulate matter concentration (red dots). Panel b: Sketch of the Stokes mass transport induced by the covariance between current velocity and water depth. Panel c: Sketch of the strain-induced periodic stratification process associated with the strain of the density profiles by the vertically-sheared horizontal currents. Arbitrary current vertical profiles are sketched.

[24]Term defined in Section 2

5.3. Internal asymmetries

Internal asymmetry modes induced by vertically-sheared tidal currents contribute to the exchange flow[25]. Consider a positive (see below), stratified estuary with isopycnals tilted seaward. Flood currents, larger near the surface than near the bottom, tend to reduce the tilting of the isopycnals, thereby reducing stratification[25] and enhancing eddy viscosity. On the contrary, out flowing ebb currents strain the isopycnals increasing their tilting and, therefore, increasing stratification. If the tilting is strong enough, the increase in stratification may inhibit vertical mixing, thus reducing eddy viscosity. This process is known as tidal straining due to the effect of the alternate M2 current field in the isopycnals. The term Strain-Induced Periodic Stratification (SIPS) has also been coined for this process (van Aken, 1986; Simpson et al., 1990; Stacey et al., 1999), emphasizing that periods of high and low-density stratification occur at intratidal scale (Figure 13.c). SIPS is dynamically significant only for intermediate values of the Simpson number (Si approx. 0.2), which compares the effects on the strain of isopycnals with those of the turbulent kinetic energy (Geyer and MacCready, 2014).

This time-dependent eddy viscosity yields overall a non-zero covariance with the vertically-sheared horizontal velocity (Eddy viscosity-Shear COvariance, ESCO). This results in a new forcing that drives a residual contribution to the exchange flow that can affect the particle trapping inside the estuary (Jay and Musiak, 1994; Dijkstra et al., 2017). ESCO includes, as a particular case, tidal straining or SIPS. In fact, not only tidal straining produces a time-dependent eddy viscosity, but also (e.g.) river discharge and wind (Dijkstra et al., 2017). Moreover, the eddy viscosity does not have to be (intra-tidally) asymmetric to result in a residual circulation: this mechanism is present even for symmetric eddy viscosity. Also, the M2 eddy viscosity does not have to be the only one that produces a residual current. Any time-varying viscosity component results in a residual circulation if there is an associated velocity component (i.e., a non-zero ESCO between them).

5.4. Estuarine circulation and hot-spots of MP accumulation

The longitudinal salinity gradient that characterises any estuary produces a baroclinic pressure gradient force that drives the (subtidal) gravitational circulation[25] (Hansen and Rattray Jr, 1966). The longitudinal salinity gradient is normally maintained by freshwater inflows from the catchment to the estuary and wind and (mainly) tidal mixing, thereby yielding a salinity decrease from the ocean toward the head of the estuary. Estuaries presenting this salinity pattern are usually referred to as positive estuaries. In the case of inverse (or negative) estuaries, which may be typically found in arid or semiarid regions, the longitudinal salinity gradient inverts its sign because the salinity increases landward due to excess evaporation (e.g. Largier et al., 1996). An estuary may change from positive to negative behaviour seasonally (Largier et al., 1997). Whereas the river flow-induced circulation is directed seaward, the gravitational circulation (in positive estuaries) is characterised by a vertically-sheared longitudinal flow separated into two layers: a seaward flow near the surface and a deep water landward flow. The term density-driven circulation is employed when both river flow-induced and gravitational circulation are lumped together.

Surface local wind stress is potentially capable of also inducing a steady two-layer circulation, viz. wind-driven circulation, with near-surface flows moving in the wind direction and compensating

[25]Term defined in Section 2

flow near the bottom moving in the opposite direction (Hansen and Rattray Jr, 1966; Geyer, 1997). Wind-driven circulation plays a relevant role in the net flow in shallow-water estuaries, tidal flats and marshes, and rias, embayments and coastal lagoons subject to long-term wind systems (see Ría de Vigo study case). Nevertheless, not-fully developed wind-driven circulation in estuaries is more common than a steady one, and, if wind is highly variable, its contribution to the net estuarine circulation is usually overwhelmed by other mechanisms (Geyer and MacCready, 2014). Additionally, remote winds on the continental shelf change the water level near the mouth. This causes a set-up or set-down of the water level depending on the wind direction that also contributes barotropically to the net estuarine circulation (Garvine, 1985).

The estuarine circulation is known to be one of the main drivers of the formation of ETM[26] (e.g. Burchard et al., 2018). Relationships between estuarine circulation and the trapping and formation of Estuarine MP Maxima (EMPM)[26], i.e. hot-spots of MP accumulation within the estuary, are less commonly reported (e.g. Bermúdez et al., 2021; Díez-Minguito and de Swart, 2020). Besides tidal and internal asymmetries, convergent flows, either on the surface or near benthic layers, induced by the estuarine circulation and bathymetric features, are key to understanding the EMPM formation where trapping of both floating and sinking MPs occurs. Similarly, flow convergence also occurs in the edge of plumes and coastal fronts, contributing to the accumulation and trapping of floating debris (Van Sebille et al., 2020). Readers can refer to Chapter 2.11 of this treatise for a detailed description of coastal front dynamics. The estuarine circulation exerts a control over the salinity mixing and stratification[26], which in turn control the fluxes of salt within the estuary. Their combined influence determines the intensity of the exchange flow. In fact, according to their vertical salinity stratification, estuaries can be classified as salt-wedge and from strongly to weakly-stratified or well-mixed (more details in Section 6). Weakly stratified or partially mixed estuaries typically exhibit the largest exchange flows (e.g. Geyer and MacCready, 2014).

6. Case studies

Four case studies are presented to illustrate MP dynamics in different types of estuaries. These are the Garonne Tidal River (GTR), Guadalquivir River Estuary (GRE), Ría de Vigo (RV), and Adour Estuary (AE) (Figure 14). This selection covers a range of types of estuaries, from well-mixed to strongly stratified, according to the classification diagram of Geyer and MacCready (2014), which has become a standard estuarine parameter space, that is utterly based on the values of the principal forcing variables, i.e. the tidal velocity and the freshwater flow (Figure 14). Each case describes the estuary and methodological aspects. A discussion of the MP dynamics is provided, focusing on the physical processes and environmental conditions driving their transport, potential accumulation and flushing toward the ocean.

[26]Term defined in Section 2

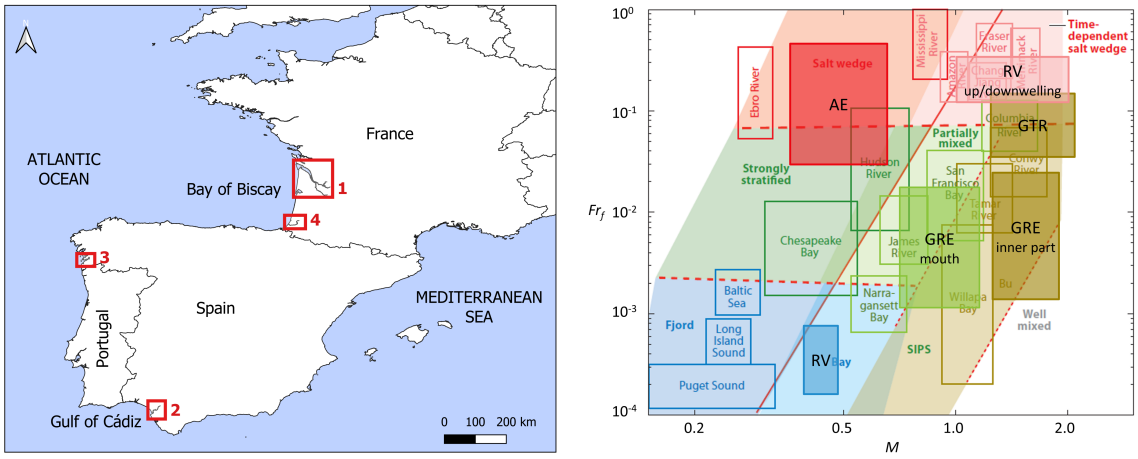

Figure 14: Left: Location of the case study sites analysed in this chapter: (1) The Garonne Tidal River, (2) The Guadalquivir River Estuary, (3) The Ría de Vigo Estuary, and (4) The Adour Estuary. Right: Mapping of the case studies in the Geyer and MacCready (2014) diagram. The nondimensional parameter M accounts for the vertical mixing, whereas Fr is the freshwater Froude number. RV estimates from Gilcoto et al. (2016), GRE estimates from Díez-Minguito and de Swart (2018), Adour estuary from Defontaine et al. (2019).

6.1. The Garonne tidal river

6.1.1. Site description

The Garonne Tidal River (GTR, SW France) is the upstream region of the Gironde-Garonne fluvial-estuarine system, located on the French Atlantic coast (Figure 15 a). It extends over 95 km between the Gironde estuary, at its confluence with the Dordogne River, and the limit of tidal influence. The Garonne river discharge varies seasonally, with maximum (up to 4720 m^3/s) and minimum values (up to 50 m^3/s) in winter and summer, respectively (data for 2005-2014; Jalón-Rojas et al. (2015)). GTR is macrotidal, with tidal ranges from 4 to 6.2 m at the rivers confluence (Jalón-Rojas et al., 2018). Tidal range[27] and current velocities increase toward the land over 60 km from the confluence of the rivers due to the convergent width (hypersynchronous behaviour), and rapidly decrease in the narrow upstream sections because of frictional dissipation (hyposynchronous behaviour). Tides and tidal currents are strongly asymmetrical, characterised by longer falling durations and greater maximum flood currents (flood dominance). This tidal asymmetry increases up-river due to the nonlinear effects of bottom friction and river discharge (Jalón-Rojas et al., 2018).

Although salinity intrusion has been observed at the lower reaches of the GTR during dry summers (Schmidt, 2020), the tidal river is hardly affected by salinity-induced density gradients and can be classified as well-mixed. Tidal pumping[27] is the main mechanism leading to landward transport and accumulating sediments in a pronounced ETM[27] (Jalón-Rojas et al., 2015, 2021).

To this day, there are no observational studies of MP pollution in the GTR. However, de Carvalho et al. (2021) have quantified the MP concentrations (size range 700 μm – 5 mm) in surface water at 14 sites across the Garonne river catchment, upstream of the GTR. Microplastic concentration averaged 0.15 items $\cdot$ m^{-3}, ranging from 0 to 3.4 items $\cdot$ m^{-3}, and showed a strong seasonal and spatial variability concentration. The level of urbanisation mainly influenced the spatial variability and

[27]Term defined in Section 2

hydrological condition drove the temporal variability, with higher concentrations in urbanised areas and warm seasons with low discharge. Furthermore, observational surveys of marine macrodebris at the Bay of Biscay highlighted peaks of debris abundance near the mouth of the Gironde estuary in winter (Galgani et al., 1995). Therefore, the GTR seems to be a significant pathway of debris and MPs to the Atlantic French coast.

6.1.2. Methods

The modelling framework iFlow (Dijkstra et al., 2017; Brouwer et al., 2018) was applied to explore the relative distribution of different types of MPs along the GTR and the underlying physical processes contributing to their longitudinal transport. iFlow is an idealised width-averaged 2DV model that uses a simplified description of the geometry and physical mechanisms (Figure 15.b), allowing for the systematic analysis of flow and sediment transport in single-branch estuaries and tidal rivers. The model is forced by an M2 tide and an M4 tide at the mouth ($x = 0$, Figure 15.b) and a constant river discharge at the landward boundary ($x = L$, Figure 15.b). The implementation of iFlow to the GTR published in Jalón-Rojas et al. (2021) was used to study sediment transport (morphology and forcings for the year 2014; domain highlighted in Fig 15.a). This implementation was fully validated for the hydrodynamics. The transport module has been extended here to study MP transport by including state-of-the-art vertical velocity parameterisations: Waldschlager et al. (2020) for spheres and fibres and Dioguardi et al. (2018) for sheets (see Section 4.3). Readers should refer to Dijkstra et al. (2017) and Jalón-Rojas et al. (2021) a detailed description of iFlow and the model settings of the GTR implementation, respectively.

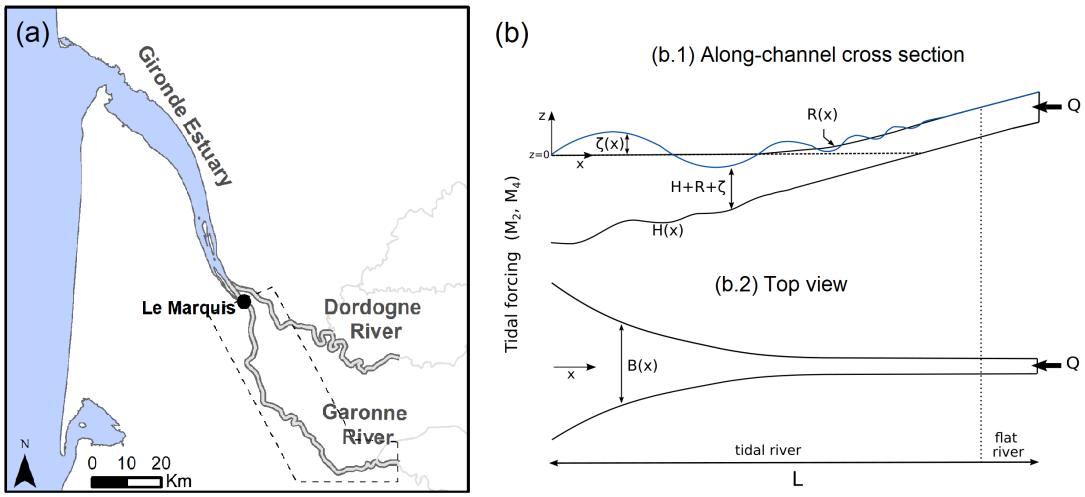

Figure 15: (a) Map of the Gironde-Garonne fluvio-estuarine system. Dotted lines delimit the model domain. (b) Geometry of the tidal river in the idealiszed model (After Jalón-Rojas et al., 2021).

The present application represents an exploratory implementation of iFlow to the study of MP transport in estuaries, particularly at the GTR. Six scenarios are presented. They combine: two contrasted hydrological conditions - low ($200\,\mathrm{m^3 s^{-1}}$) and moderate ($675\,\mathrm{m^3 s^{-1}}$) river discharge - during spring tides, and three types of particles:

(i) Particles with neutral buoyancy[28] ($w_s = 0\,\mathrm{mm \cdot s^{-1}}$), which englobe (1) MPs with a density similar to that of water, and (2) MPs with a polymer[28] density lower to that of water whose global density has increased up to get a neutral buoyancy due to biofouling.

(ii) Negative buoyant particles with a very small settling velocity ($w_s = 0.5\,\mathrm{mm \cdot s^{-1}}$), similar to that of the finest sediments presented in the estuary (Defontaine et al., 2023). This category also represents particles that start to fall down due to biofouling (Sections 3.4 and 4.3)

(iii) Negative buoyant particles with a small setting velocity ($w_s = 2\,\mathrm{mm \cdot s^{-1}}$), characteristic of polyester microfibers ($1 - 5\,\mathrm{mm}$) from fishing nets (Jalón-Rojas et al., 2022). This category may also represent flocs of small microplastics and sediments (Sections 3.3 and 4.3).

A complete assessment of MP dynamics should include a larger range of hydrodynamic conditions and types of plastics. However, as discussed in Section 6.1.3, these scenarios already provide a good picture of the mechanisms driving MP dynamics in the GTR. Other than settling velocity, the calibration of the transport module needs to provide the value of surface MP concentration at the lower boundary $c_{x=0}$. Due to the lack of data, this parameter could not be derived. Therefore, only the ratio of the tidally-averaged[28] (residual) concentration $c/c_{x=0}$ is shown (i.e. $c/c_{x=0} = 1$ at $x = 0$), allowing us to evaluate the relative distribution of MPs along the longitudinal axis.

6.1.3. Microplastic dynamics

Figure 16 illustrates the longitudinal distribution of the depth-averaged residual concentration $c/c_{x=0}$ (Fig. 16.i), and the normalised transport capacity[29], together with the different physical mechanisms contributing to it (Figure 16.ii-iv), for the three types of particles and the two river discharges considered. Readers may refer to Dijkstra et al. (2019) and Jalón-Rojas et al. (2021) for a full description of each of the physical mechanisms contributing to transport derived from iFlow. Positive and negative values of transports denote upstream and downstream transport capacity, respectively; the zero-crossing from positive to negative corresponds to convergence zones and potential hot-spots of MPs.

According to the simulations, neutrally buoyant particles ($w_s = 0\,\mathrm{mm \cdot s^{-1}}$) are completely flushed downstream the GTR, toward the Gironde estuary, for both low and moderate river discharges ($c/c_{x=0} = 0$, Figure 16.i). For both hydrological conditions, the main physical processes driving the seaward transport are river-induced flushing of MPs (river-river component) over the upper 30 km, and tidal-river interactions (river component) over the lower 70 km (e.g. tidal asymmetry caused by the tide-river interaction and river-induced flushing of tidally resuspended MPs) (Figure 16.ii). These results are transferable to higher river discharges and positive buoyant particles, which would also be flushed out by river-induced fluxes.

[28] Term defined in Section 2

[29] The MP transport that occurs when there is an abundance of MPs Dijkstra et al. (2019)

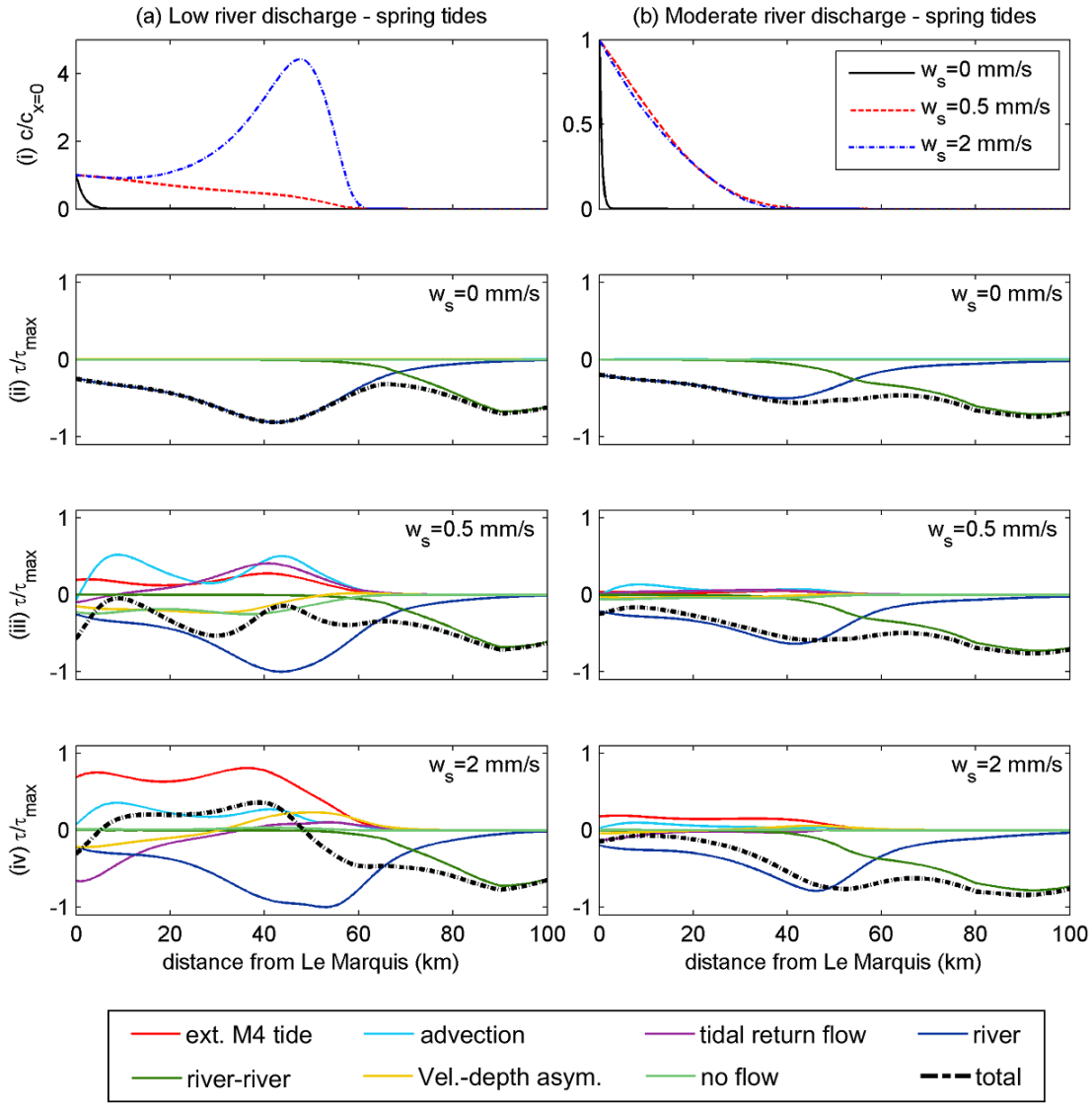

Figure 16: (i) Tidally- and depth-averaged $c/c_{x=0}$ over the GTR and (ii-iv) contribution of the different physical mechanisms to the MP transport capacity per meter width (and integrated over depth) during low (a, $200\,\mathrm{m^3 s^{-1}}$) and moderate ($675\,\mathrm{m^3 s^{-1}}$) river discharge and spring tides for three types of particles: (ii) $w_s = 0\,\mathrm{mm \cdot s^{-1}}$; (iii) $0.5\,\mathrm{mm \cdot s^{-1}}$; (iv) $2\,\mathrm{mm \cdot s^{-1}}$. Negative values indicate export, while positive values indicate import. The total net transport of all terms is plotted in a black dashed line.

These two river-related contributions also are the dominant mechanisms influencing the (seaward) total transport capacity of the two types of negatively buoyant particles during moderate river discharge (Fig 16.iii.a and Figure 16.iv.b). As a result, the potential presence of particles is limited to the vicinity of the GTR mouth, with a relative distribution of MP concentration $c/c_{x=0}$ decreasing from 1 to 0 over the lower 20 km (Figure 16.i.b). For low river discharge, the river-related seaward contribution is balanced by components leading to MP import, in particular the tidal asymmetry caused by the M2 and M4 tides entering the tidal river (external M4 tide), the tide-averaged effect of advection of MPs and, for the scenario $w_s = 0.5\,\mathrm{mm \cdot s^{-1}}$, also the contribution of the Stokes

drift[30] and the corresponding return flow (tidal return flux) (Figure 16.iii.a and 16.iv.b). The river contribution is dominant for particles with $w_s = 0.5\,\mathrm{mm \cdot s^{-1}}$, and the total transport is directed downstream. Consequently, the relative distribution of MP concentration $c/c_{x=0}$ decreases very gradually from 1 to 0 over the lower 60 km (Figure 16.i.a). For particles with $w_s = 2\,\mathrm{mm \cdot s^{-1}}$, the tidal asymmetry caused by tidal forcing is the dominant mechanism at the lower reaches. A convergence point appears indicating the trapping of MPs in a EMPM[30] at 45 km from the GTR mouth, with average concentrations up to 4.5 times higher than at the GTR mouth.

In conclusion, river flow-induced circulation and tidal-river interactions are dominant processes for the transport of: (a) positively and neutrally buoyant particles for all the hydrological conditions; (b) particles with slight negative buoyancy for moderate and high river discharges. Tidal asymmetry caused by M2 and M4 tides entering the GTR from the Gironde estuary is the main process inducing the trapping of negatively buoyant particles such as fibres from fishing nets and flocs of small microplastics and sediments in the GTR. Denser particles tend to fall near the sources and be locally resuspended near the bottom layer (see Adour Estuary case in 6.4) or be transported by bed load transport. Finally, it should be noted that this model study is highly idealised and includes simplified representations of geometry, bed friction, eddy viscosity and, consequently, some physical processes. Observations of MP concentrations are also needed to validate these trends. Even if results should be interpreted with caution, this study provides fresh insight into the main mechanisms that potentially affect MP transport in a well-mixed macrotidal tidal river such as the GTR.

6.2. The Guadalquivir River estuary

6.2.1. Site description

The Guadalquivir River Estuary (GRE) is a prototype of a well-mixed, narrow estuary. It is located in the SW part of the Iberian Peninsula (Figure 17), and extends about 110 km from its mouth, which opens to the Gulf of Cádiz (Atlantic Ocean), to the head dam at Alcalá del Río (Figure 17). The tidal river part comprises its last stretch, approximately from Seville to Alcalá del Río. The climate in the river catchment is mostly Mediterranean, which yields freshwater pulses typically occurring during the wet season (October-April), after periods of (normal) low river flows. Freshwater discharges from the head dam are usually below $40\,\mathrm{m^3 s^{-1}}$. Tides are mesotidal and semidiurnal. Different processes control the tidal propagation in the GRE (Díez-Minguito et al., 2012). In the lower part of the estuary, tidal amplitudes decrease upstream (hyposynchronous). In the middle part of the estuary, channel convergence and friction seems to be in balance. In the tidal river part, the estuary is hypersynchronous: reflection at the head dam and channel convergence overcome the effects of friction on the tidal propagation. The estuary is flood-dominated, thereby exhibiting shorter, more intense floods and longer, weaker ebbs. Despite GRE exhibits a reduced primary production because of the high suspended sediment concentration (Ruiz et al., 2017) and present socio-economic issues regarding the exploitation of the resources the estuary provides (Ruiz et al., 2015; Llope, 2017), it still constitutes a highly valuable ecosystem that has been identified as a key nursery area for many marine fish and crustacean species (González-Ortegón et al., 2015).

[30]Term defined in Section 2

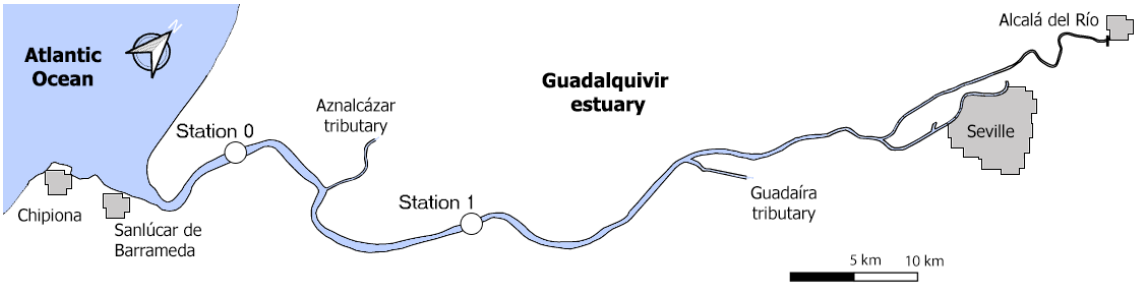

Figure 17: Map of the Guadalquivir River Estuary including the MP sampling sites (circles; Stations 0 and 1).

6.2.2. Methods

The MP dynamics in the GRE discussed below is mainly based on the joint analysis of field data, laboratory-processed samples, and idealised modelling output.

Samples of plastic debris inside the estuary were obtained from an still ongoing long-term ecological research program (e.g. González-Ortegón et al., 2012). This research program consisted of monthly field campaigns in the lower and middle part of the GRE under different runoff, salinity and precipitation conditions. Samples were collected at maximum flood and ebb on a lunar monthly basis from 2014 at Stations 0 and 1 (Figure 17) from a boat anchored to the bottom and equipped with three large manta nets. The concentration and basic properties of MPs were determined from the samples. Subsequent sieve separation, dissection by a stereo microscope, and Fourier Transform Infra-Red (FTIR) spectroscopy laboratory analyses of the samples were performed. The plastic nature of 94.3% of the particles were confirmed and plastic items were thus classified (Bermúdez et al., 2021).

Between 2008 and 2011, another extensive monitoring program was carried out in the GRE by the installation of a remote real-time monitoring network, involving acoustic Doppler current-metres, CTDs, turbidimeters, and tidal gauges that were installed close to the main axis of the navigation channel (details of the equipment and locations of the instrumentation can be found in Navarro et al., 2011). The potential physical processes affecting the MP transport are discussed from the field data produced by this monitoring network.

Regarding the idealised modelling approach, Bermúdez et al. (2021) discussed the relative influence of the river discharge, tidal straining, the density-driven, and the wind-driven circulation on the MPs distribution infered from the monitoring program by González-Ortegón et al. (2012). The model was based on a tidally-averaged 2D model that can be seen as a simplified version of the iFlow model described in Section 6.1.2 (Dijkstra et al., 2017). Model output analyses also complete the conclusions drawn from the analysis of hydrodynamic field data from the monitoring network by Navarro et al. (2011).

6.2.3. Microplastic dynamics

Similarly to what occurs in many estuarine systems, studies regarding MP pollution within the GRE are still scarce to have a full picture of the spatio-temporal variability of MP concentration and unambiguously trace MPs back to their sources. Nevertheless, there are a few notable exceptions. López-López et al. (2011) identified the urban area of the city of Seville, which hosts over 1 million inhabitants, the minor tributary river Guadaira, and the agricultural activities carried out in the

middle part of the GRE as main pollution inputs to the estuary. These authors did not explicitly consider pollution due to MPs, although a substantial contribution of MPs to the estuary is expected from these sources. First assessments of the abundance of MPs in the Gulf of Cádiz pointed to the GRE as one of the greatest contributors of MPs and suggested focusing future monitoring efforts in this area (Quintana Sepúlveda et al., 2020). Bermúdez et al. (2021) also pointed to urban activity and the intense agricultural activity developed in the Guadalquivir River catchment and near the margins of the estuary itself as potential sources that would explain the temporal variability of MP items in water samples. In fact, plastic sheeting over crops near the estuary covers nearly 8000 ha. The observed temporal variability in the number concentration of MP items showed a positive relationship with local rainfall events when there were no significant discharges from the head dam at Alcalá del Río. The predominant MPs types identified in the samples were low-density polyethylene film-type particles, most likely derived from bags and flexible packaging, according to these authors. González-Ortegón et al. (2022) reported on MP concentration values along the inner and outer shelf of the Gulf of Cádiz. These authors found the highest concentrations of MPs near the mouths of the Guadiana and Guadalquivir estuaries, showing concentrations of 64.6 and 130.5 $\mathrm{mg} \cdot \mathrm{m}^{-3}$, respectively. Specifically, values obtained near the GRE mouth represented approximately 8 times the mean MPs concentration along the continental shelf. They identified irregular shaped items like brittle fragments and films, which apparently agrees with observed shapes within the estuary by Bermúdez et al. (2021) and also seems to corroborate the hypothesis of an estuary acting as a significant source of MPs to shelf waters.

Regarding the processes controlling the MP longitudinal transport in the GRE, combined approaches of observations and modelling are showing promising results. Bermúdez et al. (2021) analysed MP items in water samples acquired during spring tides at two locations in the lower part of the GRE (Stations 0 and 1 in Figure 17). The analyses allowed the authors to validate a model in order to quantify the along-estuary transport and identify potential hot-spots of MPs (EMPM[31]), as well as estimate the relative influence of density-driven, wind-driven, and tidal straining circulation on the EMPM formation. According to the observed types of MP, these authors chose a rising velocity of 4.6 $\mathrm{mm} \cdot \mathrm{s}^{-1}$, typical for polyethylene film-type particles of 2.3 mm (Waldschlager et al., 2020).

[31] Term defined in Section 2

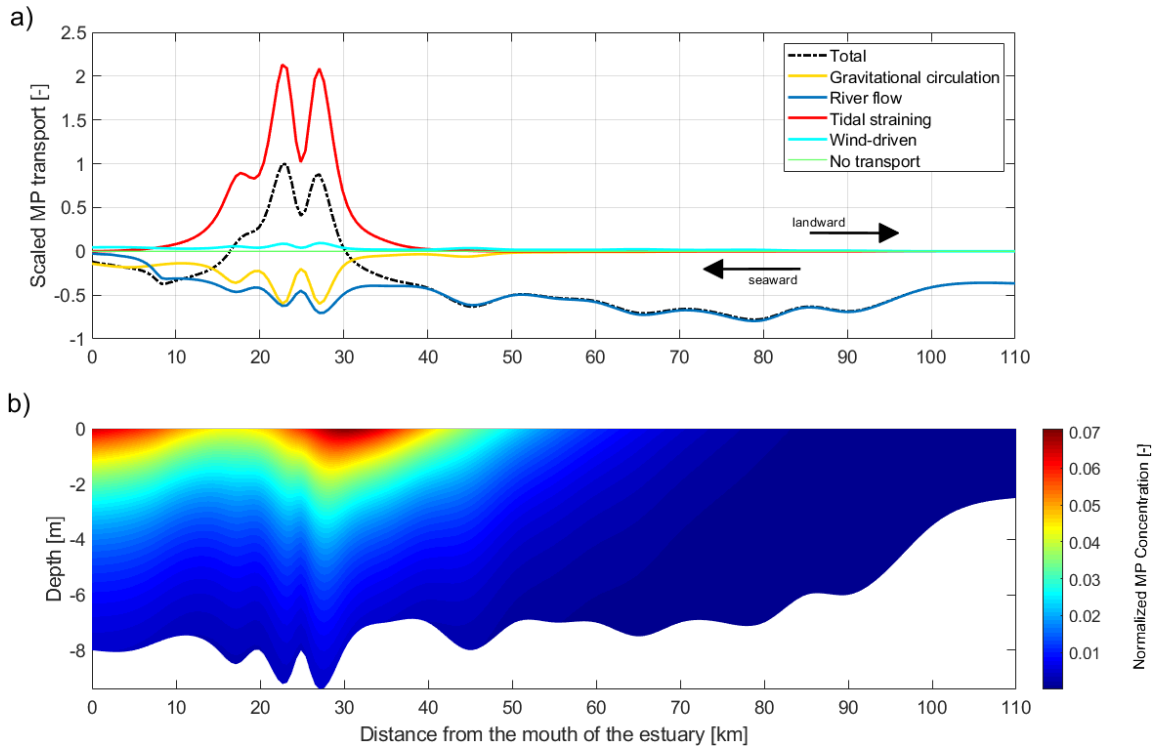

Figure 18: Panel a: Net transport of MPs (black dot line curve), which is comprised by the superposition of the gravitational circulation (yellow curve), river flow (blue curve), tidal straining (red curve), and wind-induced transports (blue curve). Black arrows indicate the transport direction. Panel b: colour plot of the 2DV normalised suspended MP concentration for normal conditions in the GRE.

The modelling results showed that the (local) wind-induced circulation within the estuary seems to be negligible, at least compared to the other contributions (Figure 18.a). The river flow dominates the circulation in the upper half of the estuary, thereby inducing a unidirectional residual down-estuary flow. On the seaward side of the estuary, the density-driven flow controls the circulation near the mouth. This is induced by a (classical) exchange flow[32]. Where the salinity gradient is higher during normal conditions of river flow, between km 10 and 40, the gravitational circulation contribution is larger. Despite of that, the circulation is dominated in that stretch by the tidal straining contribution, which apparently opposes the gravitational circulation. The net circulation is thus mostly comprised by the sum of the last three contributions, yet modulated by bathymetry as shown in Figure 19, panel b.

Modelled vertical distribution of MPs inside the estuary (Figure 18.b) shows that the highest concentrations are obtained near the surface, as expected for positive buoyancy[32], low-density particles. However, non-zero concentrations are obtained throughout the whole water column due to turbulent tidal mixing, which is quite intense in the GRE. Bermúdez et al. (2021), following Chubarenko et al. (2018b), indicated that, during both ebbs and floods, tidal shear stress[32] is high enough to entrain sinking MPs into the flow. The particular features of the vertically-sheared along-channel fluxes allowed estimating the 2D equilibrium distribution of PE film MPs in the

[32]Term defined in Section 2

GRE, which typically will tend to concentrate in the areas of flux convergence (Figure 18.b). The distribution of low-density MPs concentration showed that a minor secondary EMPM was located near the mouth, thereby indicating that a portion of items is being flushed out by the flow. The highest amount of items per unit volume (primary EMPM) were attained more up-estuary but still in the lower part of the estuary, around km 25, where the convergence of MP transports yields the trapping of MPs. This formation of an EMPM indicates that not all the low-density MPs may be flushed out of the estuary. The accumulation of low-density MPs near the ETM increases their residence time and thus their chance to be trapped in tidal flats together with sediments or, even more efficiently, by vegetation, due to windage or residual lateral circulation.

Remarkably, this EMPM occurs almost at the same location as one of the ETM[33] reported by Caballero et al. (2014) and Díez-Minguito et al. (2014). Figure 19 shows Hovmöller diagrams of the total transport comprised by the non-tidal, Stokes[33]', and tidal pumping[33] transports (panel a, and subpanels) and of the turbidity field (panel b). These transports, which were identified by Díez-Minguito et al. (2014) as the main drivers of the sediment transport in the GRE, explain the ETM formation. By analysing the tidally-averaged[33] and depth-integrated suspended sediment fluxes over time and space determined from observations, Díez-Minguito et al. (2014) pointed out the mean advection, the tidal pumping associated with the covariance between suspended sediment concentration and current, and the tidal Stokes transport as the main mechanisms that contribute to longitudinal transport, and the formation of ETM in the GRE (Figure 19.a and subpanels a1, a2, and a3). The convergence of upstream and downstream net transports (downward zero-crossings), explains the presence of the secondary turbidity maximum located at 35 km (Figure 19.b). Díez-Minguito et al. (2014) also computed the transports due to the M4 current-concentration interaction and the M2 constituent alone. They found that the locations of the ETM coincide well with the downward zero-crossings of the M2 and M4 induced transports, thereby concluding that the trapping of suspended sediment near the ETM is thus a balance between the M2 and M4 residual transports. These transports are main contributors to the tidal pumping. This may suggests that tidal pumping associated with the covariance between longitudinal currents and suspended MP concentrations is another relevant mechanism to be considered in the formation of EMPM in the Guadalquivir estuary. In fact, the occurrence at the same locations of ETM and EMPM seems to be a feature that is also observed in other estuaries (e.g. Cohen et al., 2019).

[33]Term defined in Section 2

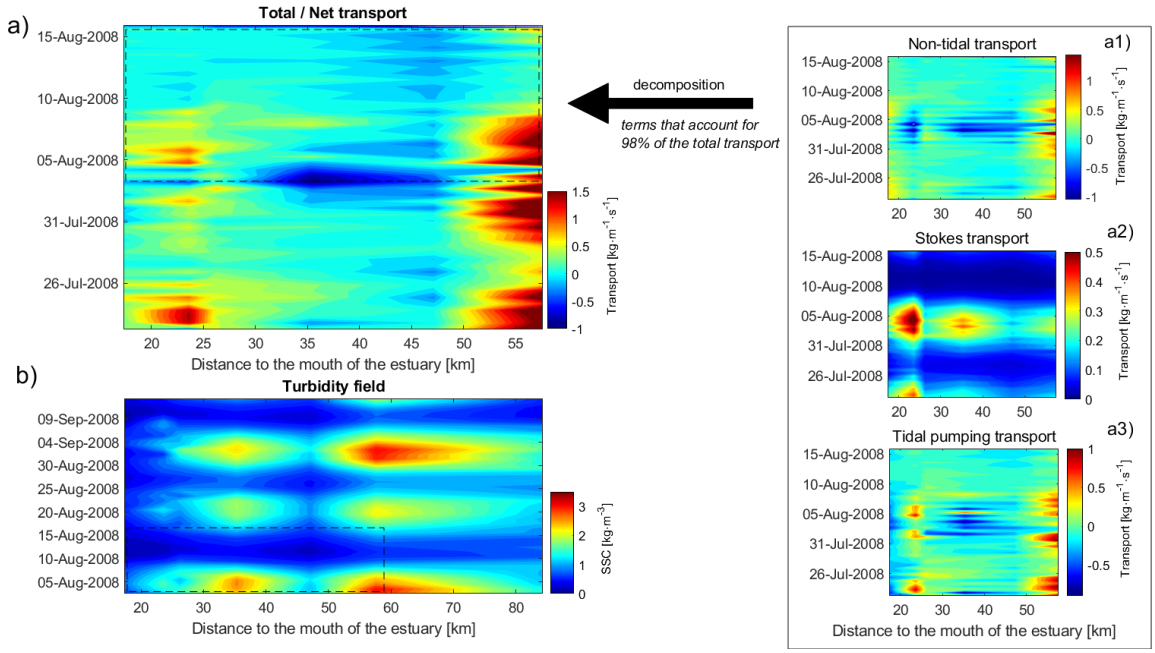

Figure 19: Hovmöller diagrams. Panel a shows the spatio-temporal variability of the along-channel total transport comprised by the non-tidal (panel a1), Stokes' (panel a2), and tidal pumping (panel a3) transports. Panel b shows the spatio-temporal variability of the suspended sediment concentration. Dashed boxes indicate the shared areas of between the Hovmöller diagrams in panels a and b.

6.3. Ría de Vigo

6.3.1. Site description

The Ría de Vigo is a mesotidal and partially mixed estuary located on the west coast of Galicia (NW Spain) with a SW-NE orientation. The total surface of the estuary is approximately 176 km^2, with a length of 35 km and a width ranging from 15 km at its mouth and 600 m at Rande Strait (Figure 20). Along-channel mean-depth is about 30 m, with its maximum near the mouth (40 m). The main river that flows into this estuary is the Oitavén-Verdugo River, with an average annual discharge of 17 $m^3.s^{-1}$. This estuary is part of a coastal upwelling ecosystem at the eastern North Atlantic. Upwelling-favourable northerly winds prevail during the spring-summer months (April to September), while downwelling-favourable southerly winds dominate the rest of the year (Álvarez-Salgado et al., 2001). During upwelling episodes, the northerly winds exert southward surface stress causing an Ekman transport offshore. The displaced surface water is replaced by the Eastern North Atlantic Central Water, colder and nutrient-richer, and the positive estuarine circulation[34] is enhanced. The runoff of rivers is very low during this period, so vertical gradients of salinity are weak. In contrast, thermal stratification[34] is generally weak in winter, when density differences are controlled by salinity rather than temperature. The upwelling dynamics contribute to high primary production rates in the estuary, which allow an important shellfish exploitation activity. It is also an area of high ecological value. The Cíes Islands, located in the mouth of the estuary, are part of the maritime-terrestrial Natural Park of the Atlantic Islands of Galicia. The estuary is, however, also subject to intense human pressures, as it is a very industrialised and populated zone. The city of

[34]Term defined in Section 2

Vigo is the main urban area, with $\sim 294,000$ inhabitants. The Vigo WasteWater Treatment Plant (WWTP), with a mean discharge rate of $4\,\mathrm{m}^3.\mathrm{s}^{-1}$ ($8\,\mathrm{m}^3.\mathrm{s}^{-1}$ peak rate), and the Port of Vigo, one of Europe's most important fishing ports, are suspected to be major inputs of MPs into de estuary.

Carretero et al. (2022) conducted the main observational study of MP abundance in the Ria, which analysed the concentration, size, shape and polymer[35] composition in the surface waters of three sampling stations monthly during 2017 (see Figure 20). The MP concentration values found ranged from 4.91 to $52.0\,\mathrm{items}\cdot\mathrm{km}^{-2}$. The largest observed fraction of MP corresponded to fibres (81%), followed by plastic paint sheets (11%). Fibres were suspected to enter the marine environment from the Vigo WWTP. Paint particles, an often overlooked component of MPs (Turner, 2021), pointed to fishing and port activities, particularly boats and vessel cleaning.

Figure 20: (a) Map of the Ría de Vigo estuary showing the main rivers that flow into the estuary, the Cíes Islands (National Park) and main urban areas (in grey), the location of the discharge of the wastewater treatment plan of Vigo (black star), the cross-sections of the numerical model (dotted lines) and the position of the sampling stations.

6.3.2. Methods

Díez-Minguito et al. (2020) developed an idealised tidally-averaged 2D model of the Ría de Vigo to explore the distribution of patterns of MPs during upwelling and downwelling conditions and to elucidate the relative importance of the local wind-driven circulation, the density gradient and the river discharge. The model is width-averaged and considers a simplified description of the geometry based on the cross-sections depicted in Figure 20. It is forced with a freshwater discharge at the landward boundary, as well as an along-estuary density gradient and wind profile. Microplastics are passively transported by the water flow and dispersed by turbulent mixing, and are characterised by a terminal velocity. Pellets, fibres and fishing line cuts, having both positive and negative buoyancy ($-20 < w_s < 20\,\mathrm{mm}\cdot\mathrm{s}^{-1}$), were the types of MPs considered.

On the other hand, Sousa et al. (2021) used a more complex numerical model, based on Delft3D modelling framework, to identify the travel path and distribution of plastics from WWTPs sources

[35]Term defined in Section 2

in the Ria. The 3D flow patterns computed with the hydrodynamic Delft3D-FLOW module were fed into the particle-tracking module Delft3D-PART. Microplastics were represented in the model by virtual passive particles floating on the water surface, whose transport is influenced by advection, diffusion and setting velocity. Polypropylene microplastics of 2.5 mm in length and $900\,\mathrm{kg}\cdot\mathrm{m}^{-3}$ in density were considered. A first set of simulations consisted of a 35-day run with a continuous and constant release of MPs from the WWTPs during the first 30 days. The concentration of particles was then analysed in a series of points along the Ría coastline. In the second set of simulations, instantaneous releases at specific tidal conditions (ebb or flood phase, during neap or spring tides) were considered to evaluate the tidal influence in the distribution of particles.

It is also worth noting that the field-based study of Carretero et al. (2022) spanned a whole year, and therefore, stations were sampled under very different hydrodynamic conditions in the Ria. The results could potentially show temporal variations at an annual scale that could, in turn, be related to the underlying hydrodynamic drivers. However, limited insights were gained in this regard due to high seasonal variability that was observed due to the winds, the rivers runoff, the sampling stations, the upwelling/downwelling periods, or the industrial activities in the Ría de Vigo. Therefore the results of this work are not discussed in the following.

6.3.3. Microplastic dynamics

The idealised model simulations of Díez-Minguito et al. (2020) showed the dominant role of the wind-induced and the gravitational circulation in the distribution of MPs, and the minor contribution of the river-induced circulation, during both upwelling and downwelling conditions. The competition between these two flows mainly controls the location of the EMPM[36]. During upwelling conditions, floating MP tend to be flushed out of the estuary (Figure 21.b), whereas sinking MPs remain trapped inside (Figure 21.c). Downwelling conditions lead to a landward displacement of floating MPs in the lower part of the Ría, where the wind effect opposes and normally exceeds that of the density gradient. A significant fraction of MPs thus remains trapped near the Rande Strait (Figure 20). The wind-induced flow also leads to a seaward displacement of MPs near the bottom (Figure 21 f). However, a significant fraction of MPs remains trapped near the head due to the gravitational circulation (Figure 21 f).

The analysis of MPs trajectories from the Vigo WWTP conducted by Sousa et al. (2021) detected the highest concentrations of MPs on the southern shore on the estuary and near the WWTP discharge point, and the lowest concentrations in the inner part of the estuary. The tidal conditions during the emission of MPs were found to be a key driver for MP transport and fate. During spring tides, the percentage of MPs that crosses the estuary mouth ranged from 25% (emission of MPs during flood) to 45% (emission during ebb), reaching open sea after 5 days 11% and 21% of the MPs, respectively. It is worth noting that a significant proportion of MPs (24%) remained around the Natural Reserve of Cíes Islands during ebb conditions. During neap tides, MP movement in the longitudinal direction of the estuary appears to be very limited, and the percentage of MPs that crossed the estuary mouth was small both under flood and ebb tides (3.7% and 5%, respectively). In this scenario, a significant fraction of MPs appears to move in the estuarine transverse direction and reach the coast opposite to the WWTP.

[36]Term defined in Section 2

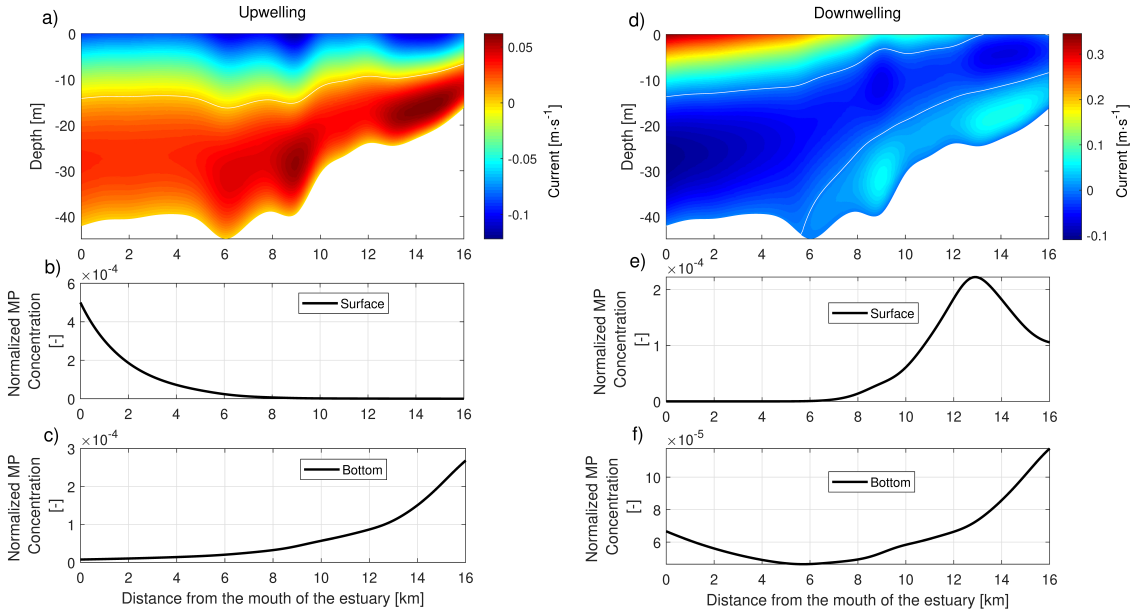

Figure 21: Configuration of the flow during upwelling (a) and downwelling conditions (b), and corresponding concentrations of MPs (fishing cuts) at the surface (b for upwelling and e for downwelling) and at the bottom (c for upwelling and f for downwelling). For figures of the circulation induced by the individual drivers (density, river and wind), the reader is referred to Díez-Minguito et al. (2020).

6.4. The Adour Estuary

6.4.1. Site description

The Adour Estuary is located in the southern Bay of Biscay (France). It extends over 70 km up to a weir in the Adour river, while the saline intrusion is limited to 20 km. The mouth of the estuary is subjected to a mesotidal forcing with a mean tidal range[37] of 2.5 m. The mean annual river discharge is 300 $m^3 s^{-1}$, but the daily river discharge varies from 80 $m^3.s^{-1}$ during the dry season to more than 3000 $m^3 s^{-1}$ during strong freshets. Such forcing applied to a narrow estuary results in a time-dependent salt-wedge estuary. Strong vertical density stratification[37] develops at flood while horizontal density gradients are produced by intense mixing periods during ebb. The lower part of the estuary is surrounded by potential sources of MP contamination. It is encompassed by the cities of Bayonne, Anglet and Boucau, and more than 160 outflows are spread along the last 10 km, from civil (e.g. WasteWater Treatment Plants, sewage network, rainwater network, storm water overflows) to industrial sources, some of which release untreated wastewaters. Inside the lower part of the estuary, there is also a harbour and a marina, which can be sources of contamination, as well as the large fishing areas in the adjacent coastal waters.

[37]Term defined in Section 2

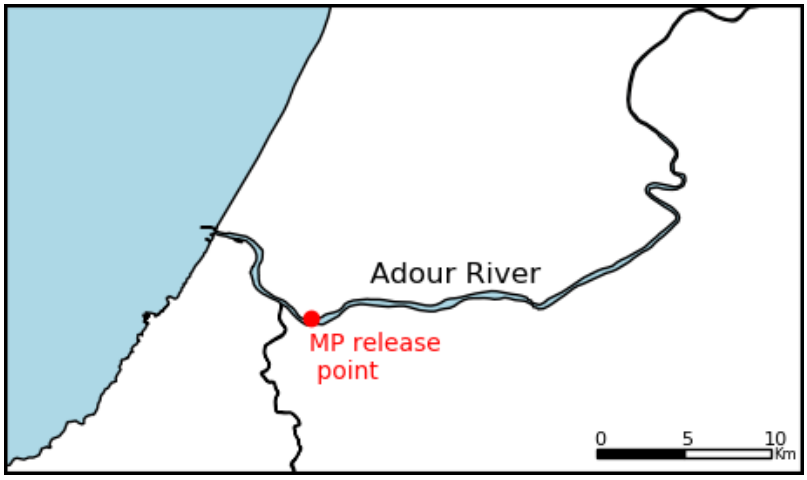

Figure 22: Map of the Adour estuarine system. Red dot represents the position where MPs were released during the simulation.

6.4.2. Methods

On June 6^{th} (freshets season) and September 26^{th} and 27^{th} (dry season) 2019, MP samples were collected over the tidal cycle at 5 km from the estuary mouth. Surface samplings with a manta net were combined with pumped water samples inside the water column (about 1 m below the surface and 1 m above the bed). The manta net had a rectangular opening 15 cm high by 30 m wide and a 300 μm mesh net, and it was equipped with a mechanical flow-metre. A 750 W immersed pump was used to collect subsurface and bottom waters, which were successively poured into sieves of 5 mm and 300 μm. Microplastics were identified and separated using a Leika M165C binocular magnifier. Dried fragments were recorded with a Zooscan device, and they were counted and measured with Image J and Plankton identifier.

TELEMAC-MASCARET modelling system was used to explore MP dispersion into the Adour Estuary with realistic 3D Eulerian simulations. The model was forced by a spring tide of 3.5 m amplitude and a river discharge of $100\,\mathrm{m^3 s^{-1}}$ for the low river discharge scenarios and 600 m^3/s for the high discharge scenarios. The hydrodynamical model was calibrated and validated with tidal gauge data, ADCP data and density profiles (Defontaine et al., 2019). Microplastics were modelized in a similar manner as sediments, i.e. by solving an advection-diffusion equation with an additional settling velocity. Simulations were run with three types of particles: S1 equivalent to a polystyrene sphere of 0.5 mm with a density of $1.05\,\mathrm{g \cdot cm^{-3}}$ ($w_s = 4\,\mathrm{mm \cdot s^{-1}}$), S2 equivalent to polycaprolactone sphere of 4.9 mm ($w_s = 127\,\mathrm{mm \cdot s^{-1}}$), and S3 a neutrally buoyant particle of 3 mm ($w_s = 0\,\mathrm{mm \cdot s^{-1}}$). Microplastics were released on day 4 of simulation at high tide at 8 km from the mouth of the estuary during 15 minutes.

A more complete description of the methodology can be found in Defontaine et al. (2020).

6.4.3. Microplastic dynamics

Observations have revealed that MP concentration was similar throughout the water column, with a mean abundance of $1.13\,items \cdot m^{-3}$. Particles collected were mostly films and fragments and the $1-2$ mm size class was the most abundant. However, size and shape distributions were depth-variable, with smaller particles near bottom, and more films and spheres at the surface than

inside the water column. MPs abundance in the different depths of the water column have shown variations throughout the tidal cycle that could be attributed to tidal processes such as resuspension and deposition mechanisms which were explored in depth with numerical simulations (Figure 24).

Numerical simulations have shown that MPs, like any particle in suspension, are very sensitive to hydrodynamics. As expected, MPs displacements followed the tidal motion, being transported in an oscillating manner landward and seaward. However, particle characteristics (size, density and settling velocity) also strongly affect their dispersion. Neutrally buoyant particles (S3) are easily flushed from the estuary, as surface waters in a time-dependent salt-wedge estuary are almost permanently flowing out the estuary (Figure 23 i and j). On the other hand, dense microplastics (S2) with high settling velocity sink at the level of the source point and move back and forth with the salt-wedge displacement (Figure 23 g and h). Particles with a density higher than marine water density and low settling velocity (S1) spread along the Adour Estuary with a variable distribution in the water column (Figure 23 e and f). S1 particle dispersion is strongly affected by tidal mechanisms and density field (Figure 24): during flood the turbulence is contained under the pycnocline and so the transport in suspension (A), while ,during ebb, intense mixing periods ($Ri < 0.25$) spread the particle throughout the water column (C). The deposition phase can be observed when the current reverses and the transport capacity reduces ($Ro > 2.5$, B). The river flow also impacts the particle dispersion with faster flushing during high river flow and landward displacement of particles during low river flow. Similarly to a back and forth displacement of an ETM with the river flow, a higher concentration of (S1) particles is localised at the estuary entrance during high river flow. In contrast, at low river flow, the concentration is higher at 8 to 10 km from the mouth of the estuary.

In conclusion, density structure, enhanced vertical mixing, and particle characteristics (size, settling velocity) have a major influence on MP dispersion and trapping, inducing spatial and temporal variability of MPs abundance and distribution. Compared to many previous numerical studies, which focused exclusively on buoyant MPs transported by surface waters, this study case demonstrates that sinking MPs transported in suspension have a behaviour analogous to suspended sediment in a salt-wedge estuary: transport in suspension restrained by the pycnocline, vertical dispersion during intense mixing periods, and accumulation in convergence areas forming potential EMPM[38].

[38]Term defined in Section 2

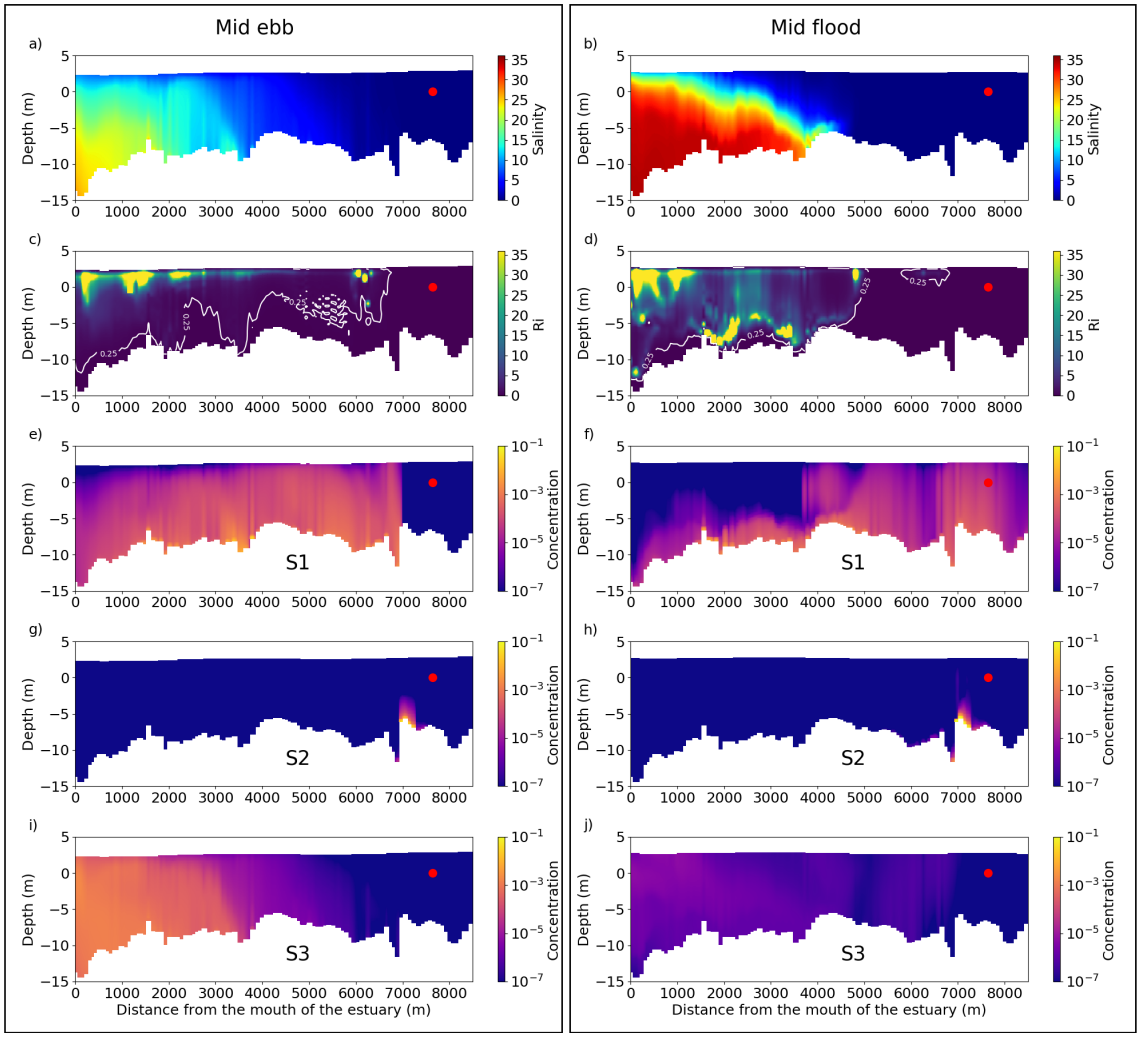

Figure 23: a) and b): longitudinal section of salinity at mid falling and rising tides. c) and d): longitudinal section of the Richardson number[40], the white line indicates the threshold value of $Ri = 0.25$ between stable and unstable configurations. e) to j): longitudinal section of microplastics concentrations in $g \cdot L^{-1}$ for the three simulation runs (S1, S2 and S3). Data were extracted about 3 h (mid ebb=left panel) and 9 h (mid flood=right panel) after the microplastic release on Day 4 under high river discharge conditions. On longitudinal sections, the red dot indicates the location of the microplastic release. After Defontaine et al. (2020).

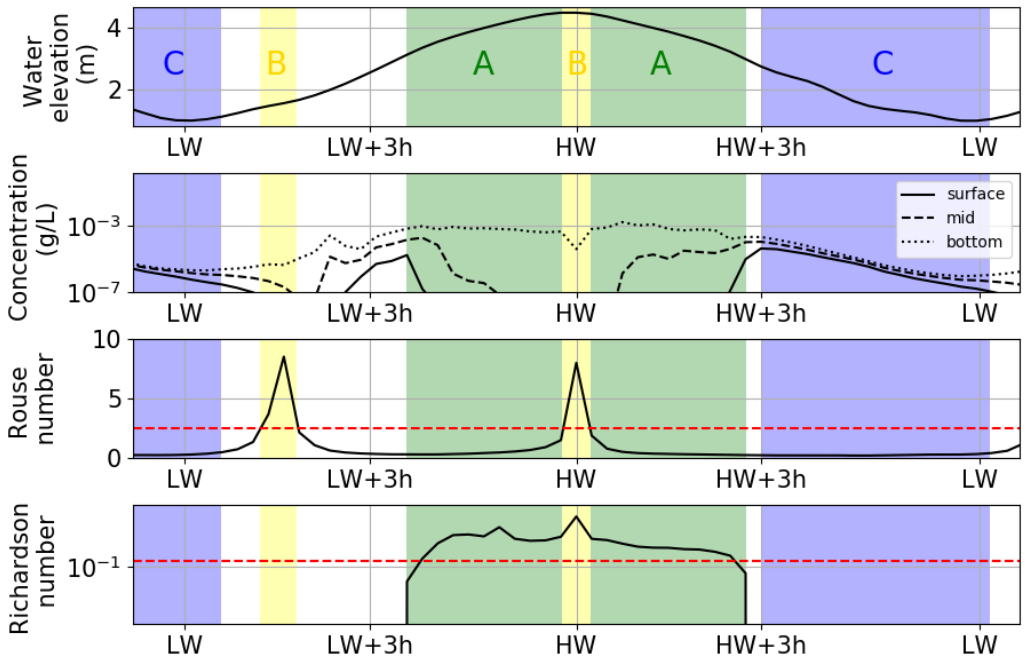

Figure 24: Time series of a) water elevation in metres, b) microplastic concentrations in grams per litre, c) Rouse number[43] and d) vertically averaged Richardson number[43]. The dashed lines indicate the threshold values for the Rouse number $Ro = 2.5$ and the Richardson number $Ri = 0.25$. Data were extracted from S1 simulation in high river flow conditions. After Defontaine et al. (2020).

7. Observation strategies and numerical simulation

7.1. Observation strategies

7.1.1. Sampling techniques

In the last decade, sampling strategies in the water compartment have been focused on floating MPs, based on the hypothesis that light MPs float while dense MPs sink and deposit on the bed (i.e. sediment compartment). Therefore, the most commonly used techniques for MP sampling in seawater are nets such as manta, plankton or Neuston nets (Gallagher et al., 2016; McEachern et al., 2019; Simon-Sánchez et al., 2019; Yonkos et al., 2014). Nets are towed at the rear of the ship during a time and at a speed that allows a large volume of water to be filtered (Figure 25). A mechanical flow-metre is generally fixed at the net opening to estimate the filtered water volume. A standard 300 μm mesh is generally mounted on nets, leading to an underestimation of the MP contamination as finer MPs are not sampled (Green et al., 2018; Tamminga et al., 2019). Trawling technique has the benefit of being easily deployed in coastal areas, and estimations of the contamination are reliable due to the high volume of water being filtered. However, such techniques are limited to sampling in relatively clear water; otherwise, they are quickly obstructed by floating debris. Clogging of net pores results in a decrease of the volume flow and the collection of smaller particles. Manta nets are

relatively difficult to manipulate under rough water so their deployment requires calm conditions (Michida et al., 2019).

Other well-known technique, increasingly used for the water column sampling, consists of pumping and pouring water through a sequence of sieves decreasing in mesh size or filtrating water at the laboratory (La Daana et al., 2017; Lusher et al., 2014; Xu et al., 2018; Zhao et al., 2015). This method allows to collect microplastics as finer as the last sieve is. The pump inlet is mounted with a pressure sensor and weights to estimate the sampling depth reliably and ensure a vertical fall. The volume of water to be filtered depends on the pump capacity, but it may require a couple of hours to collect only $10\,m^3$ of water. Pumping systems may lead to underestimating large MP concentrations due to their low abundance (Tamminga et al., 2019). Similarly, MP contamination can be estimated using bottle samples and filtration processes (Green et al., 2018; Yan et al., 2019). Such a technique allows one to consider the smaller size of MPs down to $5\,\mu m$. However, the small water volumes considered may neglect larger MP contamination to a greater extent than pumping systems.

Recently, new technologies appeared such as continuous-flow centrifuges and automatic samplers. With continuous-flow centrifuges, the pumped water is introduced in the centrifuge rotor where particles denser than the ambient water are separated. The remaining water with less dense particles flows through sieves where smaller particles are collected. This method allows the use of very fine mesh, down to $5\,\mu m$. However it may take 3 hours to process 130 L of water (Hildebrandt et al., 2019). In situ-filtration devices or automatic samplers can also filter or collect MPs directly from the surrounding waters, and can be mounted on CTD sampler or ROV (Choy et al., 2019; Li et al., 2020; Liu et al., 2019; Tekman et al., 2020). In situ filtration device used in the study by Liu et al. (2019) was composed of a high-efficiency plankton pump ($30\,m^3hr^{-1}$) combined with a $60\,\mu m$ mesh bag. This new technology showed promising results in investigating MP distribution in the water column.

The two most important parameters in MP sampling are the mesh size and the volume of sampled water. Both parameters influence the concentration of measured MPs and the type of MPs collected. For instance, a smaller mesh size may lead to concentrations of fibres several orders of magnitude higher (Dris et al., 2018). The influence of the sampling volume has been outlined in the literature. For example, (Liu et al., 2019) concluded that volume of filtered water higher than $8\,m^3$ leads to stable results. If volumes of sampled water are small (e.g. bottle sampling), it is recommended to implement replicates.

To date, no consensus has been found on sampling methods for MPs in the water compartment (Table 2), although comparative studies have shown that concentration of MPs estimated with different sampling methods can exhibit differences by orders of magnitude (Green et al., 2018). The choice of the method depends on the study purpose, the characteristics of the study site, and local hydrodynamics. There is a need to standardise sampling methods to allow comparison in MP contamination. In any case, special care should be given to inadvertent contamination during sampling. Plastic equipment should be avoided and replaced by glass or metal. Researchers should wear cotton jackets and laboratory coats during sampling and sorting. All equipment should be rinsed with ultra-pure water before covering with clean tinfoil. It is also recommended to take water replicates for quality control (Ryan et al., 2020). After sampling, different processes of density separation, filtration, sieving, visual sorting and digestion have to be carried out in the laboratory prior to identification. Such processes will not be presented in this section; the reader can refer to

recent reviews and comparative studies for more information (Cutroneo et al., 2020; Müller et al., 2020; Prata et al., 2019; Stock et al., 2019; Liu et al., 2020).

7.1.2. Field sampling in estuarine environment

Although there are some official recommendations and protocols to sample MPs in the surface, water column and sediment compartments of the aquatic environment (e.g. Galgani et al., 2013), there are no specific official recommendations to sample MPs in estuaries. Advanced knowledge of estuarine hydrodynamics is crucial to establishing an adequate protocol. This section collects a series of recommendations to improve the strategies of MP sampling in estuaries based on the estuarine dynamics discussed in previous Sections.

Estuarine dynamics largely varies over various time and space scales that should be considered when planning a sampling protocol. Temporal scales such as the tidal cycle, fortnightly cycle, and seasonal variability related to river discharge, wind, or waves should be considered. Microplastic concentrations and dynamics can also vary over the different estuarine regions. As shown in sections 5 and 6, mechanisms such as flow convergence, tidal pumping[44], stratification[44] and turbulence may accumulate MPs in EMPM[44]or disperse them depending on the type of estuary, the estuarine region, and the type of particle (Figure 12). Sampling MPs at different locations in the same estuary is thus recommended to (1) identifying potential EMPM; (2) distinguishing eventual local processes from general trends; (3) understand the relative importance of physical processes at all the estuarine regions.

The complex 3D hydrodynamics in estuaries induces the need to sample the full water column at relatively short intervals to capture variability at tidal and higher frequencies, similarly as suspended sediment concentrations. Short intervals of time are hardly compatible with collecting large volumes of water to have reliable MP concentrations for all the types of MPs. If trawling techniques benefit from filtering large volumes of water, they are challenging to deploy in estuaries where commercial navigation and recreational activities are intense and tidal currents can be strong and highly variable. Moreover, trawling techniques are generally limited to the surface. On the other hand, pumping techniques may easily sample at different depths. However, it generally requires a couple of hours to collect a volume of water sufficient to have reliable estimation of MP contamination. A compromise between time resolution and reliability on MP concentrations has to be reached depending on the study aim, local hydrodynamics and the selected technology.

Microplastics dispersion is intrinsically linked to their buoyancy[44] and thus to the ambient water density. In estuaries, water density is highly variable in time and space due to mixing/stratification[44] between salty marine water and fresh riverine water. Collecting additional observations of physical parameters simultaneously to MP sampling would be recommended. For example, conductivity, temperature and current velocities allow estimating the ambient water density and analysing the physical processes. Wind intensity and direction may also impact the dispersion and mixing of floating MPs and generate areas of accumulation (Browne et al., 2010). Measuring wind conditions during the sampling days would be therefore advised. In addition, one common feature in estuaries is the ETM[44]. In such highly turbid areas, or during algae blooms, the choice of the finer mesh size for filtration should take into account the sediment/algae concentration to avoid clogging fine sieves

[44]Term defined in Section 2

(Dris et al., 2018; Sadri and Thompson, 2014), keeping in mind that replacing one sieve during the sampling process is not straightforward.

Finally, it should be noted that estuaries are generally densely populated areas and MP pollution can be strongly correlated to the size and proximity of the urban areas (Gago et al., 2015; Lebreton et al., 2017; Naidoo et al., 2015; Rodrigues et al., 2019; Yonkos et al., 2014). The choice of the sampling locations should also consider the multiple local sources of MPs that can be found in estuaries: wastewater treatment plants, sewage network, rainwater network, port/marina, industries, densely populated areas, etc. The proximity to such sources may largely impact the estimation of the contamination. To avoid such local effects, the sampling point should be placed away from any source of MPs, unless the aim of the study is to estimate the contribution of specific sources.

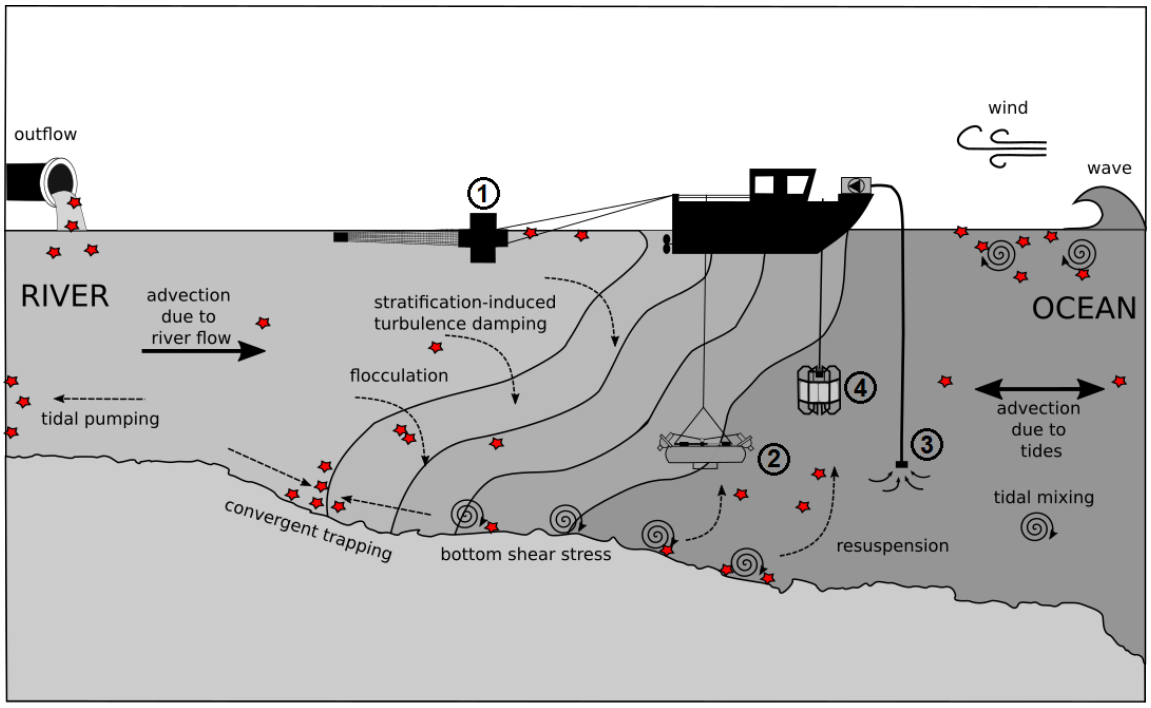

Figure 25: Schematic representation of the most commonly used techniques for MP sampling and the key processes affecting MP distribution and therefore the sampling strategy in estuarine environments (After Defontaine and Jalón-Rojas, submitted)

.

Study area	Sampling tools	Mesh size	Depth	Sampling volume	Reference
Adour Estuary, France	Manta net, pumping system	300 μm - 5 mm	Surface, subsurface (1 m), Bottom (1 m)	Net : 45 to 146 m^3, Pump : 2.8 to 5.1 m^3	Defontaine et al. (2020)
Douro Estuary, Portugal	Conical net	30 μm - 500 μm	Subsurface (1-2 m)	235 m^3	Rodrigues et al. (2019)
Tamar Estuary, UK	Manta net	300 μm - 5 mm	Surface	270 m^3	Sadri and Thompson (2014)
Solent Estuary, UK	Plankton net	300 μm - 5 mm	Surface	-	Gallagher et al. (2016)
Ebro Estuary, Spain	Neuston net	5 μm - 5 mm	Surface	-	Simon-Sánchez et al. (2019)
Ría de Vigo, Spain	Manta net	300 μm - 5 mm	Surface	60 m^3	Díez-Minguito and de Swart (2020)
Guadalquiivir, Spain	Net	1 mm - 5 mm	-	-	Bermúdez et al. (2021)
Yangtze Estuary, China	Pumping system	32 μm - 5 mm	Subsurface (1 m)	-	Zhao et al. (2014)
Changjiang Estuary, China	Pumping system	70 μm - 5 mm	Subsurface (50 cm)	100 L	Xu et al. (2018)
Minjiang Estuary, China	Pumping system	333 μm - 5 mm	Subsurface (30 cm)	20 L	Zhao et al. (2015)
Pearl Estuary, China	Water sampler	50 μm - 5 mm	Surface	5 L	Yan et al. (2019)
Winyah Bay, USA	Microlayer collection apparatus	63 μm - 2 mm	Surface	4 L	Gray et al. (2018)
Chesapeake Bay, USA	Manta net	330 μm - 5 mm	Surface	$105 - 210$ m^3	Yonkos et al. (2014), Bikker et al. (2020)
Delaware Bay, USA	Plankton net	200 μm - 5 mm	Surface	$259 - 292$ m^3	Cohen et al. (2019)
Tampa Bay, USA	Plankton net, bottle sampling	300 μm - 5 mm, 1.2 μm - 5 mm	Subsurface (1-2 m)	Net: 35 m^3, bottle : 1 L	McEachern et al. (2019)
Clyde, Bega and Hunter Estuaries, Australia	Plankton net	45 μm - 5 mm	Surface	-	Hitchcock and Mitrovic (2019)

Table 2: Comparison of sampling strategies in different estuaries (after Defontaine and Jalón-Rojas, submitted).

7.2. Numerical simulations

Numerical modelling is cheaper and faster than conducting field studies. It allows the analysis of meteorological and oceanographic conditions that did not occur during the observation period, the assessment of retrospective or prospective conditions, and testing hypotheses on MP dynamics. However, this approach is also subject to uncertainties derived from the model structure, assumptions, and setup (e.g. schematisation, time resolution,...), the parameter choice or the reliability of forcing data, and requires careful calibration with field data.

Process-based models are routinely applied to study hydrodynamic and transport processes in estuaries. Specific models of plastic abundance and distribution in these environments are instead in their infancy, but they are developing rapidly by thriving on the modelling of sediments, water or pollutant transport. These models can be divided into idealised or exploratory models and complex numerical models.

Idealised models include important simplifications in the model dimensions (typically 1D or 2D), the number of processes considered, and their parameterisations (see sketch in Fig. 17.b). Their schematisations allow for quick solutions, often analytic or semi-analytic, with a light CPU demand. These models are primarily intended to investigate the role of individual processes and the sensitivity to parameter variations on the MP distribution. In particular, identifying relevant physical processes is much more straightforward than with complex numerical models but the spatial and temporal detail is much lower. The studies in the Garonne Tidal river with iFLow (Jalón-Rojas et al., 2021) and the Ría de Vigo with the model of Díez-Minguito et al. (2020), presented in sections 6.1 and 6.3, fit into this category.

More complex numerical modelling approaches have also been applied to study MP transport and accumulation in estuarine environments. These approaches consider a fully three-dimensional representation of the flow, realistic geometries and bathymetries, and state-of-the-art parametrisations of as many physical processes as possible. They are intended to reproduce accurately and with a sufficient level of detail the hydrodynamic behaviour of the estuarine system and the transport processes therein. They allow a straightforward comparison with field data while, at the same time, can be used to fill data gaps in the absence of observations. On the other hand, this kind of model is very CPU intensive, limiting the number of simulations, and its complex setup hinders the identification of physical mechanisms driving the main trends. The studies in the Adour Estuary with TELEMAC model (Defontaine et al., 2020) and the Ría de Vigo with Delft3D model (Sousa et al., 2021), shown in Sections 6.4 and 6.3, correspond to this approach.

Complex numerical models can be based on two approaches: the Eulerian framework (e.g. Adour Estuary case) and the Lagrangian framework (e.g. Ría de Vigo case with Delft3D model). The Eulerian framework calculates concentration values in a grid. Numerical models of suspended sediment transport can also be used to simulate the transport of MPs. This approach is particularly interesting in estuaries, in which sinking, deposition and resuspension processes are fundamental. However, some model parameterizations such as terminal velocity or bed shear stress should be adapted to the dynamical behaviour of MPs as explained in Section 4.

The Lagrangian framework has been largely used to compute the trajectories of MPs at the ocean scale as they are particularly relevant to evaluate source-to-sink relationships (review by Hardesty et al., 2017). In these models, the motion of particles is typically decomposed into a deterministic component representing the advection of particles by currents, and a turbulent

unresolved component. The deterministic component uses (pre-computed) Eulerian velocity data usually derived from numerical hydrodynamic models. The unresolved contribution has to be modelled by stochastic terms such as random walk approaches. The majority of the existing applications of Lagrangian models at the ocean or regional scales focus on floating MPs and assume that they behave as passive tracers drifting within the surface layer. This assumption is particularly constraining in estuarine systems which are characterised by strong vertical dynamics. Nevertheless, more and more applications are considering the three-dimensional transport of MPs. For example, the TrackMPD model considers a wide range of transport mechanisms that are essential in estuaries (i.e., sinking, deposition, resuspension, bedload transport, beaching and re-floating), as well as empirical formulations to consider the impact of biofouling[45] on the sinking behaviours (Jalón-Rojas et al., 2019a, 2022).

8. Conclusions and outlook

This Chapter addressed the most important concepts and recent developments in microplastic (MP) dynamics and transport in estuaries. The main transport mechanisms were reviewed while highlighting the crucial role of the particle physical properties and their intrinsic evolution on the MP dynamical behaviour. Then, the typical temporal scales of estuarine variability and the main hydrodynamic processes governing the transport of MPs are presented and illustrated through four case studies, which ranged from well-mixed to strongly stratified systems.

Overall, a concise foundation of this young yet rapidly growing research field is provided. It is intended for the interdisciplinary community studying plastic pollution in estuaries, from academic researchers to advanced students, as well as for coastal and resources managers. Accordingly, a summary of the main conclusions and future perspectives on this field is provided.

- The heterogeneous nature of MPs in terms of density, size, and shape lead to distributions of their dynamical properties, such as sinking or rising terminal velocities or critical shear stress. Consequently, MPs entering an estuary may have different dynamical behaviour and be affected by different physical processes. In addition, the physical and dynamical properties of MP can evolve with the time spent in the aquatic environment due to weathering and aggregation processes. In particular, biofouling can significantly modify terminal velocities by increasing density, modifying the particle sinking orientation, or inducing motion instability. Small MP can also flocculate with sediments and behave as sediment flocs.

- Hydrodynamic processes driving MP transport in estuaries are induced by deterministic (semidiurnal or diurnal tides, spring-neap tides) and stochastic (river flow, wind, waves) environmental forcings. As a result, estuarine MP dynamics are complex, non-linear, and strongly variable over time scales ranging from seconds to years. This complexity is enhanced by the variety of MP sources and their intrinsic temporal variabilities. Despite the complexity and non-linear interactions, hydrodynamic processes can be classified into intratidal and subtidal (or tidally-averaged/residual) time scales. Intratidal variability is mainly related to tidal wave propagation and its interactions with the estuary geometry and river discharge.

[45] Term defined in Section 2

Residual circulation can be induced by non-linearities in tidal propagation, tidal rectification processes, tidal and internal asymmetries, tidal pumping, Stokes drift, river-induced circulation, gravitational circulation and wind-driven circulation. The relative importance of these processes can vary seasonally and even interannually with river discharge and wind variability.

- Understanding and predicting the source-sink transitions at the continuum river-estuary-ocean is a major challenge for scientists. Microplastic dispersion and transport trends are site-specific and highly dependent on their physical properties. In general, low-density floating MPs tend to be flushed seaward or accumulate at the lower estuarine reaches, while high-density sinking floating MPs tend to accumulate at the upper reaches. However, the spectrum of MP behaviour in a same estuary may be as wide-ranging as the variety of MPs present in the environment. Other than physical properties, the relative importance of hydrodynamic processes in the transport of MPs depends on the particular biomorphological setting of the estuary and the spatio-temporal variability of marine, atmospheric and fluvial forcing. Some examples addressed in this chapter are:

  - in a convergent tidal-dominated well-mixed estuary such as the Garonne Tidal River and the Guadalquivir Estuary, tidal pumping generated from tidal asymmetry is the main mechanism leading to landward transport, while river flow-induced circulation dominates the seaward transport.
  - in a mesotidal partially-mixed Estuary such as the Ría de Vigo, wind-induced and gravitational circulations control the distribution of MPs
  - in a mesotidal salt-wedge estuary such as the Adour River, river flow-induced circulation and the variations of the stratification and therefore the mixing conditions over the tidal cycle control in a large extent MP transport.

- However, the estuarine parameter space explored is still limited in the literature. The contribution of ephemeral estuaries to the balance of MPs released from land to the oceans is largely unexplored. Although this type of estuaries shows run-offs subject to strong low flows, González-Fernández et al. (2021) point to small estuaries as first-order pathways of MP to the ocean. Seasonal inputs from small agricultural drainage basins to (e.g.) the Mediterranean are thought to constitute a significant fraction of the total amount of MP items recorded.

- The physical integrity and mechanical properties of MP can be modified by biogeochemical and physical processes that operate on time scales similar to those of the hydrodynamic processes that transport them. This can critically influence the balance between erosion, transport and deposition processes and therefore the fate of MP. For instance, floating particles advected seaward near the surface may sink due to biofouling and be trapped in estuarine sediments before being flushed out to the ocean. This poses a real challenge for the accurate modelling of their transport and identification of accumulation points. Future numerical simulations should put special focus on the parameterisation of biochemical processes or the coupling of biochemical and transport models.

- Hot spots of MPs or EMPM[46] are expected to be generated in estuaries in a similar way than ETM[46]. The modelling of MP distribution in four different estuaries presented in this Chapter suggest that this can be a common feature of estuaries. Trapping physical processes includes gravitational circulation, tidal pumping, tidal straining, Stokes drift, wind-driven circulations and Eddy viscosity-shear covariance. For example, gravitational and wind-driver circulation may play a key role on partially-mixed estuaries, while tidal pumping can lead MP trapping at macrotidal well-mixed estuaries. In salt-wedge estuaries, the turbulence damping by density stratification induces the sinking of negatively-buoyant MPs, resulting in an accumulation at the lower water column. Other than hot-spots, the assessment of MP crossroads crossroad regions through which large amounts of MPs flow is a promising research line (Baudena et al., 2022).

- The position and dynamics of the EMPM might be similar to those of the ETM in some estuaries, particularly for sinking small MPs with similar properties as fine sediments. However, the EMPM may even overlap the ETM for other types of MPs in some estuaries. In addition, the high rates of flocculation of the finer fraction of MPs imply that the ETM and its associated bottom fluid could have a relevant role in trapping small MP in estuaries. On the other hand, bed sediments also affect MP erosion rates through the "hiding-exposure effect". Modelling together sediments and MPs is therefore a promising strategy to pinpoint MP hotspots in estuaries.

- Estuaries, and particularly intertidal zones and bottom sediment pools, may be important sinks of MPs. Vegetation can also significantly contribute to plastic straining and accumulation at intertidal zones. The assessment of the relative role of the different environmental forcings (e.g. wind, river discharge, waves) affecting MP beaching and remobilization to water can become a complex task since such forcings are controlled by the same large-scale atmospheric forcing. Nevertheless, wind direction and strength seem to play a crucial role in beaching at different estuarine regions. Tide and floods events may favour both MP straining and remobilization at intertidal zones and riverbanks.

- Understanding lateral and vertical MP fluxes in estuaries require further understanding of beaching, deposition, resuspension and burial processes and the development of formulations of erosion and deposition that consider the dependency on changing conditions. In particular, research on burial process is scarce and deserve further attention. High-resolution sediments cores could give insight into historical burial rates and the long-term evolution of MP pollution in estuaries. Moreover, the potential influence of buried MP in the cohesion of estuarine soils and morphology is yet to be determined and a promising research line. The potential environmental risks due to plastic accumulation deserve attention in future research, which could involve the inventory and analysis of stranded plastics.

- Estuaries can also be sources of ocean MPs. River floods are expected to be a major contributor of MP pollution to coastal and ocean waters due to the higher flushing capacity of the estuaries, the enhanced remobilization from riverbanks, and the higher MP input via runoff, and should

[46]Term defined in Section 2

be monitored accordingly. In general, the estimation of MP fluxes should take into account the three-dimensional structure of the flow and cover whole tidal cycles to take into account the residual transport. Fluxes calculations using a single station at a given instant can bias the estimations.

- Sampling strategy should consider the typical time scales of estuarine variability (intratidal, fortnightly cycle, and seasonal variability), the water column, and different estuarine regions. Sampling MP concentrations at different locations and water depths is recommended to (1) identifying potential EMPM; (2) distinguishing eventual local processes from general trends; (3) understand the MP distribution and the relative importance of physical processes along the estuarine axis. These requirements are challenging as sampling at short intervals of time are hardly compatible with collecting large volumes of water to have representative samples of MPs in term of concentrations and MP diversity. It is also costly in terms of time and human resources. A compromise between time resolution and reliability on MP concentrations has to be reached depending on the study aim, local hydrodynamics, and the selected technology.

- Process-based models are powerful tools to understand and predict MPs dispersion in estuaries. This tool allows filling the gaps in observations by simulating a wide range of meteorological and oceanographic conditions, testing hypothesis on MP dynamics, and assessing retrospective and prospective conditions. However, numerical simulations are subject to uncertainties derived from the model structure, assumptions and setup, the parameter choice, or the reliability of forcing data, requiring careful calibration with field data. Idealised simple models are particularly pertinent to investigate the role of individual processes and the sensitivity to parameter variations on the MP distribution. More complex numerical modelling approaches (Eulerian or Lagrangian) are intended to reproduce accurately transport trends and MPs distributions. Improved simulations are expected in the near future by improving the reproduction of hydrodynamics and the parameterisation of processes such as erosion and beaching, integrating the effect of biochemical processes, and considering the water density variability on settling velocity, among others.

Significant advances and new insights from different scientific disciplines on the transport of microplastic debris in estuaries are expected in the following few years.

References

van Aken, H.M., 1986. The onset of seasonal stratification in shelf seas due to differential advection in the presence of a salinity gradient. Continental Shelf Research 5, 475–485.

Allen, S., Allen, D., Baladima, F., Phoenix, V., Thomas, J., Le Roux, G., Sonke, J., 2021. Evidence of free tropospheric and long-range transport of microplastic at Pic du Midi Observatory. Nature communications 12, 1–10.

Alsina, J.M., Jongedijk, C.E., van Sebille, E., 2020. Laboratory measurements of the wave-induced motion of plastic particles: Influence of wave period, plastic size and plastic density. Journal of Geophysical Research: Oceans 125, e2020JC016294.

Álvarez-Salgado, X.A., Gago, J., Miguez, B., Pérez, F.F., 2001. Net ecosystem production of dissolved organic carbon in a coastal upwelling system: the Ria de Vigo, Iberian margin of the North Atlantic. Limnology and Oceanography 46, 135–146.

Amaral-Zettler, L.A., Zettler, E.R., Mincer, T.J., Klaassen, M.A., Gallager, S.M., 2021. Biofouling impacts on polyethylene density and sinking in coastal waters: A macro/micro tipping point? Water Research 201, 117289.

Andersen, T.J., Rominikan, S., Olsen, I.S., Skinnebach, K.H., Fruergaard, M., 2021. Flocculation of PVC microplastic and fine-grained cohesive sediment at environmentally realistic concentrations. The Biological Bulletin 240, 42–51.

Andrady, A.L., 2011. Microplastics in the marine environment. Marine pollution bulletin 62, 1596–1605.

Andrady, A.L., Hamid, S., Hu, X., Torikai, A., 1998. Effects of increased solar ultraviolet radiation on materials. Journal of photochemistry and photobiology B: Biology 46, 96–103.

Bagnold, R.A., 1973. The nature of saltation and of 'bed-load'transport in water. Proceedings of the Royal Society of London. A. Mathematical and Physical Sciences 332, 473–504.

Ballent, A., Purser, A., de Jesus Mendes, P., Pando, S., Thomsen, L., 2012. Physical transport properties of marine microplastic pollution. Biogeosciences Discussions 9.

Baudena, A., Ser-Giacomi, E., Jalón-Rojas, I., Galgani, F., Pedrotti, M.L., 2022. The streaming of plastic in the Mediterranean Sea. URL: https://doi.org/10.5281/zenodo.5931214, doi:10.5281/zenodo.5931214.

Becherer, J., Flöser, G., Umlauf, L., Burchard, H., 2016. Estuarine circulation versus tidal pumping: Sediment transport in a well-mixed tidal inlet. Journal of Geophysical Research: Oceans 121, 6251–6270.

Bermúdez, M., Vilas, C., Quintana, R., González-Fernández, D., Cózar, A., Díez-Minguito, M., 2021. Unravelling spatio-temporal patterns of suspended microplastic concentration in the Natura 2000 Guadalquivir estuary (SW Spain): Observations and model simulations. Marine Pollution Bulletin 170, 112622.

Bikker, J., Lawson, J., Wilson, S., Rochman, C., 2020. Microplastics and other anthropogenic particles in the surface waters of the Chesapeake Bay. Marine Pollution Bulletin 156, 111257.

Blanton, J.O., Lin, G., Elston, S.A., 2002. Tidal current asymmetry in shallow estuaries and tidal creeks. Continental Shelf Research 22, 1731–1743.

Borrelle, S.B., Ringma, J., Law, K.L., Monnahan, C.C., Lebreton, L., McGivern, A., Murphy, E., Jambeck, J., Leonard, G.H., Hilleary, M.A., et al., 2020. Predicted growth in plastic waste exceeds efforts to mitigate plastic pollution. Science 369, 1515–1518.

Bowman, D., Manor-Samsonov, N., Golik, A., 1998. Dynamics of litter pollution on Israeli Mediterranean beaches: a budgetary, litter flux approach. Journal of Coastal Research , 418–432.

Brouwer, R.L., Schramkowski, G.P., Dijkstra, Y.M., Schuttelaars, H.M., 2018. Time evolution of estuarine turbidity maxima in well-mixed, tidally dominated estuaries: The role of availability-and erosion-limited conditions. Journal of Physical Oceanography 48, 1629–1650.

Browne, M.A., Galloway, T.S., Thompson, R.C., 2010. Spatial patterns of plastic debris along estuarine shorelines. Environmental science & technology 44, 3404–3409.

Burchard, H., Schuttelaars, H.M., Ralston, D.K., 2018. Sediment trapping in estuaries. Annual review of marine science 10, 371–395.

Burns, E.E., Boxall, A.B., 2018. Microplastics in the aquatic environment: Evidence for or against adverse impacts and major knowledge gaps. Environmental toxicology and chemistry 37, 2776–2796.

Buschman, F., Hoitink, A., Van Der Vegt, M., Hoekstra, P., 2009. Subtidal water level variation controlled by river flow and tides. Water Resources Research 45.

Caballero, I., Morris, E.P., Ruiz, J., Navarro, G., 2014. Assessment of suspended solids in the Guadalquivir estuary using new DEIMOS-1 medium spatial resolution imagery. Remote Sensing of Environment 146, 148–158.

Carretero, O., Gago, J., Filgueiras, A.V., Viñas, L., 2022. The seasonal cycle of micro and mesoplastics in surface waters in a coastal environment (Ría de Vigo, NW Spain). Science of The Total Environment 803, 150021.

de Carvalho, A.R., Garcia, F., Riem-Galliano, L., Tudesque, L., Albignac, M., Ter Halle, A., Cucherousset, J., 2021. Urbanization and hydrological conditions drive the spatial and temporal variability of microplastic pollution in the Garonne River. Science of the Total Environment 769, 144479.

Castelle, B., Dodet, G., Masselink, G., Scott, T., 2017. A new climate index controlling winter wave activity along the Atlantic coast of Europe: The West Europe Pressure Anomaly. Geophysical Research Letters 44, 1384–1392.

Choy, C.A., Robison, B.H., Gagne, T.O., Erwin, B., Firl, E., Halden, R.U., Hamilton, J.A., Katija, K., Lisin, S.E., Rolsky, C., et al., 2019. The vertical distribution and biological transport of marine microplastics across the epipelagic and mesopelagic water column. Scientific reports 9, 1–9.

Chubarenko, I., Esiukova, E., Bagaev, A., Bagaeva, M., Grave, A., 2018a. Three-dimensional distribution of anthropogenic microparticles in the body of sandy beaches. Science of the total environment 628, 1340–1351.

Chubarenko, I., Esiukova, E., Bagaev, A., Isachenko, I., Demchenko, N., Zobkov, M., Efimova, I., Bagaeva, M., Khatmullina, L., 2018b. Behavior of microplastics in coastal zones, in: Microplastic contamination in aquatic environments. Elsevier, pp. 175–223.

Cohen, J.H., Internicola, A.M., Mason, R.A., Kukulka, T., 2019. Observations and simulations of microplastic debris in a tide, wind, and freshwater-driven estuarine environment: the Delaware Bay. Environmental Science & Technology 53, 14204–14211.

Cole, M., Lindeque, P., Halsband, C., Galloway, T.S., 2011. Microplastics as contaminants in the marine environment: a review. Marine pollution bulletin 62, 2588–2597.

Cooper, D.A., Corcoran, P.L., 2010. Effects of mechanical and chemical processes on the degradation of plastic beach debris on the island of Kauai, Hawaii. Marine pollution bulletin 60, 650–654.

Cózar, A., Martí, E., Duarte, C.M., García-de Lomas, J., Van Sebille, E., Ballatore, T.J., Eguíluz, V.M., González-Gordillo, J.I., Pedrotti, M.L., Echevarría, F., et al., 2017. The Arctic Ocean as a dead end for floating plastics in the North Atlantic branch of the Thermohaline Circulation. Science advances 3, e1600582.

Cutroneo, L., Reboa, A., Besio, G., Borgogno, F., Canesi, L., Canuto, S., Dara, M., Enrile, F., Forioso, I., Greco, G., et al., 2020. Microplastics in seawater: sampling strategies, laboratory methodologies, and identification techniques applied to port environment. Environmental Science and Pollution Research 27, 8938–8952.

Defontaine, S., Jalón-Rojas, I., submitted. Physical processes matters! recommendations for sampling microplastics in estuarine waters based on hydrodynamics. Enviornmental and Science Technology Letters .

Defontaine, S., Jalón-Rojas, I., Sottolichio, A., Gratiot, N., Cédric, L., 2023. Settling dynamics of cohesive sediments in a highly turbid tidal river. Marine Geology 457, 106995.

Defontaine, S., Sous, D., Morichon, D., Verney, R., Monperrus, M., 2019. Hydrodynamics and SPM transport in an engineered tidal estuary: the Adour river (France). Estuarine, Coastal and Shelf Science 231, 106445.

Defontaine, S., Sous, D., Tesan, J., Monperrus, M., Lenoble, V., Lanceleur, L., 2020. Microplastics in a salt-wedge estuary: Vertical structure and tidal dynamics. Marine Pollution Bulletin 160, 111688.

Dietrich, W.E., 1982. Settling velocity of natural particles. Water resources research 18, 1615–1626.

Díez-Minguito, M., Baquerizo, A., Ortega-Sánchez, M., Navarro, G., Losada, M., 2012. Tide transformation in the Guadalquivir estuary (SW Spain) and process-based zonation. Journal of Geophysical Research: Oceans 117.

Díez-Minguito, M., Baquerizo, A., de Swart, H., Losada, M., 2014. Structure of the turbidity field in the Guadalquivir estuary: Analysis of observations and a box model approach. Journal of Geophysical Research: Oceans 119, 7190–7204.

Díez-Minguito, M., Bermúdez, M., Gago, J., Carretero, O., Viñas, L., 2020. Observations and idealized modelling of microplastic transport in estuaries: the exemplary case of an upwelling system (Ría de Vigo, NW Spain). Marine Chemistry 222, 103780.

Díez-Minguito, M., de Swart, H.E., 2018. Observational Evidences of Strain-induced Periodic Stratification (SIPS) in the Guadalquivir Estuary, in: Proceedings of V Encuentro de Oceanografia Fisica 2018 (EOF), Vigo (Spain).

Díez-Minguito, M., de Swart, H.E., 2020. Relationships Between Chlorophyll-a and Suspended Sediment Concentration in a High-Nutrient Load Estuary: An Observational and Idealized Modeling Approach. Journal of Geophysical Research: Oceans 125, e2019JC015188.

Dijkstra, Y.M., Brouwer, R.L., Schuttelaars, H.M., Schramkowski, G.P., 2017. The iflow modelling framework v2. 4: a modular idealized process-based model for flow and transport in estuaries. Geoscientific Model Development 10, 2691–2713.

Dijkstra, Y.M., Schuttelaars, H.M., Schramkowski, G.P., Brouwer, R.L., 2019. Modeling the transition to high sediment concentrations as a response to channel deepening in the Ems River Estuary. Journal of Geophysical Research: Oceans 124, 1578–1594.

Dioguardi, F., Mele, D., Dellino, P., 2018. A new one-equation model of fluid drag for irregularly shaped particles valid over a wide range of Reynolds number. Journal of Geophysical Research: Solid Earth 123, 144–156.

Dris, R., Gasperi, J., Rocher, V., Tassin, B., 2018. Synthetic and non-synthetic anthropogenic fibers in a river under the impact of Paris Megacity: Sampling methodological aspects and flux estimations. Science of the Total Environment 618, 157–164.

Dronkers, J.J., 1964. Tidal computations in rivers and coastal waters .

Dyer, K.R., 1988. Fine sediment particle transport in estuaries, in: Physical processes in estuaries. Springer, pp. 295–310.

Dyer, K.R., 1995. Sediment transport processes in estuaries, in: Developments in Sedimentology. Elsevier. volume 53, pp. 423–449.

ECHA, 2020. Opinion of the Committee for Risk Assessment and Opinion of the Committee for Socio-economic Analysis on an Annex XV dossier proposing restrictions of the manufacture, placing on the market or use of a substance within the EU. .

Elahi, M., Jalón-Rojas, I., Wang, X., Ritchie, E., 2020. Influence of seasonal river discharge on tidal propagation in the Ganges-Brahmaputra-Meghna Delta, Bangladesh. Journal of Geophysical Research: Oceans 125, e2020JC016417.

van Emmerik, T., Mellink, Y., Hauk, R., Waldschläger, K., Schreyers, L., 2022. Rivers as plastic reservoirs. Front. Water 3, 786936.

Fan, Y., Zheng, K., Zhu, Z., Chen, G., Peng, X., 2019. Distribution, sedimentary record, and persistence of microplastics in the Pearl River catchment, China. Environmental Pollution 251, 862–870.

Fazey, F.M., Ryan, P.G., 2016. Biofouling on buoyant marine plastics: An experimental study into the effect of size on surface longevity. Environmental pollution 210, 354–360.

Fick, A., 1855. V. on liquid diffusion. The London, Edinburgh, and Dublin Philosophical Magazine and Journal of Science 10, 30–39.

Fischer, H.B., List, J.E., Koh, C.R., Imberger, J., Brooks, N.H., 1979. Mixing in inland and coastal waters. Academic press.

Fischer, R., Lobelle, D., Kooi, M., Koelmans, A., Onink, V., Laufkötter, C., Amaral-Zettler, L., Yool, A., van Sebille, E., 2021. Modeling submerged biofouled microplastics and their vertical trajectories. Biogeosciences Discussions , 1–29.

Forsberg, P.L., Sous, D., Stocchino, A., Chemin, R., 2020. Behaviour of plastic litter in nearshore waters: First insights from wind and wave laboratory experiments. Marine pollution bulletin 153, 111023.

Frias, J., Nash, R., 2019. Microplastics: finding a consensus on the definition. Marine pollution bulletin 138, 145–147.

Friedrichs, C.T., Aubrey, D.G., 1988. Non-linear tidal distortion in shallow well-mixed estuaries: a synthesis. Estuarine, Coastal and Shelf Science 27, 521–545.

Gago, J., Henry, M., Galgani, F., 2015. First observation on neustonic plastics in waters off nw spain (spring 2013 and 2014). Marine environmental research 111, 27–33.

Galgani, F., Burgeot, T., Bocquene, G., Vincent, F., Leaute, J., Labastie, J., Forest, A., Guichet, R., 1995. Distribution and abundance of debris on the continental shelf of the Bay of Biscay and in Seine Bay. Marine Pollution Bulletin 30, 58–62.

Galgani, F., Hanke, G., Werner, S., De Vrees, L., 2013. Marine litter within the European marine strategy framework directive. ICES Journal of Marine Science 70, 1055–1064.

Gall, S.C., Thompson, R.C., 2015. The impact of debris on marine life. Marine pollution bulletin 92, 170–179.

Gallagher, A., Rees, A., Rowe, R., Stevens, J., Wright, P., 2016. Microplastics in the Solent estuarine complex, UK: an initial assessment. Marine Pollution Bulletin 102, 243–249.

Garvine, R.W., 1985. A simple model of estuarine subtidal fluctuations forced by local and remote wind stress. Journal of Geophysical Research: Oceans 90, 11945–11948.

Gasperi, J., Cachot, J., 2021. Projet Plastic-Seine: Flux et impacts des microplastiques dans l'estuaire de la Seine. Ph.D. thesis. Programme Seine-Aval 6.

Geyer, R., Jambeck, J.R., Law, K.L., 2017. Production, use, and fate of all plastics ever made. Science advances 3, e1700782.

Geyer, W., 1997. Influence of wind on dynamics and flushing of shallow estuaries. Estuarine, coastal and shelf science 44, 713–722.

Geyer, W.R., MacCready, P., 2014. The estuarine circulation. Annual review of fluid mechanics 46, 175–197.

Geyer, W.R., Scully, M.E., Ralston, D.K., 2008. Quantifying vertical mixing in estuaries. Environmental fluid mechanics 8, 495–509.

Gigault, J., Ter Halle, A., Baudrimont, M., Pascal, P.Y., Gauffre, F., Phi, T.L., El Hadri, H., Grassl, B., Reynaud, S., 2018. Current opinion: what is a nanoplastic? Environmental pollution 235, 1030–1034.

Gilcoto, M., Graña, R., Piedracoba, S., Montero, P., Villacieros-Robineau, R., Largier, J., Barton, E., 2016. Estuarine Classification of the Ría de Vigo Based on Seasonal Cycles of Stratification and Mixing, in: Abstracts book of IV Encuentro de Oceanografia Fisica 2016 (EOF), Alicante (Spain).

Godin, G., 1985. Modification of river tides by the discharge. Journal of waterway, port, coastal, and ocean engineering 111, 257–274.

Godin, G., 1991. Frictional effects in river tides. Tidal hydrodynamics 379, 402.

Gonçalves, M., Schmid, K., Andrade, M.C., Andrades, R., Pegado, T., Giarrizzo, T., 2020. Are the tidal flooded forests sinks for litter in the Amazonian estuary? Marine Pollution Bulletin 161, 111732.

González-Fernández, D., Cózar, A., Hanke, G., Viejo, J., Morales-Caselles, C., Bakiu, R., Barceló, D., Bessa, F., Bruge, A., Cabrera, M., et al., 2021. Floating macrolitter leaked from europe into the ocean. Nature Sustainability 4, 474–483.

González-Ortegón, E., Baldó, F., Arias, A., Cuesta, J.A., Fernández-Delgado, C., Vilas, C., Drake, P., 2015. Freshwater scarcity effects on the aquatic macrofauna of a European Mediterranean-climate estuary. Science of the total environment 503, 213–221.

González-Ortegón, E., Sendra, M., Sparaventi, E., Leal, R.F.S., de los Ríos, I., Baldó, F., González-Fernández, D., Yeste, M.P., 2022. Coastal gradients of small microplastics and associated pollutants influenced by estuarine sources. Marine Pollution Bulletin 174, 113292.

González-Ortegón, E., Subida, M.D., Arias, A.M., Baldó, F., Cuesta, J.A., Fernández-Delgado, C., Vilas, C., Drake, P., 2012. Nekton response to freshwater inputs in a temperate European Estuary with regulated riverine inflow. Science of the total environment 440, 261–271.

Gray, A.D., Wertz, H., Leads, R.R., Weinstein, J.E., 2018. Microplastic in two South Carolina Estuaries: Occurrence, distribution, and composition. Marine pollution bulletin 128, 223–233.

Green, D.S., Kregting, L., Boots, B., Blockley, D.J., Brickle, P., Da Costa, M., Crowley, Q., 2018. A comparison of sampling methods for seawater microplastics and a first report of the microplastic litter in coastal waters of Ascension and Falkland Islands. Marine pollution bulletin 137, 695–701.

Guo, L., van der Wegen, M., Jay, D.A., Matte, P., Wang, Z.B., Roelvink, D., He, Q., 2015. River-tide dynamics: Exploration of nonstationary and nonlinear tidal behavior in the Yangtze River estuary. Journal of Geophysical Research: Oceans 120, 3499–3521.

Hallermeier, R.J., 1981. Terminal settling velocity of commonly occurring sand grains. Sedimentology 28, 859–865.

Hansen, D.V., Rattray Jr, M., 1966. Gravitational circulation in straits and estuaries .

Hardesty, B.D., Harari, J., Isobe, A., Lebreton, L., Maximenko, N., Potemra, J., Van Sebille, E., Vethaak, A.D., Wilcox, C., 2017. Using numerical model simulations to improve the understanding of micro-plastic distribution and pathways in the marine environment. Frontiers in marine science 4, 30.

Hildebrandt, L., Voigt, N., Zimmermann, T., Reese, A., Proefrock, D., 2019. Evaluation of continuous flow centrifugation as an alternative technique to sample microplastic from water bodies. Marine environmental research 151, 104768.

Hinata, H., Mori, K., Ohno, K., Miyao, Y., Kataoka, T., 2017. An estimation of the average residence times and onshore-offshore diffusivities of beached microplastics based on the population decay of tagged meso-and macrolitter. Marine pollution bulletin 122, 17–26.

Hitchcock, J.N., Mitrovic, S.M., 2019. Microplastic pollution in estuaries across a gradient of human impact. Environmental Pollution 247, 457–466.

Hoitink, A., Hoekstra, P., Van Maren, D., 2003. Flow asymmetry associated with astronomical tides: Implications for the residual transport of sediment. Journal of Geophysical Research: Oceans 108.

Horrevoets, A., Savenije, H., Schuurman, J., Graas, S., 2004. The influence of river discharge on tidal damping in alluvial estuaries. Journal of Hydrology 294, 213–228.

Isobe, A., Kubo, K., Tamura, Y., Nakashima, E., Fujii, N., et al., 2014. Selective transport of microplastics and mesoplastics by drifting in coastal waters. Marine pollution bulletin 89, 324–330.

Iwasaki, S., Isobe, A., Kako, S., Uchida, K., Tokai, T., 2017. Fate of microplastics and mesoplastics carried by surface currents and wind waves: A numerical model approach in the Sea of Japan. Marine Pollution Bulletin 121, 85–96.

Jahnke, A., Arp, H.P.H., Escher, B.I., Gewert, B., Gorokhova, E., Kuhnel, D., Ogonowski, M., Potthoff, A., Rummel, C., Schmitt-Jansen, M., et al., 2017. Reducing uncertainty and confronting ignorance about the possible impacts of weathering plastic in the marine environment. Environmental Science & Technology Letters 4, 85–90.

Jalón-Rojas, I., Castelle, B., 2021. Climate control of multidecadal variability in river discharge and precipitation in western europe. Water 13, 257.

Jalón-Rojas, I., Dijkstra, Y., Schuttelaars, H., Brouwer, R., Schmidt, S., Sottolichio, A., 2021. Multidecadal Evolution of the Turbidity Maximum Zone in a Macrotidal River Under Climate and Anthropogenic Pressures. Journal of Geophysical Research: Oceans 126, e2020JC016273.

Jalón-Rojas, I., Romero-Ramirez, A., Fauquembergue, K., Rossignol, L., Cachot, J., Sous, D., Morin, B., 2022. Effects of biofilm and particle physical properties on the rising and settling velocities of microplastic fibers and sheets. Environmental and Science Technology 56, 8114–8123.

Jalón-Rojas, I., Schmidt, S., Sottolichio, A., 2015. Turbidity in the fluvial Gironde Estuary (southwest France) based on 10-year continuous monitoring: sensitivity to hydrological conditions. Hydrology and Earth System Sciences 19, 2805–2819.

Jalón-Rojas, I., Sottolichio, A., Hanquiez, V., Fort, A., Schmidt, S., 2018. To what extent multidecadal changes in morphology and fluvial discharge impact tide in a convergent (turbid) tidal river. Journal of Geophysical Research: Oceans 123, 3241–3258.

Jalón-Rojas, I., Wang, X.H., Fredj, E., 2019a. A 3D numerical model to track marine plastic debris (TrackMPD): sensitivity of microplastic trajectories and fates to particle dynamical properties and physical processes. Marine pollution bulletin 141, 256–272.

Jalón-Rojas, I., Wang, X.H., Fredj, E., 2019b. On the importance of a three-dimensional approach for modelling the transport of neustic microplastics. Ocean Science 15, 717–724.

Jay, D.A., 1991. Estuarine salt conservation: A Lagrangian approach. Estuarine, Coastal and Shelf Science 32, 547–565.

Jay, D.A., 2010. Estuarine variability. Cambridge University Press. p. 62–99. doi:10.1017/CBO9780511676567.005.

Jay, D.A., Musiak, J.D., 1994. Particle trapping in estuarine tidal flows. Journal of Geophysical Research: Oceans 99, 20445–20461.

Jay, D.A., Talke, S.A., Hudson, A., Twardowski, M., 2015. Estuarine turbidity maxima revisited: Instrumental approaches, remote sensing, modeling studies, and new directions. Developments in sedimentology 68, 49–109.

Johnson, S.W., 1989. Deposition, fate, and characteristics of derelict trawl web on an Alaskan beach. Marine pollution bulletin 20, 164–168.

Johnson, S.W., Eiler, J.H., 1999. Fate of radio-tagged trawl web on an Alaskan beach. Marine pollution bulletin 38, 136–141.

Kaiser, D., Kowalski, N., Waniek, J.J., 2017. Effects of biofouling on the sinking behavior of microplastics. Environmental research letters 12, 124003.

Karkanorachaki, K., Syranidou, E., Kalogerakis, N., 2021. Sinking characteristics of microplastics in the marine environment. Science of The Total Environment 793, 148526.

Karthik, R., Robin, R., Purvaja, R., Ganguly, D., Anandavelu, I., Raghuraman, R., Hariharan, G., Ramakrishna, A., Ramesh, R., 2018. Microplastics along the beaches of southeast coast of India. Science of The Total Environment 645, 1388–1399.

Kataoka, T., Hinata, H., 2015. Evaluation of beach cleanup effects using linear system analysis. Marine Pollution Bulletin 91, 73–81.

Khatmullina, L., Isachenko, I., 2017. Settling velocity of microplastic particles of regular shapes. Marine pollution bulletin 114, 871–880.

Kooi, M., Koelmans, A.A., 2019. Simplifying microplastic via continuous probability distributions for size, shape, and density. Environmental Science & Technology Letters 6, 551–557.

Kooi, M., Nes, E.H.v., Scheffer, M., Koelmans, A.A., 2017. Ups and downs in the ocean: effects of biofouling on vertical transport of microplastics. Environmental science & technology 51, 7963–7971.

Kowalski, N., Reichardt, A.M., Waniek, J.J., 2016. Sinking rates of microplastics and potential implications of their alteration by physical, biological, and chemical factors. Marine pollution bulletin 109, 310–319.

Kvale, K.F., Friederike Prowe, A., Oschlies, A., 2020. A critical examination of the role of marine snow and zooplankton fecal pellets in removing ocean surface microplastic. Frontiers in Marine Science 6, 808.

La Daana, K.K., Officer, R., Lyashevska, O., Thompson, R.C., O'Connor, I., 2017. Microplastic abundance, distribution and composition along a latitudinal gradient in the Atlantic Ocean. Marine pollution bulletin 115, 307–314.

Lanzoni, S., Seminara, G., 1998. On tide propagation in convergent estuaries. Journal of Geophysical Research: Oceans 103, 30793–30812.

Largier, J., Hollibaugh, J.T., Smith, S., 1997. Seasonally hypersaline estuaries in Mediterranean-climate regions. Estuarine, Coastal and Shelf Science 45, 789–797.

Largier, J.L., Hearn, C.J., Chadwick, D.B., 1996. Density structures in "low inflow estuaries". Buoyancy Effects on Coastal and Estuarine Dynamics 53, 227–241.

Lebreton, L., Van Der Zwet, J., Damsteeg, J.W., Slat, B., Andrady, A., Reisser, J., 2017. River plastic emissions to the world's oceans. Nature communications 8, 1–10.

Lefebvre, C., Rojas, I.J., Lasserre, J., Villette, S., Lecomte, S., Cachot, J., Morin, B., 2021. Stranded in the high tide line: Spatial and temporal variability of beached microplastics in a semi-enclosed embayment (Arcachon, France). Science of The Total Environment 797, 149144.

Li, D., Liu, K., Li, C., Peng, G., Andrady, A.L., Wu, T., Zhang, Z., Wang, X., Song, Z., Zong, C., et al., 2020. Profiling the vertical transport of microplastics in the West Pacific Ocean and the East Indian Ocean with a novel in situ filtration technique. Environmental Science & Technology 54, 12979–12988.

Liu, K., Zhang, F., Song, Z., Zong, C., Wei, N., Li, D., 2019. A novel method enabling the accurate quantification of microplastics in the water column of deep ocean. Marine Pollution Bulletin 146, 462–465.

Liu, P., Zhan, X., Wu, X., Li, J., Wang, H., Gao, S., 2020. Effect of weathering on environmental behavior of microplastics: Properties, sorption and potential risks. Chemosphere 242, 125193.

Llope, M., 2017. The ecosystem approach in the Gulf of Cadiz. A perspective from the southernmost European Atlantic regional sea. ICES Journal of Marine Science 74, 382–390.

Lo, H.S., Lee, Y.K., Po, B.H.K., Wong, L.C., Xu, X., Wong, C.F., Wong, C.Y., Tam, N.F.Y., Cheung, S.G., 2020. Impacts of Typhoon Mangkhut in 2018 on the deposition of marine debris and microplastics on beaches in Hong Kong. Science of the Total Environment 716, 137172.

Lobelle, D., Kooi, M., Koelmans, A.A., Laufkötter, C., Jongedijk, C.E., Kehl, C., van Sebille, E., 2021. Global modeled sinking characteristics of biofouled microplastic. Journal of Geophysical Research: Oceans 126, e2020JC017098.

López-López, J.A., García-Vargas, M., Moreno, C., 2011. A chemometric approach to the evaluation of atmospheric and fluvial pollutant inputs in aquatic systems: The Guadalquivir River estuary as a case study. Environmental Pollution 159, 1136–1143.

Losada, M., Díez-Minguito, M., Reyes-Merlo, M., 2017. Tidal-fluvial interaction in the Guadalquivir River Estuary: Spatial and frequency-dependent response of currents and water levels. Journal of Geophysical Research: Oceans 122, 847–865.

Lusher, A.L., Burke, A., O'Connor, I., Officer, R., 2014. Microplastic pollution in the Northeast Atlantic Ocean: validated and opportunistic sampling. Marine pollution bulletin 88, 325–333.

Martin, C., Almahasheer, H., Duarte, C.M., 2019. Mangrove forests as traps for marine litter. Environmental Pollution 247, 499–508.

McEachern, K., Alegria, H., Kalagher, A.L., Hansen, C., Morrison, S., Hastings, D., 2019. Microplastics in tampa bay, florida: abundance and variability in estuarine waters and sediments. Marine pollution bulletin 148, 97–106.

McIlgorm, A., Campbell, H.F., Rule, M.J., 2011. The economic cost and control of marine debris damage in the Asia-Pacific region. Ocean & Coastal Management 54, 643–651.

Michida, Y., Chavanich, S., Chiba, S., Cordova, M.R., Cozsar Cabanas, A., Glagani, F., Hagmann, P., Hinata, H., Isobe, A., Kershaw, P., et al., 2019. Guidelines for Harmonizing Ocean Surface Microplastic Monitoring Methods. Version 1.1. .

Miró, J.M., Megina, C., Donázar-Aramendía, I., Reyes-Martínez, M.J., Sánchez-Moyano, J.E., García-Gómez, J.C., 2020. Environmental factors affecting the nursery function for fish in the main estuaries of the Gulf of Cadiz (south-west Iberian Peninsula). Science of the Total Environment 737. doi:10.1016/j.scitotenv.2020.139614.

Morales-Caselles, C., Viejo, J., Martí, E., González-Fernández, D., Pragnell-Raasch, H., González-Gordillo, J.I., Montero, E., Arroyo, G.M., Hanke, G., Salvo, V.S., et al., 2021. An inshore–offshore sorting system revealed from global classification of ocean litter. Nature Sustainability 4, 484–493.

Müller, Y.K., Wernicke, T., Pittroff, M., Witzig, C.S., Storck, F.R., Klinger, J., Zumbülte, N., 2020. Microplastic analysis—are we measuring the same? results on the first global comparative study for microplastic analysis in a water sample. Analytical and Bioanalytical Chemistry 412, 555–560.

Naidoo, T., Glassom, D., Smit, A.J., 2015. Plastic pollution in five urban estuaries of KwaZulu-Natal, South Africa. Marine pollution bulletin 101, 473–480.

Napper, I.E., Wright, L.S., Barrett, A.C., Parker-Jurd, F.N., Thompson, R.C., 2022. Potential microplastic release from the maritime industry: Abrasion of rope. Science of the Total Environment 804, 150155.

Navarro, G., Gutiérrez, F.J., Díez-Minguito, M., Losada, M.A., Ruiz, J., 2011. Temporal and spatial variability in the Guadalquivir estuary: a challenge for real-time telemetry. Ocean Dynamics 61, 753–765.

Njeru, J., 2006. The urban political ecology of plastic bag waste problem in Nairobi, Kenya. Geoforum 37, 1046–1058.

Oben Mbeng, L., David, M., Ntyanm Ondo, S., 2021. Classification Study of Ingested Plastic Particles in Marine Organisms using Electron Microscope: A Case Study of Cameroon Beaches .

Okubo, A., Ebbesmeyer, C.C., 1976. Determination of vorticity, divergence, and deformation rates from analysis of drogue observations, in: Deep Sea Research and Oceanographic Abstracts, Elsevier. pp. 349–352.

Parker, B.B., 1991. The relative importance of the various nonlinear mechanisms in a wide range of tidal interactions. Tidal hydrodynamics 13, 237–268.

Parvin, F., Jannat, S., Tareq, S.M., 2021. Abundance, characteristics and variation of microplastics in different freshwater fish species from Bangladesh. Science of The Total Environment 784, 147137.

Phuong, N.N., Poirier, L., Lagarde, F., Kamari, A., Zalouk-Vergnoux, A., 2018. Microplastic abundance and characteristics in french atlantic coastal sediments using a new extraction method. Environmental Pollution 243, 228–237.

Pinheiro, L.M., Monteiro, R.C., do Sul, J.A.I., Costa, M.F., 2019. Do beachrocks affect microplastic deposition on the strandline of sandy beaches? Marine pollution bulletin 141, 569–572.

Prata, J.C., da Costa, J.P., Duarte, A.C., Rocha-Santos, T., 2019. Methods for sampling and detection of microplastics in water and sediment: a critical review. TrAC Trends in Analytical Chemistry 110, 150–159.

Quintana Sepúlveda, R., González Fernández, D., Cózar Cabañas, A., Vilas Fernández, C., González Ortegón, E., Baldo Martínez, F., Morales Caselles, C., 2020. Plastic waste input from Guadalquivir River to the ocean, in: EGU General Assembly Conference Abstracts, p. 19268.

van Rijn, L.C., 1998. Principles of coastal morphology.

Rodrigues, S., Almeida, C.M.R., Silva, D., Cunha, J., Antunes, C., Freitas, V., Ramos, S., 2019. Microplastic contamination in an urban estuary: abundance and distribution of microplastics and fish larvae in the Douro estuary. Science of the Total Environment 659, 1071–1081.

Rozman, U., Kalčíková, G., 2022. Seeking for a perfect (non-spherical) microplastic particle–the most comprehensive review on microplastic laboratory research. Journal of Hazardous Materials 424, 127529.

Ruiz, J., Macías, D., Navarro, G., 2017. Natural forcings on a transformed territory overshoot thresholds of primary productivity in the Guadalquivir estuary. Continental Shelf Research 148, 199–207.

Ruiz, J., Polo, M.J., Díez-Minguito, M., Navarro, G., Morris, E.P., Huertas, E., Caballero, I., Contreras, E., Losada, M.A., 2015. The Guadalquivir estuary: A hot spot for environmental and human conflicts, in: Finkl, C.W., Makowski, C. (Eds.), Environmental Management and Governance. Springer. volume 8 of *Coastal Research Library*, pp. 199–232.

Rummel, C.D., Jahnke, A., Gorokhova, E., Kuhnel, D., Schmitt-Jansen, M., 2017. Impacts of biofilm formation on the fate and potential effects of microplastic in the aquatic environment. Environmental science & technology letters 4, 258–267.

Ryan, P.G., 2015. Does size and buoyancy affect the long-distance transport of floating debris? Environmental Research Letters 10, 084019.

Ryan, P.G., Perold, V., Osborne, A., Moloney, C.L., 2018. Consistent patterns of debris on South African beaches indicate that industrial pellets and other mesoplastic items mostly derive from local sources. Environmental Pollution 238, 1008–1016.

Ryan, P.G., Suaria, G., Perold, V., Pierucci, A., Bornman, T.G., Aliani, S., 2020. Sampling microfibres at the sea surface: The effects of mesh size, sample volume and water depth. Environmental Pollution 258, 113413.

Sadri, S.S., Thompson, R.C., 2014. On the quantity and composition of floating plastic debris entering and leaving the Tamar Estuary, Southwest England. Marine pollution bulletin 81, 55–60.

Savenije, H.H., 2005. Salinity and tides in alluvial estuaries. Gulf Professional Publishing.

Schmidt, S., 2020. A 14-Year Multi-sites and High-Frequency Monitoring of Salinity in the Tidal Garonne River (SW France) Reveals Marked Inter-annual Variability in Marine Intrusion, in: Estuaries and Coastal Zones in Times of Global Change. Springer, pp. 3–11.

Scully, M.E., Friedrichs, C.T., 2007. Sediment pumping by tidal asymmetry in a partially mixed estuary. Journal of Geophysical Research: Oceans 112.

Shields, A., 1936. Anwendung der aehnlichkeitsmechanik und der turbulenzforschung auf die geschiebebewegung. PhD Thesis Technical University Berlin .

Simon-Sánchez, L., Grelaud, M., Garcia-Orellana, J., Ziveri, P., 2019. River Deltas as hotspots of microplastic accumulation: The case study of the Ebro River (NW Mediterranean). Science of the total environment 687, 1186–1196.

Simpson, J.H., Brown, J., Matthews, J., Allen, G., 1990. Tidal straining, density currents, and stirring in the control of estuarine stratification. Estuaries 13, 125–132.

Sipe, J.M., Bossa, N., Berger, W., von Windheim, N., Gall, K., Wiesner, M.R., 2022. From bottle to microplastics: Can we estimate how our plastic products are breaking down? Science of The Total Environment 814, 152460.

Smith, S.D., 2012. Marine debris: A proximate threat to marine sustainability in Bootless Bay, Papua New Guinea. Marine Pollution Bulletin 64, 1880–1883.

Song, Y.K., Hong, S.H., Jang, M., Han, G.M., Jung, S.W., Shim, W.J., 2017. Combined effects of UV exposure duration and mechanical abrasion on microplastic fragmentation by polymer type. Environmental science & technology 51, 4368–4376.

Sousa, M.C., DeCastro, M., Gago, J., Ribeiro, A.S., Des, M., Gómez-Gesteira, J.L., Dias, J.M., Gomez-Gesteira, M., 2021. Modelling the distribution of microplastics released by wastewater treatment plants in Ria de Vigo (NW Iberian Peninsula). Marine Pollution Bulletin 166, 112227.

Speer, P., Aubrey, D., 1985. A study of non-linear tidal propagation in shallow inlet/estuarine systems Part II: Theory. Estuarine, Coastal and Shelf Science 21, 207–224.

Stacey, M.T., Monismith, S.G., Burau, J.R., 1999. Observations of turbulence in a partially stratified estuary. Journal of Physical Oceanography 29, 1950–1970.

Stock, F., Kochleus, C., Bänsch-Baltruschat, B., Brennholt, N., Reifferscheid, G., 2019. Sampling techniques and preparation methods for microplastic analyses in the aquatic environment–a review. TrAC Trends in Analytical Chemistry 113, 84–92.

do Sul, J.A.I., Costa, M.F., Silva-Cavalcanti, J.S., Araújo, M.C.B., 2014. Plastic debris retention and exportation by a mangrove forest patch. Marine pollution bulletin 78, 252–257.

Tamminga, M., Stoewer, S.C., Fischer, E.K., 2019. On the representativeness of pump water samples versus manta sampling in microplastic analysis. Environmental pollution 254, 112970.

Tekman, M.B., Wekerle, C., Lorenz, C., Primpke, S., Hasemann, C., Gerdts, G., Bergmann, M., 2020. Tying up loose ends of microplastic pollution in the Arctic: distribution from the sea surface through the water column to deep-sea sediments at the HAUSGARTEN observatory. Environmental science & technology 54, 4079–4090.

Ter Halle, A., Ghiglione, J.F., 2021. Nanoplastics: A Complex, Polluting Terra Incognita. Environmental Science & Technology 55, 14466–14469.

Tramoy, R., Gasperi, J., Colasse, L., Silvestre, M., Dubois, P., Noûs, C., Tassin, B., 2020a. Transfer dynamics of macroplastics in estuaries–New insights from the Seine estuary: Part 2. Short-term dynamics based on GPS-trackers. Marine Pollution Bulletin 160, 111566.

Tramoy, R., Gasperi, J., Colasse, L., Tassin, B., 2020b. Transfer dynamic of macroplastics in estuaries—New insights from the Seine estuary: Part 1. Long term dynamic based on date-prints on stranded debris. Marine Pollution Bulletin 152, 110894.

Treilles, R., Gasperi, J., Gallard, A., Saad, M., Dris, R., Partibane, C., Breton, J., Tassin, B., 2021. Microplastics and microfibers in urban runoff from a suburban catchment of Greater Paris. Environmental Pollution 287, 117352.

Turner, A., 2021. Paint particles in the marine environment: An overlooked component of microplastics. Water Research X 12, 100110.

Turner, J.S., Turner, J.S., 1979. Buoyancy effects in fluids. Cambridge university press.

Uncles, R., Elliott, R., Weston, S., 1985. Dispersion of salt and suspended sediment in a partly mixed estuary. Estuaries 8, 256–269.

Valle-Levinson, A., 2008. Density-driven exchange flow in terms of the Kelvin and Ekman numbers. Journal of Geophysical Research: Oceans 113.

Van Melkebeke, M., Janssen, C., De Meester, S., 2020. Characteristics and sinking behavior of typical microplastics including the potential effect of biofouling: implications for remediation. Environmental science & technology 54, 8668–8680.

Van Rijn, L.C., et al., 1993. Principles of sediment transport in rivers, estuaries and coastal seas. volume 1006. Aqua publications Amsterdam.

Van Sebille, E., Aliani, S., Law, K.L., Maximenko, N., Alsina, J.M., Bagaev, A., Bergmann, M., Chapron, B., Chubarenko, I., Cózar, A., et al., 2020. The physical oceanography of the transport of floating marine debris. Environmental Research Letters 15, 023003.

Waldschlager, K., Born, M., Cowger, W., Gray, A., Schuettrumpf, H., 2020. Settling and rising velocities of environmentally weathered micro-and macroplastic particles. Environmental Research 191, 110192.

Waldschlager, K., Schuttrumpf, H., 2019a. Effects of particle properties on the settling and rise velocities of microplastics in freshwater under laboratory conditions. Environmental science & technology 53, 1958–1966.

Waldschlager, K., Schuttrumpf, H., 2019b. Erosion behavior of different microplastic particles in comparison to natural sediments. Environmental science & technology 53, 13219–13227.

Winterwerp, J.C., Van Kesteren, W.G., 2004. Introduction to the physics of cohesive sediment dynamics in the marine environment. Elsevier.

Wright, S.L., Thompson, R.C., Galloway, T.S., 2013. The physical impacts of microplastics on marine organisms: a review. Environmental pollution 178, 483–492.

Xu, P., Peng, G., Su, L., Gao, Y., Gao, L., Li, D., 2018. Microplastic risk assessment in surface waters: A case study in the Changjiang Estuary, China. Marine pollution bulletin 133, 647–654.

Yan, M., Nie, H., Xu, K., He, Y., Hu, Y., Huang, Y., Wang, J., 2019. Microplastic abundance, distribution and composition in the Pearl River along Guangzhou city and Pearl River estuary, China. Chemosphere 217, 879–886.

Yonkos, L.T., Friedel, E.A., Perez-Reyes, A.C., Ghosal, S., Arthur, C.D., 2014. Microplastics in four estuarine rivers in the Chesapeake Bay, USA. Environmental science & technology 48, 14195–14202.

Zhang, H., 2017. Transport of microplastics in coastal seas. Estuarine, Coastal and Shelf Science 199, 74–86.

Zhao, S., Zhu, L., Li, D., 2015. Microplastic in three urban estuaries, China. Environmental Pollution 206, 597–604.

Zhao, S., Zhu, L., Wang, T., Li, D., 2014. Suspended microplastics in the surface water of the Yangtze Estuary System, China: first observations on occurrence, distribution. Marine pollution bulletin 86, 562–568.